

A COMPARISON OF ADVECT CLOUD MODEL
AND FIFTH-GENERATION MESOSCALE MODEL
TOTAL FRACTIONAL CLOUD FORECASTS

THESIS

Brian D. Pukall, Captain, USAF

AFIT/GM/ENP/98M-08

19980409 021

DEPARTMENT OF THE AIR FORCE **DTIC QUALITY INSPECTED 4**
AIR UNIVERSITY
AIR FORCE INSTITUTE OF TECHNOLOGY

Wright-Patterson Air Force Base, Ohio

AFIT/GM/ENP/98M-08

**A COMPARISON OF ADVECT CLOUD MODEL
AND FIFTH-GENERATION MESOSCALE MODEL
TOTAL FRACTIONAL CLOUD FORECASTS**

THESIS

Brian D. Pukall, Captain, USAF

AFIT/GM/ENP/98M-08

Approved for public release; distribution unlimited

The views expressed in this thesis are those of the author and do not reflect the official policy or position of the U.S. Air Force, Department of Defense, or the U.S. Government.

AFIT/GM/ENP/98M-08

**A COMPARISON OF ADVECT CLOUD MODEL AND FIFTH-GENERATION
MESOSCALE MODEL TOTAL FRACTIONAL CLOUD FORECASTS**

THESIS

**Presented to the Faculty of the Graduate School of Engineering
of the Air Force Institute of Technology**

Air University

Air Education and Training Command

**In Partial Fulfillment of the Requirement for the
Degree of Master of Science in Meteorology**

Brian D. Pukall, B.A.

Captain, USAF


March 1998

Approved for public release; distribution unlimited

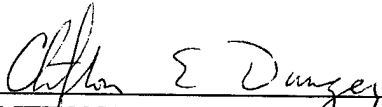
A COMPARISON OF ADVECT CLOUD MODEL AND FIFTH-GENERATION
MESOSCALE MODEL TOTAL FRACTIONAL CLOUD FORECASTS

Brian D. Pukall, B.A.
Captain, USAF

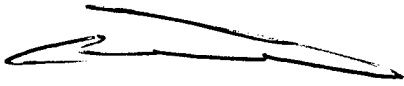
Approved:


MICHAEL K. WALTERS, LtCol, USAF
Chairman, Advisory Committee

12 Feb 98
Date


CLIFTON E. DUNGEY, Maj, USAF
Member, Advisory Committee

12 Feb 98
Date


GLEN P. PERRAM, LtCol, USAF
Member, Advisory Committee

12 Feb 98
Date

Approved for public release; distribution unlimited

Acknowledgments

I would like to thank God for giving me the perseverance and insight to make it through this thesis and through the entire program. I need to thank my wife, Alessandra, for her support, encouragement, and understanding throughout the past 18 months. Without her, it would have been a dreary time indeed. I would also like to acknowledge my infant daughter, Vittoria, whose incredibly sweet demeanor allowed me to sleep through the night almost from the time she was born, a definite benefit the night before a test.

Here at AFIT I would especially like to thank my thesis advisor, Lieutenant Colonel Michael K. Walters, for giving me the pushes I needed to produce a quality thesis. I would also like to thank the other members of my committee, Major Clifton Dungey and Lieutenant Colonel Glen Perram for their comments and assistance in the writing of this document. I must also thank Master Sergeant Pete Rahe for babysitting my data and making sure none of it mysteriously disappeared into computer limbo.

Finally, I would like to thank all those at the Air Force Weather Agency who aided me in gathering data, transferring it to AFIT, and decoding it once it arrived. I would especially like to express my gratitude to Ms. Tanya Spero, Captain Margaret Wonsick, Dr. Tom Kopp, and Captain Lou Cantrell.

Table of Contents

	Page
Acknowledgments	ii
Table of Contents	iii
List of Figures	viii
List of Tables	xiv
Abstract	xviii
I. Introduction	1
1.1 Background	1
1.2 Importance of the Research	2
1.2.1 Military Impacts	2
1.2.2 Cloud Forecasting Approaches	3
1.2.2.1 Diagnostic Approach	3
1.2.2.2 Prognostic Approach	4
1.3 Statement of the Problem	4
1.4 Benefit from solving the Problem	5
1.5 Research Objective	5
1.6 Procedure	6
1.7 Thesis Organization	7
II. Literature Review	8
2.1 RTNEPH	8
2.1.1 RTNEPH Background	8

2.1.2	RTNEPH Weaknesses	12
2.1.3	RTNEPH Strengths	14
2.2	ADVCLD	15
2.2.1	ADVCLD Background	15
2.2.2	Moisture Initialization in ADVCLD	16
2.2.3	Advection in ADVCLD	21
2.3	MM5	22
2.3.1	MM5 Background	22
2.3.2	MM5 Characteristics	23
2.3.3	Moisture in the MM5	25
2.4	Total Fractional Cloudiness Forecasts from MM5 Output Variables ...	27
2.4.1	RH Schemes	27
2.4.1.1	Sundqvist Method	28
2.4.1.2	Kvamstø Method	29
2.4.2	Total Cloud Condensate Schemes	30
III.	Methodology	31
3.1	Introduction	31
3.2	Scope	31
3.3	Procedure	31
3.3.1	RTNEPH and ADVCLD Data	31
3.3.2	MM5 Data	32
3.3.3	Implementation of FC Schemes from MM5 Variables	32

3.3.3.1 RH Schemes	33
3.3.3.2 Vertical Column Method	33
3.3.3.3 Layered Method	34
3.3.4 Data Processing	35
3.4 Quality Control of the Data	37
3.4.1 Objective Quality Control	37
3.4.2 Subjective Quality Control	37
3.5 Statistical Analysis	40
3.5.1 Scalar Measures of Forecast Accuracy	42
3.5.2 Sharpness as a Measure of Forecast Performance	44
3.5.3 Contingency Table Statistics	44
3.5.4 Forecast Skill	47
3.5.5 Statistical Significance Testing	48
3.6 Subjective Analysis	49
IV. Results	51
4.1 Significance Testing Results	52
4.2 Scalar Measures of Accuracy Results	53
4.2.1 Mean Error Results	53
4.2.2 Mean Absolute Error Results	53
4.2.3 Root-Mean-Squared Error Results	58
4.3 Sharpness (20/20 Score) Results	67
4.3.1 Sharpness for Clear Skies (0-19 Score) Results	67

4.3.2 Sharpness for Overcast Skies (81-100 Score) Results	67
4.4 Contingency Table Results	76
4.4.1 Hit Rate Results	76
4.4.2 Critical Success Index Results	81
4.4.3 Probability of Detection Results	86
4.4.4 False Alarm Rate Results	86
4.5 Skill Score Results	95
4.5.1 Hit Rate Skill Score Results	95
4.5.2 Critical Success Index Skill Score Results	95
4.6 Subjective Analysis Results	104
V. Conclusions and Recommendations	110
5.1 Conclusions.....	110
5.1.1 Conclusions From Comparisons of ADVCLD and MM5.....	110
5.1.2 Conclusions From Comparisons of MM5 Schemes	112
5.1.3 Conclusions Based on Persistence	113
5.1.4 Summary of Conclusions	114
5.2 Recommendations	114
5.2.1 Recommendations for Operational Implementation	114
5.2.2 Recommendations for Further Research	115
Appendix A: Tables used in ADVCLD to relate CPS and FC amounts	117
Appendix B: Relationship between CPS and dew point depression	122
Appendix C: MM5 forecast cycles and initialization models used	123

Appendix D: Sigma (σ) Coordinate System Description	127
Appendix E: Pressure levels used by MM5	128
Appendix F: Total cloud condensate threshold values-vertical column method....	129
Appendix G: Total cloud condensate threshold values-layered method	130
Bibliography	133
Vita	135

List of Figures

	Page
Figure 1. Representation of the area (shaded gray area) centered on a model grid point for which a total fractional cloudiness forecast is valid	2
Figure 2. The 64 northern hemisphere RTNEPH grid boxes (Kiess and Cox, 1988)	11
Figure 3. Geographical region covered by the Bosnia grid	24
Figure 4. Infrared satellite image for 12 UTC on 8 October 1997	39
Figure 5. ADVCLD FC analysis for 12 UTC on 8 October 1997. Black corresponds to total FC amounts of zero percent and white corresponds to 100 percent	39
Figure 6. An example of a frequency count array used to perform the statistical analysis. The original array was 21 x 21, binned to a 10 x 10 array for display. The columns represent RTNEPH total FC values, while the rows represent ADVCLD total FC values	41
Figure 7. An example of a 2 x 2 contingency table	45
Figure 8. ME versus forecast hour for August 1997. The thick solid line represents ADVCLD, the thin solid line is persistence, the thick dotted line is the Kvamstø method, the thin dotted line is the Sundqvist method, the thick dashed line is the vertical column method, and the thin dashed line is the layered method. Average hourly ME values are plotted. See Table 2 for descriptive statistics	54
Figure 9. As in Figure 8 for September 1997. See Table 3 for descriptive statistics	55
Figure 10. As in Figure 8 for October 1997. See Table 4 for descriptive statistics	56
Figure 11. As in Figure 8 for November 1997. See Table 5 for descriptive statistics	57
Figure 12. MAE versus forecast hour for August 1997. The thick solid line represents ADVCLD, the thin solid line is persistence, the thick dotted line is the Kvamstø method, the thin dotted line is the Sundqvist method, the thick dashed line is the vertical column method, and the	

thin dashed line is the layered method. Average hourly MAE values are plotted. See Table 6 for descriptive statistics	59
Figure 13. As in Figure 12 for September 1997. See Table 7 for descriptive statistics	60
Figure 14. As in Figure 12 for October 1997. See Table 8 for descriptive statistics	61
Figure 15. As in Figure 12 for November 1997. See Table 9 for descriptive statistics	62
Figure 16. RMSE versus forecast hour for August 1997. The thick solid line represents ADVCLD, the thin solid line is persistence, the thick dotted line is the Kvamstø method, the thin dotted line is the Sundqvist method, the thick dashed line is the vertical column method, and the thin dashed line is the layered method. Average hourly RMSE values are plotted. See Table 10 for descriptive statistics	63
Figure 17. As in Figure 16 for September 1997. See Table 11 for descriptive statistics	64
Figure 18. As in Figure 16 for October 1997. See Table 12 for descriptive statistics	65
Figure 19. As in Figure 16 for November 1997. See Table 13 for descriptive statistics	66
Figure 20. 0-19 score versus forecast hour for August 1997. The thick solid line represents ADVCLD, the thin solid line is persistence, the thick dotted line is the Kvamstø method, the thin dotted line is the Sundqvist method, the thick dashed line is the vertical column method, and the thin dashed line is the layered method. RTNEPH is the thick dashed/dotted line. Average hourly 0-19 scores are plotted. See Table 14 for descriptive statistics	68
Figure 21. As in Figure 20 for September 1997. See Table 15 for descriptive statistics	69
Figure 22. As in Figure 20 for October 1997. See Table 16 for descriptive statistics	70
Figure 23. As in Figure 20 for November 1997. See Table 17 for descriptive statistics	71

Figure 24. 81-100 score versus forecast hour for August 1997. The thick solid line represents ADVCLD, the thin solid line is persistence, the thick dotted line is the Kvamstø method, the thin dotted line is the Sundqvist method, the thick dashed line is the vertical column method, and the thin dashed line is the layered method. RTNEPH is the thick dashed/dotted line. Average hourly 81-100 scores are plotted. See Table 18 for descriptive statistics	72
Figure 25. As in Figure 24 for September 1997. See Table 19 for descriptive statistics	73
Figure 26. As in Figure 24 for October 1997. See Table 20 for descriptive statistics	74
Figure 27. As in Figure 24 for November 1997. See Table 21 for descriptive statistics	75
Figure 28. Hit rate for a broken cloudiness forecast versus forecast hour for August 1997. The thick solid line represents ADVCLD, the thin solid line is persistence, the thick dotted line is the Kvamstø method, the thin dotted line is the Sundqvist method, the thick dashed line is the vertical column method, and the thin dashed line is the layered method. Average hourly hit rate values are plotted. See Table 22 for descriptive statistics	77
Figure 29. As in Figure 28 for September 1997. See Table 23 for descriptive statistics	78
Figure 30. As in Figure 28 for October 1997. See Table 24 for descriptive statistics	79
Figure 31. As in Figure 28 for November 1997. See Table 25 for descriptive statistics	80
Figure 32. Critical success index versus forecast hour for August 1997. The thick solid line represents ADVCLD, the thin solid line is persistence, the thick dotted line is the Kvamstø method, the thin dotted line is the Sundqvist method, the thick dashed line is the vertical column method, and the thin dashed line is the layered method. Average hourly CSI values are plotted. See Table 26 for descriptive statistics	82
Figure 33. As in Figure 32 for September 1997. See Table 27 for descriptive statistics	83

Figure 34. As in Figure 32 for October 1997. See Table 28 for descriptive statistics	84
Figure 35. As in Figure 32 for November 1997. See Table 29 for descriptive statistics	85
Figure 36. Probability of detection versus forecast hour for August 1997. The thick solid line represents ADVCLD, the thin solid line is persistence, the thick dotted line is the Kvamstø method, the thin dotted line is the Sundqvist method, the thick dashed line is the vertical column method, and the thin dashed line is the layered method. Average hourly POD values are plotted. See Table 30 for descriptive statistics	87
Figure 37. As in Figure 36 for September 1997. See Table 31 for descriptive statistics	88
Figure 38. As in Figure 36 for October 1997. See Table 32 for descriptive statistics	89
Figure 39. As in Figure 36 for November 1997. See Table 33 for descriptive statistics	90
Figure 40. False alarm rate versus forecast hour for August 1997. The thick solid line represents ADVCLD, the thin solid line is persistence, the thick dotted line is the Kvamstø method, the thin dotted line is the Sundqvist method, the thick dashed line is the vertical column method, and the thin dashed line is the layered method. Average hourly FAR values are plotted. See Table 34 for descriptive statistics	91
Figure 41. As in Figure 40 for September 1997. See Table 35 for descriptive statistics	92
Figure 42. As in Figure 40 for October 1997. See Table 36 for descriptive statistics	93
Figure 43. As in Figure 40 for November 1997. See Table 37 for descriptive statistics	94
Figure 44. HR skill score versus forecast hour for August 1997. The thick solid line represents ADVCLD, the thick dotted line is the Kvamstø method, the thin dotted line is the Sundqvist method, the thick dashed line is the vertical column method, and the thin dashed line is the layered method. Average hourly HR skill score values against a reference persistence forecast are plotted as percentages. See Table 38 for descriptive statistics	96

Figure 45. As in Figure 44 for September 1997. See Table 39 for descriptive statistics	97
Figure 46. As in Figure 44 for October 1997. See Table 40 for descriptive statistics	98
Figure 47. As in Figure 44 for November 1997. See Table 41 for descriptive statistics	99
Figure 48. CSI skill score versus forecast hour for August 1997. The thick solid line represents ADVCLD, the thick dotted line is the Kvamstø method, the thin dotted line is the Sundqvist method, the thick dashed line is the vertical column method, and the thin dashed line is the layered method. Average hourly CSI skill score values against a reference persistence forecast are plotted as percentages. See Table 42 for descriptive statistics	100
Figure 49. As in Figure 48 for September 1997. See Table 43 for descriptive statistics	101
Figure 50. As in Figure 48 for October 1997. See Table 44 for descriptive statistics	102
Figure 51. As in Figure 48 for November 1997. See Table 45 for descriptive statistics	103
Figure 52. 24-hour total FC forecast valid 8 October at 12 UTC obtained from the Kvamstø method. This is the same valid time as Figures 4 and 5 shown in chapter 3. Black corresponds to total FC amounts of zero percent and white corresponds to 100 percent	106
Figure 53. As in Figure 52 for the 24-hr forecast using the Sundqvist method	106
Figure 54. As in Figure 52 for the 24-hr forecast using the vertical column method	107
Figure 55. As in Figure 52 for the 24-hr forecast using the layered method	107
Figure 56. As in Figure 52 for the 24-hr ADVCLD forecast	108
Figure 57. RTNEPH analysis valid for 9 September at 15 UTC. Grayscale as in Figure 52	108

Figure 58. 15-hour total FC forecast valid 9 September at 15 UTC obtained from the Kvamstø method. This is the same valid time as the RTNEPH analysis shown in Figure 57. Grayscale as in Figure 52	109
Figure 59. As in Figure 58 for a 15-hr forecast using the layered method	109

List of Tables

	Page
Table 1. Resolutions of the various mesh sizes used at the AFWA	10
Table 2. Monthly average RTNEPH 20/20 scores given as percentages. Inspection of the values reveals that September was the month with the least cloudiness in this study while November was the cloudiest month in the study	52
Table 3. Descriptive statistics for Figure 8. Mean error for August 1997	54
Table 4. Descriptive statistics for Figure 9. Mean error for September 1997	55
Table 5. Descriptive statistics for Figure 10. Mean error for October 1997	56
Table 6. Descriptive statistics for Figure 11. Mean error for November 1997	57
Table 7. Descriptive statistics for Figure 12. MAE for August 1997	59
Table 8. Descriptive statistics for Figure 13. MAE for September 1997	60
Table 9. Descriptive statistics for Figure 14. MAE for October 1997	61
Table 10. Descriptive statistics for Figure 15. MAE for November 1997	62
Table 11. Descriptive statistics for Figure 16. RMS error for August 1997	63
Table 12. Descriptive statistics for Figure 17. RMS error for September 1997	64
Table 13. Descriptive statistics for Figure 18. RMS error for October 1997	65
Table 14. Descriptive statistics for Figure 19. RMS error for November 1997	66
Table 15. Descriptive statistics for Figure 1. 0-19 score for August 1997	68
Table 16. Descriptive statistics for Figure 2. 0-19 score for September 1997	69
Table 17. Descriptive statistics for Figure 3. 0-19 score for October 1997	70
Table 18. Descriptive statistics for Figure 4. 0-19 score for November 1997	71
Table 19. Descriptive statistics for Figure 24. 81-100 score for August 1997	72

Table 20. Descriptive statistics for Figure 25. 81-100 score for September 1997 ...	73
Table 21. Descriptive statistics for Figure 26. 81-100 score for October 1997	74
Table 22. Descriptive statistics for Figure 27. 81-100 score for November 1997 ...	75
Table 23. Descriptive statistics for Figure 28. Hit rate for August 1997	77
Table 24. Descriptive statistics for Figure 29. Hit rate for September 1997	78
Table 25. Descriptive statistics for Figure 30. Hit rate for October 1997	79
Table 26. Descriptive statistics for Figure 31. Hit rate for November 1997	80
Table 27. Descriptive statistics for Figure 32. Critical success index for August 1997	82
Table 28. Descriptive statistics for Figure 33. Critical success index for September 1997	83
Table 29. Descriptive statistics for Figure 34. Critical success index for October 1997	84
Table 30. Descriptive statistics for Figure 35. Critical success index for November 1997	85
Table 31. Descriptive statistics for Figure 36. Probability of detection for August 1997	87
Table 32. Descriptive statistics for Figure 37. Probability of detection for September 1997	88
Table 33. Descriptive statistics for Figure 38. Probability of detection for October 1997	89
Table 34. Descriptive statistics for Figure 39. Probability of detection for November 1997	90
Table 35. Descriptive statistics for Figure 40. False alarm rate for August 1997	91
Table 36. Descriptive statistics for Figure 41. False alarm rate for September 1997	92
Table 37. Descriptive statistics for Figure 42. False alarm rate for October 1997...	93

Table 38. Descriptive statistics for Figure 43. False alarm rate for November 1997	94
Table 39. Descriptive statistics for Figure 44. Hit rate skill score for August 1997	96
Table 40. Descriptive statistics for Figure 45. Hit rate skill score for September 1997	97
Table 41. Descriptive statistics for Figure 46. Hit rate skill score for October 1997	98
Table 42. Descriptive statistics for Figure 47. Hit rate skill score for November 1997	99
Table 43. Descriptive statistics for Figure 48. CSI skill score for August 1997	100
Table 44. Descriptive statistics for Figure 49. CSI skill score for September 1997	101
Table 45. Descriptive statistics for Figure 50. CSI skill score for October 1997	102
Table 46. Descriptive statistics for Figure 51. CSI skill score for November 1997	103
Table A1. Conversion from fractional cloudiness to CPS for 850 mb. Units of cloud percent form the abscissa and tens of cloud percent form the ordinate. CPS values are located in the interior of the table	117
Table A2. Conversion from fractional cloudiness to CPS for 700 mb. Units of cloud percent form the abscissa and tens of cloud percent form the ordinate. CPS values are located in the interior of the table	118
Table A3. Conversion from fractional cloudiness to CPS for 500 mb. Units of cloud percent form the abscissa and tens of cloud percent form the ordinate. CPS values are located in the interior of the table	118
Table A4. Conversion from fractional cloudiness to CPS for 300 mb. Units of cloud percent form the abscissa and tens of cloud percent form the ordinate. CPS values are located in the interior of the table	119
Table A5. Conversion from CPS to fractional cloudiness for 850 mb. Units of CPS form the abscissa and tens of CPS form the ordinate. Cloud percent values are located in the interior of the table	119

Table A6. Conversion from CPS to fractional cloudiness for 700 mb. Units of CPS form the abscissa and tens of CPS form the ordinate. Cloud percent values are located in the interior of the table	120
Table A7. Conversion from CPS to fractional cloudiness for 500 mb. Units of CPS form the abscissa and tens of CPS form the ordinate. Cloud percent values are located in the interior of the table	120
Table A8. Conversion from CPS to fractional cloudiness for 300 mb. Units of CPS form the abscissa and tens of CPS form the ordinate. Cloud percent values are located in the interior of the table	121
Table C1. MM5 forecast cycles used together with model that was used to provide the initial and boundary conditions for August 1997	123
Table C2. MM5 forecast cycles used together with model that was used to provide the initial and boundary conditions for September 1997	124
Table C3. MM5 forecast cycles used together with model that was used to provide the initial and boundary conditions for October 1997	125
Table C4. MM5 forecast cycles used together with model that was used to provide the initial and boundary conditions for November 1997	126
Table F1. Total cloud condensate thresholds used to convert to FC amounts for the vertical column method. FC amounts are expressed in percent while total cloud condensate is in units of kg of condensate per kg of air	129
Table G1. Total cloud condensate thresholds used to convert to FC amounts for MM5 model layers between 950 mb and 750 mb. FC amounts are expressed in percent while total cloud condensate is in units of kg of condensate per kg of air	130
Table G2. Total cloud condensate thresholds used to convert to FC amounts for MM5 model layers between 700 mb and 400 mb. FC amounts are expressed in percent while total cloud condensate is in units of kg of condensate per kg of air	131
Table G3. Total cloud condensate thresholds used to convert to FC amounts for MM5 model layers between 350 mb and 200 mb. FC amounts are expressed in percent while total cloud condensate is in units of kg of condensate per kg of air	132

Abstract

Total fractional cloudiness (FC) forecasts from the advect cloud (ADVCLD) model and total FC forecasts diagnosed from the relative humidity and total cloud condensate (snow, ice, rain water, and cloud water) fields from the fifth-generation mesoscale model (MM5) were statistically and subjectively compared to determine which model produced the better total FC forecasts from August through November 1997 for a forecast window centered on Bosnia. The real-time nephanalysis (RTNEPH) model was used to represent the true state of the atmosphere. ADVCLD and MM5 forecasts were also compared against a persistence forecast to provide a minimal skill baseline. The Air Force Weather Agency (AFWA) provided all model data.

The Kvamstø and Sundqvist schemes were used to transform the relative humidity forecasted at individual grid points by MM5 into a total FC forecast. Two other methods, the vertical column and layered methods, based on threshold techniques and devised by the author were used to transform the total cloud condensate forecasted by MM5 into a total FC forecast.

The results indicate that ADVCLD produced the better total FC forecasts for the first 33 hours of the 36-hr forecast period despite having a tendency to produce too much cloudiness. Overall, the MM5 displayed a significant negative bias in both the relative humidity and total cloud condensate fields. The MM5 was found to significantly underforecast cloud cover over the Adriatic Sea and slightly overforecast cloudiness over mountainous regions. ADVCLD demonstrated skill against persistence throughout the forecast cycle, however, MM5 demonstrated skill only after the 12-hr forecast point.

A COMPARISON OF ADVECT CLOUD MODEL AND FIFTH-GENERATION MESOSCALE MODEL TOTAL FRACTIONAL CLOUD FORECASTS

I. Introduction

1.1 Background

Total fractional cloud forecasts produced by a numerical weather prediction model represent the amount of cloud cover in an area centered on a model grid point, as depicted in Figure 1. The total fractional cloud forecast is made for each grid point in the model's domain and is usually expressed as a percent between 0 and 100. A fractional cloud forecast of 100 percent indicates that the entire area is covered with clouds, while a 25 percent fractional cloud forecast implies that only one quarter of the area is covered with clouds, however, the exact location of the clouds within the area is not specified. By adding "total" to the phrase "fractional cloud forecast", one is implying that the forecast is for the entire vertical column above a particular grid point without taking into consideration at what altitude the clouds are located.

Thus a total fractional cloud forecast is an estimate of the cloud cover a satellite sees as it looks toward the Earth. If in a particular vertical column no clouds are detected by the satellite, then the total fractional cloudiness for that column is zero. If, on the other hand, the satellite sees no part of the Earth in a particular vertical column because half of the column is totally obscured by clouds at 20,000 feet and the other half of the column is completely obscured by clouds at 5,000 feet, the total fractional cloudiness for that vertical column is 100 percent.

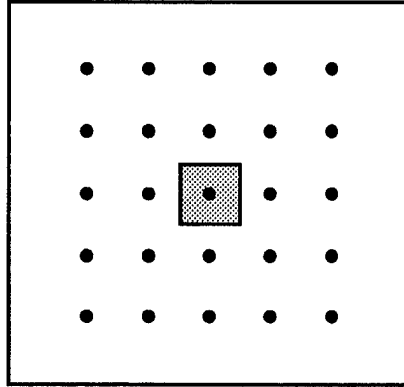


Figure 1. Representation of the area (shaded gray area) centered on a model grid point for which a total fractional cloudiness forecast is valid.

1.2 Importance of the Research

1.2.1 Military Impacts

Cloud cover has a tremendous impact on a wide range of military operations including aerial reconnaissance, air-to-ground weapons delivery, air refueling, airlift, airdrop, and air-to-air intercept. Advance knowledge of cloud locations and the amount of cloud coverage is vitally important to commanders tasked with planning a bomb strike or a pass over hostile territory to gather reconnaissance information. Literally millions of dollars can be saved if commanders are provided with accurate, dependable total fractional cloud forecasts. Accurate cloud forecasts give commanders the power to make the most efficient and effective possible use of the assets at their disposal.

The problem of producing accurate cloud forecasts is even older than numerical weather prediction, and the Air Force Weather Agency (AFWA) has been providing cloud forecasts in support of a wide variety of military operations for approximately 30 years.

During this period, a constant effort has been expended to improve cloud forecasts.

Unfortunately, moisture, which is essential for cloud formation, is generally recognized as one of the most difficult meteorological parameters to correctly forecast.

The inherent difficulty of cloud forecasting has led to a credibility problem that is familiar to all meteorologists who have ever issued a forecast. If the meteorologist issues a correct forecast but is not believed, the forecast is useless. Accurate information gets thrown away, and sometimes this means that missiles get thrown away, dropped harmlessly into the sea, instead of reaching their intended targets. In order to prevent this from happening, a method of cloud forecasting must be developed that produces a consistently accurate depiction of what actually occurs in the atmosphere. When this happens, commanders and decision makers will feel confident that they “own the weather” and will exploit it to their advantage.

1.2.2 Cloud Forecasting Approaches

Historically, there have been two methods used to forecast cloud cover, namely the diagnostic approach and the prognostic approach. The advect cloud (ADVCLD) model uses a diagnostic approach while the fifth-generation mesoscale model (MM5), on the other hand, uses a prognostic approach to forecast cloud condensate.

1.2.2.1 DIAGNOSTIC APPROACH

The diagnostic approach to cloud forecasting uses a set of governing equations which does not include equations for the conservation of condensed water (snow, ice, rain water, cloud water). Rather, other model variables, such as vertical velocity and relative humidity, are used in some manner to produce an estimate for the amount of cloud cover. This approach is not computationally expensive, however, it does ignore many of the

physical processes which lead to the production of condensed water. This is the old approach that was used extensively due to the lack of computing speed and available computer memory, the lack of good deterministic cloud models, and the difficulty in prescribing accurate initial conditions. ADVCLD uses the diagnostic approach to cloud forecasting.

1.2.2.2 PROGNOSTIC APPROACH

The prognostic approach, on the other hand, explicitly solves differential equations for the conservation of condensed water. This method is more computationally demanding and was not feasible before the advent of super-fast computers and expanded memory. Many more physical processes and dynamical effects are parameterized using this approach. This, in turn, should lead to a more accurate representation of the atmosphere. The MM5 uses the prognostic approach and explicitly forecasts for condensed water in the forms of snow, ice, rain water, and cloud water.

1.3. Statement of the Problem

Part of the process of producing an accurate cloud forecast is the decision of which forecast model to use as the basis for the cloud forecast. How does one make this choice? Obviously, the meteorologist wants to use the model which consistently outputs the most reliable cloud forecasts. The AFWA is currently running many numerical weather prediction models. Two of those which are used to make cloud cover forecasts are ADVCLD and MM5.

Which of these models does a better job of forecasting moisture in the atmosphere? Which of these models should the forecaster in the field use as a basis for cloudiness forecasts to commanders and operators? Does a crossover point exist in the

forecast period? That is, is there a point in time where, one model, initially performing poorly, begins to consistently outperform the other model? For example, does ADVCLD produce a better representation of the moisture found in the atmosphere for the first 12 hours of the forecast period with MM5 producing the better moisture forecasts after that point?

1.4 Benefit from Solving the Problem

While a forecast model's ability to forecast total fractional cloudiness well does not guarantee that it will be able to correctly forecast cloud layers, the opposite is true. That is, if the model cannot forecast total fractional cloudiness well, there is little chance that it will be able to forecast the cloud layers accurately. Thus knowledge of which model can be made to perform better at forecasting total fractional cloudiness gives a strong indication of which model should be used in making all cloud forecasts. Use of the correct forecast model at the correct time should in turn lead to more accurate and credible cloud forecasts, which is the ultimate goal.

1.5 Research Objective

This thesis compares the performance of total fractional cloudiness forecasts produced by ADVCLD and total fractional cloudiness forecasts produced from the relative humidity and total cloud condensate (snow, ice, rain water, and cloud water) fields outputted from the MM5. This was done qualitatively (through subjective analysis) and quantitatively (through statistical analysis) for the late summer and autumn period of 1997 for a forecast window that is centered on Bosnia. The real-time nephanalysis (RTNEPH), also produced by the AFWA, was used to represent the true state of the atmosphere against which ADVCLD and MM5 forecasts were compared.

1.6 Procedure

The MM5 being run at AFWA produces forecasts valid every 3 hours out to the 36-hour point and is run twice a day (usually with initial analyses valid for 00 UTC and 12 UTC). ADVCLD is run eight times a day and produces forecasts valid at 3 hour intervals out past the 36-hour point. The RTNEPH is produced every three hours. Thus the comparison was made at 3-hour intervals out to 36 hours.

ADVCLD produces total fractional cloudiness forecasts as output, however, MM5 does not. Therefore, two diagnostic methods were used to transform the relative humidity at individual grid points forecasted by MM5 into a total fractional cloudiness forecast, the Kvamstø method (Kvamstø 1991) and the Sundqvist method (Sundqvist 1989). These two methods will be discussed in more detail in chapter two.

Two other methods were used to transform the total cloud condensate (cloud water, rain water, snow, and ice) produced at individual grid points by MM5 into a total fractional cloudiness forecast. The first method summed the total cloud condensate in a vertical column at each grid point. The vertically summed cloud condensate value was then turned into a total fractional cloudiness forecast using an empirically derived threshold technique. The second method assigned various percentages of fractional cloudiness to each grid point at each model layer using a cloud condensate threshold technique and then summed the fractional cloudiness values. These two methods will be discussed in more detail in chapter two.

The ADVCLD and MM5 total fractional cloudiness forecasts were also compared against a forecast based on persistence to provide a minimal skill baseline. This was done by persisting the ADVCLD initial analysis throughout the 36-hour forecast period. The

choice of ADVCLD rather than RTNEPH to represent persistence will be discussed in chapter three.

Statistical measures of accuracy, bias, and skill were computed for ADVCLD, the two MM5 relative humidity schemes, the two MM5 cloud condensate schemes, and for persistence. Based on those statistics, the two forecast models were compared.

1.7 Thesis Organization

Chapter two provides a succinct synopsis of the information found in the literature which has a direct bearing on the problem. The RTNEPH, ADVCLD, and MM5 models will be briefly described. The four methods to produce a total fractional cloudiness forecast from MM5 output variables mentioned in section 1.6 will also be described in more detail.

Chapter three discusses the methodology employed to ensure a valid comparison was made. Quality control of the data will be addressed along with an overview of the data processing that was done. The statistical methods used to analyze and evaluate ADVCLD and MM5 along with the significance of each statistic are also described. The subjective analysis that was done will also be outlined.

Chapter four summarizes the results of the statistical and subjective analyses.

Chapter five, the last chapter, draws conclusions based on the data, and makes recommendations for future research and operational implementation.

II. Literature Review

2.1 RTNEPH

This section gives background information about the AFWA's RTNEPH model and outlines its strengths and weaknesses. The RTNEPH is used in this study to represent the true state of the atmosphere against which ADVCLD and MM5 total fractional cloudiness forecasts were compared.

2.1.1 RTNEPH Background

Six main programs make up the RTNEPH. They are the satellite data mapper, the surface temperature analysis and forecast model, the satellite data processor, the conventional data processor, the merge processor, and the bogus processor. The RTNEPH replaced the 3-Dimensional Nephanalysis (3DNEPH) model as AFWA's cloud analysis model in August, 1983, and its primary purpose is to initialize cloud forecast models, such as ADVCLD, that are run at the AFWA (Crum, 1987). It differs from its predecessor in that the RTNEPH can place clouds in one of four floating layers in the vertical instead of being restricted to one of 15 fixed layers employed by 3DNEPH. Like 3DNEPH, the RTNEPH merges visible and infrared satellite imagery and conventional data sources to create a coherent cloud database that is designed to maximize the probability of cloud detection (Hamill *et al.*, 1992).

The RTNEPH analysis is performed every three hours and produces as its output a time-flagged total fractional cloudiness amount which ranges between 0 and 100 percent. In addition, fractional cloudiness amounts are given for up to four floating layers (Kopp, 1997 personal communication). The RTNEPH also assigns a cloud type, a cloud base

height, and a cloud thickness to each of the four floating layers. Lastly, if a ceiling (defined as the lowest height above ground level at which 60 percent of the sky is covered with clouds) is determined to exist, the ceiling height is also reported.

The time of the observation is appended to the fractional cloudiness amount to aid in deciding which data should be persisted in the next RTNEPH analysis cycle. If newer information is available it is used, if not, the old fractional cloudiness amount gets persisted to the next RTNEPH analysis (Kiess and Cox, 1988). However, no RTNEPH persisted data points were used as verification points in this study. The choice of verification points, as well as the entire verification process, will be described in detail in chapter three.

The grid for the RTNEPH is overlayed on a polar-stereographic projection true at 60° latitude (Hamill *et al.*, 1992). The polar-stereographic projection is centered at the poles relative to the surface of the Earth. There are, in fact, two RTNEPH grids, one for each hemisphere. Each of these hemispheric grids is a subset of the AFWA whole-mesh reference grid which has a nominal horizontal resolution of 381 kilometers (true at 60°). The resolution increases toward the poles and decreases toward the equator due to the curvature of the Earth. The hemispheric grids, however, have a nominal horizontal resolution of 47.625 km (true at 60°), which is 8 times finer than the whole-mesh grid. Thus, these hemispheric grids are known as eighth-mesh grids (Hamill *et al.*, 1992). Table 1 summarizes the various grid mesh sizes used at the AFWA.

Each eighth-mesh grid is a 512 x 512 matrix and contains a total of 262,144 points (Kiess and Cox, 1988). Both hemispheric grids are further divided into two sets of 64 RTNEPH boxes with each box containing a 64 x 64 matrix. This gives a total of 4,096

points in each RTNEPH box. Figure 2 shows the 64 northern hemisphere boxes. The RTNEPH box that was used in this study is box number 30 in Figure 2.

Table 1. Resolutions of the various mesh sizes used at the AFWA.

Grid Size	Nominal Horizontal Resolution in km (true at 60° N)
Whole-Mesh	381
Half-Mesh	190.5
Quarter-Mesh	95.25
Eighth-Mesh	47.625
64 th -Mesh	5.953

As mentioned earlier, the vertical RTNEPH grid structure consists of up to four floating layers at each grid point. These layers can range from the surface to 21,900 m mean sea level (MSL), and they have a spatial resolution of 30 m below 6,000 m MSL, and 300 m above 6,000 m MSL (Kiess and Cox, 1988).

The RTNEPH ingests data from many sources including Defense Meteorological Satellite Program (DMSP) satellites, National Oceanic and Atmospheric Administration (NOAA) polar-orbiting satellites, conventional cloud observations, radiosondes, pilot reports (PIREPS), and surface analyses. Although it can ingest data from many sources, most of the data analyzed by the RTNEPH comes from DMSP satellites (Hamill *et al.*, 1992). As of December 1997, the RTNEPH did not have the capability of ingesting data from geostationary satellites.

In addition to automatically ingesting data from the above sources, a manual correction (bogus) is performed by forecasters at the AFWA to ensure that the RTNEPH analysis mirrors, to the greatest extent possible, the true state of the atmosphere. Inserting

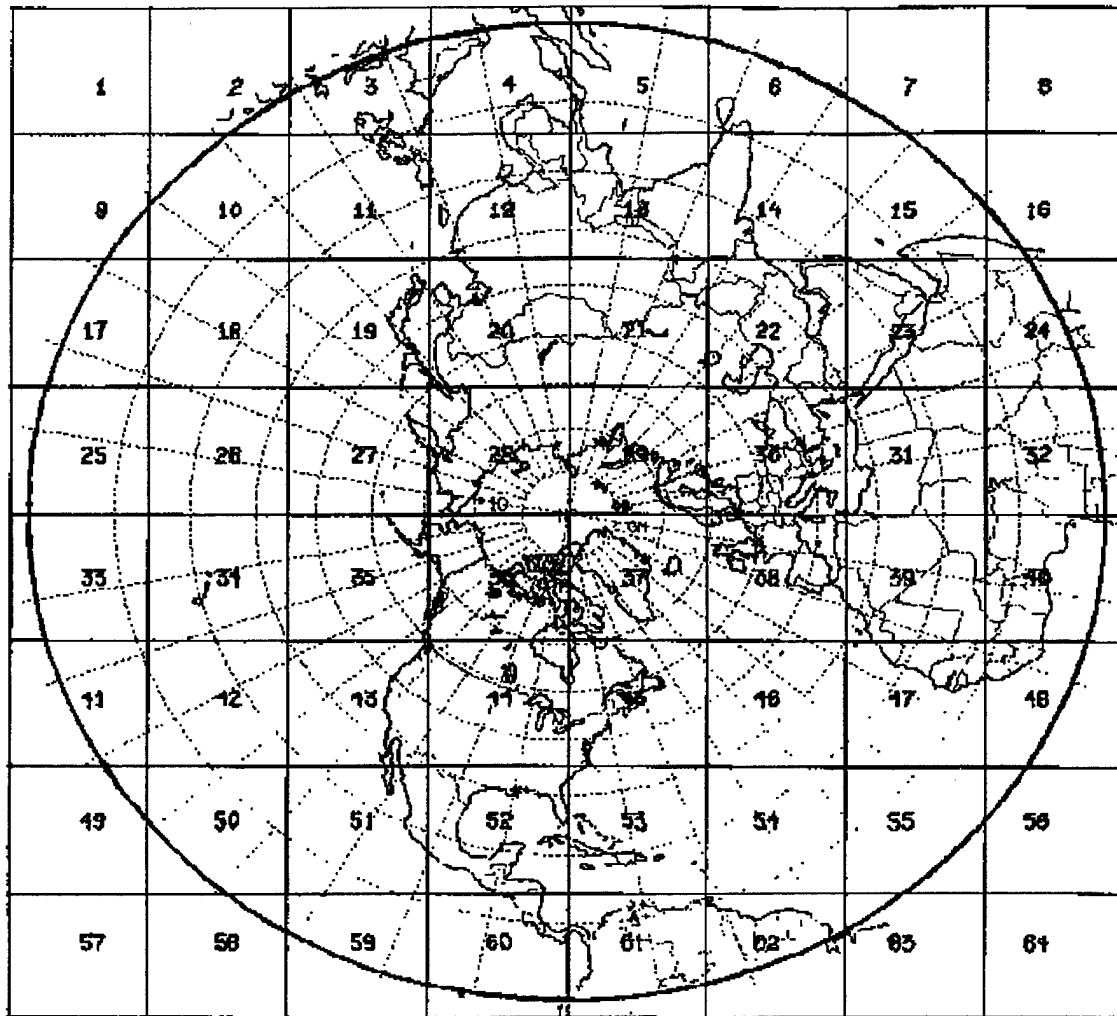


Figure 2. The 64 northern hemisphere RTNEPH grid boxes (Kiess and Cox, 1988).

all new cloud layers into the RTNEPH analysis is the primary purpose of bogusing (Kiess and Cox, 1988). All available information, including data from geostationary satellites, is used by the analysts to perform the bogus. Analysts look for areas on the initial RTNEPH analysis that differ from satellite imagery, surface observations, or other data with the same valid time as the RTNEPH analysis. The forecaster then corrects any discrepancies by either inserting data into the RTNEPH analysis or removing data from the RTNEPH analysis as appropriate. This corrected RTNEPH analysis is then processed further.

As mentioned above, the RTNEPH uses satellite data, both visible and infrared, as well as conventional data sources to produce its final analysis. The visible satellite data, infrared satellite data, and the conventional data get processed separately (Kiess and Cox, 1988). In order to produce a coherent final RTNEPH analysis, the infrared and visible satellite analyses must be merged with the conventional data analysis. This task is accomplished by the merge processor.

As the merge processor runs, it produces a final cloud analysis from the three data sources mentioned above and the persisted (previous) RTNEPH cloud analysis (Hamill *et al.*, 1992). For more detailed information on the merge processor, the reader is directed to AFGWC/TN-88/001. It is this final cloud analysis that is used to initialize other AFWA cloud forecast models.

2.1.2 RTNEPH Weaknesses

The RTNEPH has several known analysis deficiencies. The first is a tendency to underinterpret low clouds (Kiess and Cox, 1988). This occurs when infrared satellite data is the only available data source. The RTNEPH, which uses a global database of background surface temperatures, frequently cannot distinguish between the background surface temperature and the temperature of low clouds. Thus low clouds are missed, interpreted instead as the surface of the Earth.

Another known weakness has to do with how RTNEPH interprets coastline areas. Cloud cover near coastlines can be either over-forecasted or under-forecasted due to the difficulty in assigning a representative background temperature to grid points near coastal areas (Kiess and Cox, 1988). Sea-surface temperatures are almost always different than the land temperatures nearby, and this difference can lead to the misrepresentation of the

actual surface temperature and ultimately to the misrepresentation of the cloud cover in coastal areas. The third area in which the RTNEPH is somewhat deficient is its ability to detect small-scale clouds, such as fair weather cumulus. These clouds are underestimated on a routine basis (Kiess and Cox, 1988).

Another major error in the RTNEPH analysis is the tendency to overanalyze both clear and overcast conditions while underanalyzing partly cloudy conditions (Hamill *et al.*, 1992). The accuracy of layered cloud information is also suspect, especially when the RTNEPH detects a high-level obscuring cloud deck. Unless there are nearby surface observations, the RTNEPH has no way of detecting clouds that may be present at lower levels. Also, if there is an upper-level cloud deck, assigning an accurate cloud thickness is quite difficult.

The accuracy of the cloud height information in the RTNEPH has not been studied in great detail, however, it is widely believed that the RTNEPH underanalyzes thin clouds, especially cirrus, and places these thin clouds at elevations which are lower than where the clouds actually occur (Hamill *et al.*, 1992). Another major source of error is introduced when cloud heights are assigned according to cloud type by means of a default table. In this way, clouds are only allowed at certain predefined levels. This method is, in fact, the procedure most frequently used by the RTNEPH to assign cloud heights (Kiess and Cox, 1988).

The RTNEPH analysis also has problems in data sparse areas where much of the analysis is made up of conventional observations which get spread to surrounding grid points. Such data is known as spread data. As a result of this data spreading, the RTNEPH analysis in data sparse regions contains large blocks of identical data. Spread

data also makes up a small percentage of the RTNEPH analysis in data rich regions. In these data rich areas, the spread data often contrasts sharply with adjacent points which are based on satellite data (USAFETAC/UH-86/001 Rev).

The use of spread data leads to a somewhat unrealistic representation of the actual cloud cover but is sometimes unavoidable. This is especially true in regions of the Earth, such as near the equator, where the circumference of the Earth is larger. A greater percentage of areal coverage is achieved by a polar-orbiting satellite at 45° N, for example, than at the equator due to the fact that the distance between successive satellite passes is greatest at the equator.

Added to all of the above limitations is the fact that the RTNEPH currently uses data only from polar-orbiting satellites. There are not enough polar-orbiting satellites to provide continual satellite coverage for the whole Earth. Thus, large areas of the RTNEPH analysis cannot be updated every three hours with satellite data. This leads to large regions of RTNEPH points being persisted from one analysis to the next, and it compounds the problem of spread data because timely conventional observations are preferred over persisted data.

2.1.3 RTNEPH Strengths

Notwithstanding the numerous limitations just described, the RTNEPH analysis has many positive attributes. First, it is a global cloud analysis model. Second, it uses actual satellite data and surface cloud observations to create the cloud analysis. The inclusion of satellite data gives the RTNEPH cloud analysis a distinct advantage over cloud analyses that are generated without the benefit of satellite data. The fact that the

RTNEPH analysis is manually bogused also adds to the quality of the final product (Kopp, 1997 personal communication).

Another indication of the acceptance of the RTNEPH cloud analysis is the fact that scientists are willing to use it to represent the true state of the atmosphere. Phillips Laboratory performed a 30-month study (Nehrkorn *et al.*, 1994) evaluating numerical weather prediction models and cloud forecasts from the Advanced Physics Global Spectral Model. In their study, the RTNEPH cloud analysis was used as the ground truth against which the cloud forecasts were compared.

Actual surface observations of cloudiness were not verified against in this study because of the tendency of European observers to report CAVOK (ceiling and visibility OK) instead of reporting actual cloudiness and visibility observations. An observer in Europe is allowed to report CAVOK if there is no cloudiness below 5,000 ft and the visibility is at least 10 km. Thus, if the sky is overcast, for example, at 20,000 ft with unrestricted visibility, this can be reported as CAVOK. It would have been impossible to objectively verify total fractional cloudiness forecasts using CAVOK observations, so no surface observations were used in this study.

2.2 ADVCLD

This section gives background information about the AFWA's ADVCLD model. It also describes ADVCLD's moisture initialization and advection schemes. ADVCLD total fractional cloudiness forecasts were compared against MM5 total fractional cloudiness forecasts in this study.

2.2.1 ADVCLD Background

ADVCLD is a real-time, global cloud forecast model that is initialized using actual cloud amounts from the RTNEPH. ADVCLD produces its global fractional cloudiness forecasts at eighth-mesh resolution out to 12 hours, and at quarter-mesh resolution out to 48 hours (see Table 1). The model is run every three hours (8 times a day) and makes forecasts that are valid at three-hour intervals out to the 48-hour point (Cantrell, 1997 personal communication). In other words, every time a new RTNEPH analysis is created, a new ADVCLD forecast is made.

Each cloud forecast consists of fractional cloud forecasts at five different levels, as well as a total fractional cloudiness forecast at every grid point. The five levels are the gradient level, 850 mb, 700 mb, 500 mb, and 300 mb. ADVCLD does not, however, forecast cloud bases, cloud tops, or ceilings (Kopp, 1997 personal communication). ADVCLD took the place of the AFWA's older 5LAYER model and greatly improved the horizontal resolution of the cloud forecasts as the 5LAYER model was run on a half-mesh grid.

2.2.2 Moisture Initialization in ADVCLD

As mentioned above, the ADVCLD moisture field is initialized using data inputted from the RTNEPH for grid points at which the RTNEPH total fractional cloudiness is not equal to zero. At all such points, the first step in the initialization process is to populate the five ADVCLD layers with fractional cloudiness amounts derived from the floating RTNEPH layers that contain non-zero fractional cloudiness amounts.

To spread the clouds vertically, the top and base of each RTNEPH cloud layer are checked to determine which of the fixed ADVCLD layers they overlap. The RTNEPH layer fractional cloudiness amount is then inserted into the overlapped ADVCLD layers

provided that the receiving layers do not already have larger amounts in them. This process is repeated for every RTNEPH layer that contains a non-zero fractional cloudiness amount (Crum, 1987). The resultant layer fractional cloudiness amounts at each point are later quality controlled and, if necessary, adjusted so that the total fractional cloudiness amount at each point is within 2 percent of the RTNEPH total fractional cloudiness amount at the same point. The adjustment process will be described later in this section.

Before describing the adjustment process, the entire total fractional cloudiness computation process should be described. The total fractional cloudiness amount at a particular ADVCLD grid point for which the equivalent RTNEPH grid point contains a non-zero total fractional cloudiness amount is calculated from the statistical union of the layered cloud amounts, the maximum layer amount, and the average separation of the cloud layers (Crum, 1987).

An estimate of the correlation between the layers is calculated since layered cloud amounts may be separated by thousands of meters. The correlation between two layers is constrained to lie somewhere between zero and one. The assumption made in ADVCLD is that layers that are separated by the depth of the troposphere (assumed to be 11,000 m) are not correlated, and thus have a correlation equal to zero (Crum, 1987). Adjacent layers are assumed to be perfectly correlated and thus have a correlation equal to one. The correlation between other layers is given by the equation,

$$r = 1 - \frac{H_1 - H_2}{11000}, \quad (2.1)$$

where r is the correlation between two layers, H_1 is the height (in meters) of the upper layer, and H_2 is the height (in meters) of the lower layer. If there are more than two cloud

layers, the average of all possible pair-wise separations of the cloud layers is divided by 11,000. This value is then subtracted from one to determine the overall correlation, r_{tot} , that exists between all layers that contain non-zero fractional cloudiness amounts (Crum, 1987).

Once an overall correlation has been calculated, a three-step process is used to determine the total cloud amount at each grid point (Crum, 1987). First, the largest cloud amount in any one layer is determined. This value is the minimum possible total cloud amount. Next, the statistical union of the layer cloud amounts is calculated. This value is the maximum possible total cloud amount. Finally, the results from steps one and two are used, together with the correlation, to determine the total fractional cloudiness amount according to the equation,

$$FC_{tot} = FC_{min} + (FC_{max} - FC_{min}) * r_{tot}, \quad (2.2)$$

where FC_{tot} is the total fractional cloudiness amount, FC_{min} is the minimum possible total cloud amount from step one, FC_{max} is the maximum possible total cloud amount from step two, and r_{tot} is the overall correlation between cloudy model layers as determined above.

The total fractional cloudiness amount, FC_{tot} , is then used to adjust the ADVCLD layered fractional cloudiness amounts if necessary. In this process, FC_{tot} is checked against the RTNEPH total fractional cloudiness amount at that grid point. An adjustment factor, α , is calculated using,

$$\alpha = \frac{FC_{neph}}{FC_{tot}}, \quad (2.3)$$

where FC_{neph} is the RTNEPH total fractional cloudiness amount. If the adjustment factor is greater than 1.02 or less than 0.98, all of the ADVCLD layer amounts are multiplied by α to increase or decrease the layer totals, and then the whole adjustment process is repeated (Crum, 1987). The above procedure ensures that the ADVCLD total fractional cloudiness analysis field is consistent with the RTNEPH analysis.

Although ADVCLD initializes with fractional cloudiness amounts, it does not explicitly forecast fractional cloudiness. Rather, the initial total fractional cloudiness (FC) amounts at each of the five layers are transformed into condensation pressure spread (CPS) values which are then advected along with the forecast wind (Kopp, 1997 personal communication). CPS amounts are explicitly forecasted at each model time step, and then converted back into total FC values at 3-hour intervals. The advection procedure will be described in more detail later.

CPS is defined to be the difference (in millibars) between the pressure of an air parcel and the pressure at which condensation would take place if the that air parcel were to be lifted dry adiabatically. CPS is given by the equation,

$$CPS = p - p_s, \quad (2.4)$$

where p is the pressure of the air parcel and p_s is the saturation pressure (the pressure at the level where condensation first occurs).

Now that CPS has been defined, the relationship between FC and CPS used in ADVCLD becomes clearer. By examining equation 2.4, one would expect that small CPS values should lead to large FC amounts while large CPS values should lead to small FC amounts. That is, the smaller the vertical distance between a parcel and its lifting condensation level (LCL), the greater the cloud cover, and vice versa. Within ADVCLD,

CPS and FC are interchanged using the conversion tables that are found in Appendix A. These tables are based on empirical curves presented in 1965 by Edson (Crum, 1987).

A relationship also exists between CPS (in millibars) and dew point depression (in Kelvin). The mathematical expression of this relationship, as presented by Crum (1987), is given in Appendix B. Therefore, by using CPS as the intermediary, a link has been established between FC amounts and dew point depressions. This is a critically important connection due to the way in which ADVCLD initializes moisture at grid points for which there is no FC information available from the RTNEPH.

At grid points for which the corresponding RTNEPH total FC amount is zero or at least 3 hours old, another method is used to initialize the moisture. In such cases, CPS values are assigned by using the relationship between CPS and dew point depression described in Appendix B. The needed temperature, pressure, and moisture information is provided to ADVCLD by the Navy Operational Global Analysis and Prediction System (NOGAPS). This NOGAPS data has a resolution of $2.5^{\circ} \times 2.5^{\circ}$ (approximately 283 km) and must first be interpolated to the eighth mesh grid before it can be inputted into ADVCLD (Kopp, 1997 personal communication).

There are definite advantages to using CPS as the moisture parameter. First, it provides the link between FC and dew point depression. Second, and more importantly, CPS links changes in cloud amount to vertical motion (Crum, 1987). For example, consider an initially unsaturated air parcel which is lifted dry adiabatically. As it rises, it cools, the dew point depression narrows, the vertical distance (CPS) between the parcel and its LCL shrinks, and the FC amount increases. For descending motion, the situation is reversed. CPS (in millibars) offers a way of directly modifying cloud amounts by using the

net vertical displacement (in millibars) experienced by a parcel of air along its trajectory during the forecast period.

2.2.3 *Advection in ADVCLD*

In order to compute trajectories for each of the grid points, it is necessary to have initial and predicted values for the three-dimensional wind field. The wind data, too, is inputted from NOGAPS. The NOGAPS wind forecasts are used to calculate an "upstream" trajectory from the terminal point (the 48-hour forecast point) back in time at 3-hour intervals until the initial point of origin (the analysis point) is determined (Crum, 1987).

The points of origin, however, rarely coincide with ADVCLD grid points, and so it is necessary to interpolate the CPS values at nearby ADVCLD grid points to the origin points. The interpolation is accomplished by combining a two-point interpolation scheme and an eight-point interpolation scheme (Crum, 1987). More information about the specifics of the ADVCLD interpolation technique can be found in AFGWC/TN-87/001. It is from these interpolated points of origin that the CPS amounts get advected and modified as they follow their individual trajectories. Parcel trajectories are calculated from every terminal grid point at each vertical level in ADVCLD.

As a parcel of air follows its trajectory, its CPS value is modified by upward and downward displacements. The effect of vertical motion on the CPS value is given by

$$CPS_f = CPS_i + \Delta p, \quad (2.5)$$

where CPS_f is the CPS value at the final time step, CPS_i is the CPS value at the initial time step, and Δp is the vertical trajectory component in pressure units. In ADVCLD, vertical motion has the greatest modifying effect on the initial CPS values. However, it is

not the only means by which the initial CPS amounts can be modified. ADVCLD also contains parameterizations for entrainment, diurnal effects, and the evaporation of precipitation, all of which act to modify existing CPS values. For a more detailed discussion of these parameterizations the reader is directed to AFGWC/TN-87/001.

Obviously, the quality of the final cloud forecast using this method is heavily dependent upon the accuracy of the wind data that is input. Small errors in the initial winds field can cause ADVCLD to have significant phase errors by the 48-hour point. However, the fact that ADVCLD is initialized with actual cloud information permits it to avoid the moisture "spin-up" problem that is common in numerical weather prediction models (Kopp, 1997 personal communication).

2.3 MM5

This section gives a brief background of the MM5 and describes the general characteristics of the model, with special emphasis on how it handles moisture.

2.3.1 MM5 Background

The MM5, as its name implies, is a mesoscale model which was developed by the Pennsylvania State University (PSU) in conjunction with the National Center for Atmospheric Research (NCAR). Initial work on this model began in 1971 at PSU. Constant effort has been expended at PSU and NCAR to improve the model, and the one currently in use is the fifth-generation (fifth-version), hence the name MM5. The AFWA began running its version of MM5 in early 1997. The MM5, as run at the AFWA, is discussed in the following sections.

2.3.2 MM5 Characteristics

The MM5 used in this study generates forecasts valid at 3-hour intervals out to the 36-hour point twice per day (usually with initial analyses valid at 00 UTC and 12 UTC) for a window centered over the Bosnia region in Europe. The European window was selected because of the importance of the Bosnia region to recent Air Force operations. It was also, however, the only one available at the commencement of the research. As of December 1997, though, the AFWA was producing MM5 forecasts for windows over the United States and Asia as well.

The area covered by the Bosnia grid used in this study is depicted in Figure 3. It includes a grid composed of 101 x 101 (10,201) grid points with a 10.2 km horizontal resolution in the center of the grid. The MM5 used the 1° x 1° resolution aviation model (AVN) for initial conditions and boundary conditions, when it was available to the AFWA. When the AVN was not available, the 2.5° x 2.5° resolution NOGAPS data was used for the initial conditions and boundary conditions (Spero, 1997 personal communication). Appendix C gives a list of the dates and times of the MM5 analyses used in this study together with the model (AVN or NOGAPS) that was used to initialize them.

The boundary conditions were forced at 3-hour intervals using the nudging technique in conjunction with the sponge technique (Grell *et al.*, 1995). An upper radiative boundary condition was also incorporated at each model time step. This boundary condition allows wave energy to pass through the top unreflected. For a more detailed explanation of the boundary conditions used in the MM5, the reader is directed to NCAR/TN-398+STR.

The MM5 produces forecasts on 26 different “full” sigma levels for vertical velocity, and produces forecasts on 25 “half” sigma levels for horizontal wind

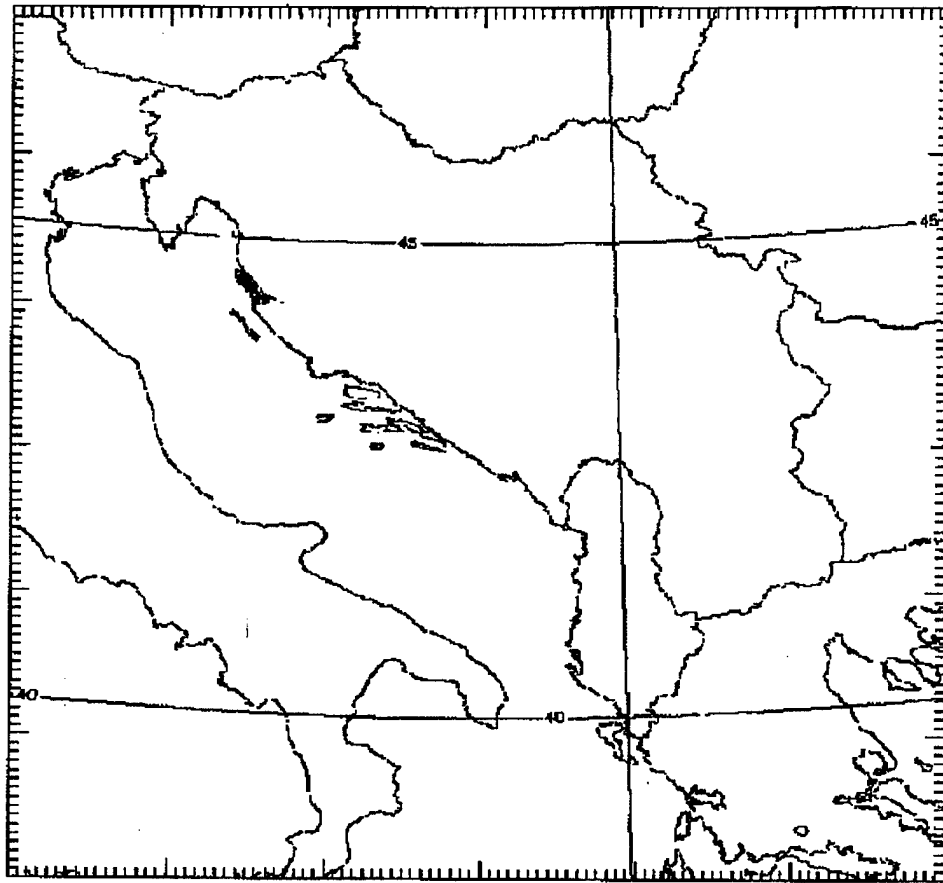


Figure 3. Geographical region covered by the Bosnia grid.

components, temperature, specific humidity, cloud water, cloud ice, snow, rain water, and other prognostic variables (Spero, 1997 personal communication). The full sigma levels and half sigma levels are tabulated in Appendix D. These sigma-level forecasts are then post-processed to generate forecasts of temperature, relative humidity, vertical velocity, wind speed and direction, and total cloud condensate (cloud water, cloud ice, snow, rain water), as well as other weather parameters, on various pressure levels (Spero, 1997 personal communication). The pressure levels used in the MM5 are found in Appendix E. The data used to conduct this research was pressure-level data.

The MM5 uses a method developed by Blackadar to parameterize the planetary boundary layer (PBL). The atmospheric radiation option in the MM5 provides two schemes, a long-wave (infrared) scheme and a short-wave (visible) scheme, that interact with the atmosphere, cloud and precipitation fields, and with the surface (Grell *et al.*, 1995). This method was developed by Dudhia. For more information on the Blackadar and Dudhia schemes, the reader is directed to NCAR/TN-398+STR.

2.3.3 Moisture in the MM5

As mentioned in the introduction, the MM5 uses a prognostic approach to cloud forecasting in that it explicitly forecasts cloud water, cloud ice, snow, and rain water (total cloud condensate). However, although relative humidity is initialized using NOGAPS data, the total cloud condensate is initialized to zero (Spero, 1997 personal communication). Thus forecasts of total water condensate have a "spin-up" problem. That is, considering that the time step of the model is only 30 seconds, several hundred model integrations are needed before the forecasted values for total cloud condensate become realistic.

Precipitation processes are parameterized in the MM5, with Marshall-Palmer size distributions assumed for rain and snow (Grell *et al.*, 1995). The MM5 also includes a mixed-phase ice scheme in which supercooled water can exist below 0° C, and snow can exist above 0° C. Again a complete description of the above can be found in NCAR/TN-398+STR.

The MM5, as implemented at the AFWA, uses the Grell scheme to parameterize convection. In this parameterization, clouds are thought of as two steady-state circulations which are caused by an updraft and a downdraft. No direct mixing occurs

between the cloud and the rest of the environment except at the top and the bottom of the circulations (Grell *et al.*, 1995). There is no entrainment or detrainment along the cloud edges; these occur only at the top and bottom of the clouds. Mass flux is assumed to be constant with height, and maximum buoyancy is allowed for in the updraft and in the downdraft. This type of convection is called deep convection, as it can extend throughout the troposphere. In using this method, the cloud base is not restricted to the boundary layer. Clouds bases can be at any level in the troposphere. This is the type of convection that produces precipitation.

In addition to parameterizing deep convection, the MM5 also simulates shallow convection. The shallow convection scheme serves two primary tasks. First, it parameterizes PBL forced non-precipitating convection, and, second, it accounts for mid-tropospheric shallow convection caused by other sub-grid scale effects such as the radiational cooling of cloud tops (Grell *et al.*, 1995). This is done by simulating bubbles which are forced by surface heating and moisture fluxes. In this case, strong lateral mixing is permitted. These bubbles rise (usually no more than 75 mb) and lose their buoyancy (Grell *et al.*, 1995). The clouds produced using this shallow convection scheme are generally non-precipitating and contain no convective scale downdrafts. The interested reader is directed to NCAR/TN-398+STR for a complete discussion of the convective schemes used in the MM5.

2.4 Total Fractional Cloudiness Forecasts from MM5 Output Variables

Although the MM5 contains parameterizations for many complex physical processes, it does not explicitly output total fractional cloudiness forecasts. Thus, in order to make a comparison against ADVCLD, a method (or methods) was needed to convert

MM5 output variables, such as relative humidity (RH) or total cloud condensate, into total FC forecasts. This section describes two RH schemes found in the literature, as well as two total cloud condensate schemes devised by the author, that were used in this study to make that conversion.

2.4.1 RH Schemes

Mocko and Cotton (1995) date the implementation of fractional cloudiness parameterizations in computer models back to Sommeria and Deardorff and Manton and Cotton in 1977. In Mocko and Cotton's article (1995), they evaluated several fractional cloudiness schemes using the Regional Atmospheric Modeling System (RAMS) compared against satellite imagery and aircraft measurements of fractional cloudiness. Their study was conducted on 7 July 1987 off the coast of California and was primarily focused on cloudiness in the boundary layer. They found that two of the methods which used only relative humidity to predict cloudiness, the Sundqvist and Kvamstø methods, outperformed all of the others. These two schemes, which are described in detail below, depended upon the concept of a critical relative humidity (the relative humidity at which condensation is allowed to take place).

Another study that used the critical relative humidity concept was done by PSU and NCAR in November through December of 1991. MM5 predictions of cloud occurrence and vertical location were statistically compared and validated against data obtained from the PSU 94-GHz cloud radar (Seaman *et al.*, 1995). This study was conducted in Kansas as part of the Second International Satellite Cloud Climatology Project Regional Experiment campaign.

As mentioned above, MM5 cloud forecasts were made based on the critical relative humidity concept. It was discovered that for the 12 km resolution model forecasts, the critical relative humidities in the low, middle, and high layers of the atmosphere were, respectively, 89 percent, 72 percent, and 65 percent (Seaman *et al.*, 1995).

2.4.1.1 SUNDQVIST METHOD

Sundqvist *et al.* (1989) used a diagnostic method based solely on the relative humidity found in the grid volume. Their fractional cloudiness equation was:

$$FC = 1 - \sqrt{\frac{RH_s - RH}{RH_s - RH_{cc}}}, \quad (2.6)$$

where $RH_s = 1.0$ is the saturated value of relative humidity, RH is the actual relative humidity, and RH_{cc} is a threshold value when condensation is allowed to take place (i.e. the critical relative humidity).

This scheme was used in conjunction with a modified version of the operational fine mesh model of the Norwegian Meteorological Institute (DNMI) that already parameterized convective condensation and stratiform condensation and produced cloud water as a prognostic variable. In this sense then, this mesoscale model is similar to MM5.

Using equation 2.6, a FC value was calculated for every grid point at each vertical level in the model. However, no condensation was allowed to take place in the well-mixed boundary layer. The grid points in a vertical column were then summed to produce a total fractional cloudiness forecast according to the equation

$$FC_{tot} = 1 - \prod_{j=2}^k \frac{1 - \max(FC_{j-1}, FC_j)}{1 - FC_{j-1}}, \quad (2.7)$$

where FC_{tot} is the resulting fractional cloud cover from layers 1 through k and FC_j is the fractional cloudiness amount at level j computed using equation 2.6. In a vertical column with monotonically increasing or decreasing cloud cover with height, FC_{tot} is equal to the maximum FC_j (this is maximum overlapping). When the cloud cover does not increase or decrease monotonically, equation 2.7 represents random overlapping, and FC_{tot} is larger than the largest FC_j (Sundqvist, 1989).

2.4.1.2 KVAMSTØ METHOD

Kvamstø (1991) also suggested a diagnostic method based solely on relative humidity. The fractional cloudiness equation used was:

$$FC = \left(\frac{FC_{\max} - FC_{\min}}{RH_c - RH_{cc}} \right) (RH - RH_{cc}), \quad (2.8)$$

where $FC_{\max} = 1.0$, $FC_{\min} = 0.0$, and the other parameters are the same as for the Sundqvist method. Equation 2.8 was used to calculate the FC amount for every grid point at each vertical level. Equation 2.7 was then used to sum the individual layer values and arrive at the final total fractional cloudiness amount.

Kvamstø was primarily interested in stratiform cloudiness in his study. He, too, used mesoscale model data from the DNMI which had a horizontal resolution of 50 km. Kvamstø found a pronounced correlation between fractional stratiform cloud cover and relative humidity (Kvamstø, 1991). Above the boundary layer and below 238 K, both Kvamstø and Sundqvist used values for RH_{cc} of 0.75 over land and 0.85 over water. As

mentioned previously, no condensation was allowed in the well-mixed boundary layer, while above 238 K, RH_{cc} increased asymptotically to a value near 1.00.

2.4.2 Total Cloud Condensate Schemes

In addition to the two relative humidity methods described in the previous section, FC was predicted using two schemes involving the total cloud condensate explicitly forecasted by MM5 at every grid point. The two cloud condensate schemes, which will be described in detail in the next chapter, will be referred to as the vertical column method and the layered method.

The total condensed water content in actual clouds varies according to temperature. For two clouds with different cloud-base temperatures, the cloud with the warmer base has a greater probability for producing a significant amount of condensed liquid-water. The total ice-water content (IWC) in clouds also shows a strong dependence on temperature, with larger values of IWC associated with higher temperatures (Cotton and Anthes, 1989). This dependence of water content on temperature was incorporated into the layered method.

This concludes the literature review. More information about the two cloud condensate methods and the specific implementation of the two RH schemes is presented in the next chapter.

III. Methodology

3.1 Introduction

This chapter describes the specific implementation of the four schemes used to convert MM5 variables in total FC amounts as well as the steps taken to quality control the data. The statistical and subjective analyses used in this study are also described.

3.2 Scope

This study compares total fractional cloudiness forecasts made by ADVCLD and MM5 at 3-hourly intervals out to the 36-hour point over a region centered on Bosnia. RTNEPH analyses were used to represent the true state of the atmosphere against which ADVCLD and MM5 forecasts were compared. Four separate MM5 total FC forecasts, one forecast for each method used to convert MM5 variables to total FC amounts, were compared against the ADVCLD total FC forecast. Selected days from the months of August, September, October, and November, 1997, were used to conduct the study. The validation days and times were chosen based on the availability of the three models needed to make the comparison.

3.3 Procedure

3.3.1 RTNEPH and ADVCLD Data

Output from the RTNEPH and ADVCLD models was provided by the AFWA. The data, produced at eighth-mesh and quarter-mesh resolution, was interpolated to the 101 x 101 MM5 grid using the nearest-neighbor technique. That is, the FC amount at each of the points in the 101 x 101 grid was assigned to be the total FC value of the

nearest RTNEPH (ADVCLD) eighth-mesh (eighth-mesh or quarter-mesh) point. The interpolation was accomplished at the AFWA.

As mentioned earlier, the RTNEPH analyses contain persisted FC data, however, at all grid points with data more than 2 hours old, the total FC values were replaced with a value of 99999. This, too, was accomplished at the AFWA. RTNEPH fractional cloudiness amounts were provided in increments of 5 percent (i.e. values ranged between 0 and 100 in increments of 5), while ADVCLD FC amounts were provided in 1 percent intervals. Total fractional cloudiness amounts were supplied for each model, thus no further manipulation of the data outputted from these two models was required.

3.3.2 MM5 Data

Output from the MM5 model was also provided by the AFWA. Three output variables, relative humidity, total cloud condensate, and vertical velocity, were supplied at 21 post-processed pressure levels (Appendix E). The values of relative humidity ranged between 0 and 1, while the total cloud condensate was given in units of kilograms of condensate per kilogram of dry air (kgkg^{-1}). Vertical velocity was not used in this study.

3.3.3 Implementation of FC Schemes from MM5 Variables

Sixteen vertical layers were used in transforming relative humidity and total cloud condensate values to total fractional cloudiness forecasts using the two schemes described in section 2.4. These were MM5 pressure levels 04-19 listed in Appendix E. Levels 01 and 02 (1100 mb and 1050 mb) were excluded for the obvious reason that they are underground. Level 03 (1000mb) was not considered in keeping with Sundqvist's idea to disallow condensation in the well-mixed boundary layer. Levels 20 and 21 (150 mb and

100 mb) were excluded due to the lack of observed cirrus at these levels (this is similar to the condition imposed above 238 K in the RH schemes mentioned in section 2.4.1.2).

These sixteen vertical layers were further divided into low, middle, and high cloud regions. The low cloud region included layers between 950 mb and 750 mb. The middle cloud region contained layers between 700 mb and 400 mb, while the high cloud region consisted of layers between 350 mb and 200 mb. The division into low, middle, and high regions was done to allow for the dependence of both the critical relative humidity (Seaman *et al.*, 1995) and the liquid and ice-water contents (Cotton and Anthes, 1989) on temperature.

3.3.3.1 RH SCHEMES

The Kvamstø and Sundqvist schemes were implemented as described in section 2.4.1 using critical relative humidities of 0.70, 0.65, and 0.60 for the low, middle, and high cloud regions respectively. Trials done with the critical relative humidities of 0.89, 0.72, and 0.65 used in the PSU/NCAR study (Seaman *et al.*, 1995) and the constant critical RH of 0.75 used by Kvamstø (1991) and Sundqvist (1989) in their studies were also performed. Those critical RH values, however, produced FC forecasts that had a significant negative bias. That is, they did not produce enough cloudiness.

3.3.3.2 VERTICAL COLUMN METHOD

In the first of the total cloud condensate schemes, referred to as the vertical column method, the total cloud condensate was simply summed in a vertical column above a particular grid point. That is

$$VCC = \sum_k TCC_k, \quad (3.1)$$

where VCC is the total cloud condensate in a vertical column above a grid point and TCC_k is the total cloud condensate at each vertical model level, k .

This method made no attempt to diagnose FC at each individual level, but rather sought to relate VCC to the total fractional cloudiness at each grid point, as prescribed by the RTNEPH. This was done by using various thresholds of VCC to correspond to FC amounts between 0% and 100%. These thresholds, which were determined empirically using data from the month of August, are found in Appendix F.

3.3.3.3 LAYERED METHOD

The second total cloud condensate method used in this study was the layered method. In this scheme, fractional cloudiness amounts were established at every grid point for each vertical model level. This was done, again, by using thresholds of total cloud condensate to diagnose FC values. Different thresholds were used depending on the vertical model level under consideration. Three sets of threshold values were used. They were for low-level clouds (950 mb - 750 mb), mid-level clouds (700 mb - 400 mb), and high-level clouds (350 mb - 200 mb).

The division into three sets was done to simulate the dependence of cloud water content on temperature. By using three sets of threshold values, a given total cloud condensate value is converted to a higher fractional cloudiness amount at 250 mb than it is at 700 mb or 925 mb. This is in accordance with the findings presented in Cotton and Anthes (1989). These three sets of thresholds, which were determined empirically using data from the month of August, are listed in Appendix G.

After fractional cloudiness amounts were assigned to every grid point at each vertical model level, the layered FC values were then summed according to equation 2.7.

The resultant value was the final total fractional cloudiness forecast produced by the layered method.

3.3.4 Data Processing

All of the processing done on the data from the RTNEPH, ADVCLD, and MM5 models as well as some of the statistical computation (described in later in this chapter) was done using FORTRAN programs written by the author. These programs were written in standard FORTRAN 77.

First, the total FC forecasts from the ADVCLD model and the total FC amounts from the RTNEPH analysis were read into 101 x 101 arrays. Then the 16 layers of MM5 relative humidity and total cloud condensate values were read into 101 x 101 arrays. The valid time for all three models was the same (i.e. a 3-hour total FC forecast valid at 15 UTC on 26 August 1997 from the 12 UTC ADVCLD forecast cycle was compared against a 3-hour total FC forecast valid at 15 UTC on 26 August 1997 from the 12 UTC MM5 forecast cycle using the RTNEPH total FC analysis valid at 15 UTC on 26 August 1997). Before running the program, a check (performed manually by the author for every 3-hour forecast valid time) was done to ensure that all three models used in the comparison had the same valid time. If data was not available from any one of the three models, no comparison was made.

The next step in the algorithm was to calculate the total FC amounts at all 10,201 grid points for the Kvamstø, Sundqvist, vertical column, and layered methods as presented in the preceding sections. A total fractional cloudiness amount was also calculated for the persistence method. This was done by using the ADVCLD analysis total FC values and persisting them into the future. For example, the forecast used as the persistence 9-hour

total FC forecast valid at 21 UTC on 26 August 1997 was the ADVCLD analysis valid at 12 UTC on 26 August 1997.

The ADVCLD model was chosen to be persisted due to the fact that the RTNEPH analyses always contained some grid points (with assigned total FC values of 99999) that were more than two hours old; moreover, the grid points at which there were total FC amounts of 99999 were not the same for all RTNEPH analyses. Total FC values at these grid points were not used to make the statistical comparisons. Since the ADVCLD model uses the RTNEPH analysis, where possible, to initialize its total FC amounts and uses CPS at points where the RTNEPH data is missing, the ADVCLD always has valid total FC amounts to persist (instead of 99999) at each of the 10,201 grid points. For this reason, the ADVCLD analysis field was persisted.

Once this was done, the FC values from the ADVCLD model, the Kvamstø method, the Sundqvist method, and persistence were rounded to the nearest 5 percent (i.e. 7 percent was rounded to 5 percent while 8 percent was rounded to 10 percent) since the RTNEPH data was given in 5 percent intervals. Thresholds for the vertical column method and the layered method were specified solely at 5 percent intervals (see Appendices D and E).

A check was then made to determine which RTNEPH points contained values of 99999, and a count was kept of the number of timely RTNEPH points. Only the grid points with RTNEPH total FC amounts other than 99999 were used throughout the remainder of the program. At this point, the statistics described in section 3.5 were computed.

3.4 Quality Control of the Data

Before discussing the statistical methods employed to make the comparison between ADVCLD total FC forecasts and MM5 total FC forecasts, the steps taken to quality control (QC) the data will be described.

3.4.1 Objective Quality Control

In order to ensure that a valid statistical comparison was ultimately performed, the values read into the FORTRAN program from the three models were compared against the data files sent by the AFWA which contained the original values. This was done to ensure that the data values were read in correctly. Each time an equation was programmed, the result of the program's calculation was checked against a calculation done by hand to make sure that the program was indeed calculating the intended quantity.

3.4.2 Subjective Quality Control

In addition to the objective quality control, a subjective quality control was also performed. As part of the subjective QC, the RTNEPH analyses as well as the ADVCLD, and MM5 total FC forecasts were compared against satellite imagery. This was done to determine if the rows and columns of data were read into the program in the correct positions. By comparing against the satellite imagery, it was also possible to verify that the dates and times that corresponded to each data file were correct. In addition, it provided a check as to how well the RTNEPH analysis actually represented reality. The visualizations necessary to perform this subjective check were created using the Grid Analysis and Display System (GrADS®) version 1.6.

To illustrate the subjective analysis that was done, consider figures 4 and 5. Figure 4 is an infrared satellite image for 12 UTC on 8 October 1997, taken by the Meteosat 5

satellite. Figure 5, which was created using GrADS[®], is a representation of the 0-hour (analysis) ADVCLD total fractional cloudiness amounts for the same date and time.

In comparing Figures 4 and 5 it is necessary to understand that in Figure 4 the whitest pixels represent the highest cloud tops. In Figure 5, however, the whitest pixels represent the greatest fractional cloudiness amounts (i.e. white in Figure 5 signifies a FC amount of 100 percent). Keeping these differences in mind, one notes that the ADVCLD analysis, and thus the RTNEPH analysis from which it was derived, is quite accurate in its representation of the cloudiness found in the atmosphere. Obviously, the rows and columns of data were read in correctly.

ADVCLD does an excellent job with the frontal cloudiness that extends from just north of Rome to the north and east into Croatia and Slovenia. It also detected the overcast conditions that were present over the boot of Italy as well as the area of clear skies extending from Serbia east into Bulgaria. An area that, at first glance, appears to be a discrepancy between ADVCLD and the satellite is the area around Aviano in northeastern Italy. This apparent difference, however, can be explained by closely examining the satellite image. Low clouds, which appear darker than high clouds, are evident in this area, and they cover a large percentage of northeastern Italy. Figures 4 and 5 seem different around Aviano due to the differences, described in the preceding paragraph, in interpreting the images.

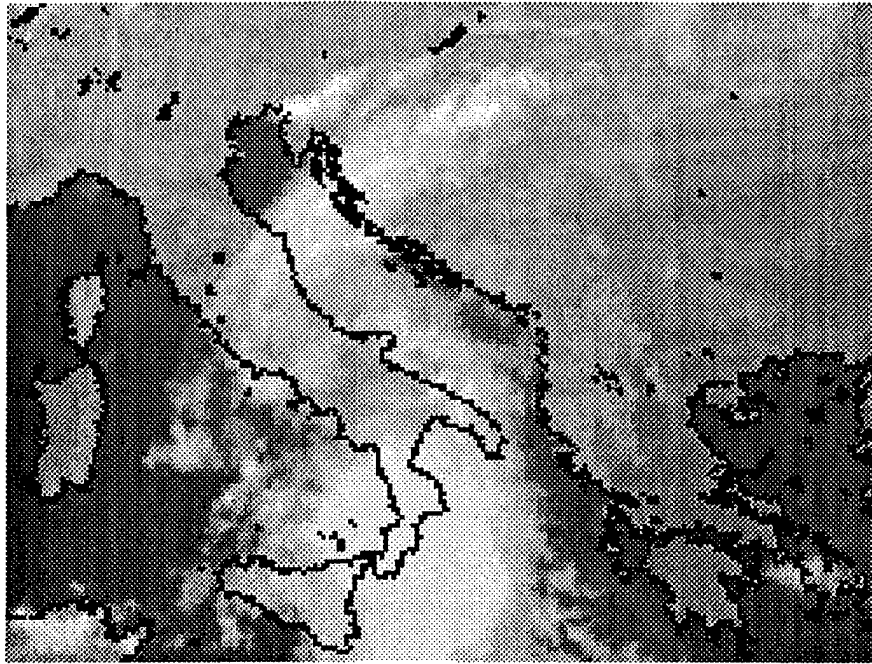


Figure 4. Infrared satellite image for 12 UTC on 8 October 1997.

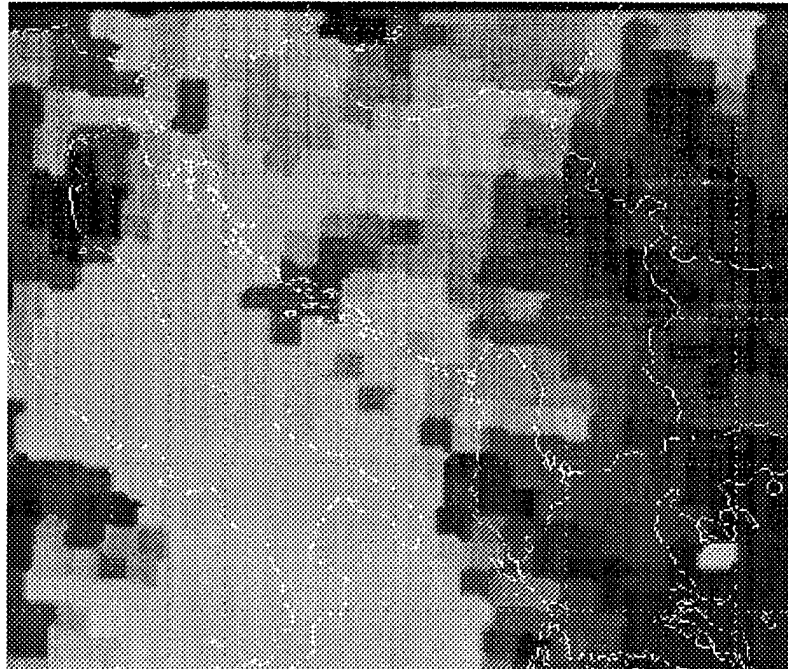


Figure 5. ADVCLD FC analysis for 12 UTC on 8 October 1997. Black corresponds to total FC amounts of zero percent and white corresponds to 100 percent.

By studying the visualizations of the RTNEPH analyses and the ADVCLD 0-hour analyses, which should have been identical at grid points where the RTNEPH total FC amounts were not zero or missing (Wonsick, 1997 personal communication), a gridding mismatch was detected. This mismatch, which was verified by inspection of the data, was traced back to the original eighth-mesh/quarter-mesh ADVCLD hemispheric grid area that was selected at the AFWA for interpolation to the MM5 grid. The area chosen for interpolation was the correct size but was slightly to the west and south of the actual MM5 grid area. This area was, nonetheless, interpolated to the MM5 grid. The result of the interpolation was an ADVCLD total FC field that was shifted two grid points up (north) and two grid points to the right (east) of the RTNEPH total FC analysis.

To correct this gridding mismatch, the ADVCLD total FC amounts were shifted two grid points down (south) and two grid points right (west) in the FORTRAN program that read in the model data. As a result of this programmed correction, the RTNEPH analysis and the ADVCLD 0-hour analysis were once again in good agreement, however, the values at the grid points in the northernmost (top) two rows and the easternmost (right) two columns were no longer valid total FC amounts. Thus, instead of using the entire 101 x 101 grid to make the statistical comparisons, a 99 x 99 grid (9,801 points) of total FC values was used. Figure 5 is an example of a corrected ADVCLD total FC analysis field.

3.5 Statistical Analysis

After the total fractional cloudiness values for each method were calculated and the quality control was completed, the next step was to perform the statistical analyses needed to compare the various methods. This section describes the specific statistics

used to make the determination of which model better forecasted total FC amounts. All statistics were calculated for ADVCLD, the Kvamstø scheme, the Sundqvist scheme, the vertical column method, the layered method, and for persistence.

In order to make the statistical comparisons, it was necessary to construct arrays of frequency counts for each of the six fractional cloudiness forecasts. These arrays accounted for every value of cloud increment forecasted or observed by RTNEPH, from 0 to 100 percent in 5 percent increments, since the RTNEPH data was only supplied in 5 percent intervals. Thus each array had 21 rows and 21 columns.

An example of one of these arrays is shown in Figure 6 for illustration purposes only. The columns of Figure 6 represent the RTNEPH total FC values, while the rows represent the ADVCLD total FC values. Figure 6, however, is binned to 10 percent

RTNEPH Observed Total FC %											
		0-10	11-20	21-30	31-40	41-50	51-60	61-70	71-80	81-90	91-100
A											
D											
V	0-10	520	15	25	10	12	19	22	25	17	39
C	11-20	15	22	12	23	34	11	9	14	11	20
L	21-30	21	33	89	40	45	15	10	27	8	28
D	31-40	11	14	29	25	47	9	7	18	6	16
	41-50	42	16	23	31	22	20	19	13	4	19
F	51-60	33	3	46	17	57	31	43	21	5	32
C	61-70	12	9	32	8	31	13	39	35	10	37
S	71-80	19	4	20	6	19	30	47	46	16	58
T	81-90	12	2	28	11	29	14	16	70	15	69
	91-100	21	7	15	13	45	11	19	55	23	99
%											

Figure 6. An example of a frequency count array used to perform the statistical analysis. The original array was 21 x 21, binned to a 10 x 10 array for display. The columns represent RTNEPH total FC values, while the rows represent ADVCLD total FC values.

increments (instead of the 5 percent increments actually used) for display purposes. The statistics in this study were computed using the full 21 x 21 arrays.

3.5.1 Scalar Measures of Forecast Accuracy

Three scalar measures of forecast accuracy were calculated: the mean error (ME), the mean absolute error (MAE), and the root-mean-square error (RMSE). The mean error was calculated in order to determine the bias of the model's forecasts. The formula used to calculate mean error is

$$ME = 5 \cdot \left[\frac{\sum_{i=0}^{20} \sum_{j=0}^{20} ARRAY_{i,j} \cdot (i - j)}{CNT} \right], \quad (3.2)$$

where i represents the rows, j represents the columns, $ARRAY_{i,j}$ is the count in the i^{th} row and the j^{th} column of the 21 x 21 frequency count array, and CNT is the number of MM5 grid points (from a possible 9,801) for which there was a valid RTNEPH total FC value (i.e. the value was not 99999).

The sum inside the brackets in equation 3.2 represents the mean error in 5 percent increments, that is, a value inside the brackets of 1 corresponds to a total FC error of 5 percent, and a value inside the brackets of 20 correspond to a total FC error of 100 percent. Therefore, the value inside the brackets was multiplied by 5. A negative mean error indicates that a model is underforecasting, while a positive mean error indicates that a model is overforecasting.

Cancellation of the errors at each individual point may occur when calculating the mean error. To illustrate this point, consider a sample of 100 points for which total FC

forecasts were made. Suppose that the mean error for these points was zero. This could mean that a correct forecast was made for each of the 100 points (highly unlikely) or that 50 points were overforecasted by 10 percent each and the other 50 points were underforecasted by 10 percent each. Nonetheless, in the above example there was no forecast bias.

In order to obtain an idea of the magnitude of the forecast errors, two other scalar measures of forecast accuracy were used in this study. They are the MAE and the RMSE. The formulas used to compute them are

$$MAE = 5 \cdot \left[\frac{\sum_{i=0}^{20} \sum_{j=0}^{20} |ARRAY_{i,j} \cdot (i - j)|}{CNT} \right], \quad (3.3)$$

and

$$RMSE = 5 \cdot \sqrt{\frac{\sum_{i=0}^{20} \sum_{j=0}^{20} ARRAY_{i,j} \cdot (i - j)^2}{CNT}}. \quad (3.4)$$

These are the best known scalar measures of forecast accuracy (Wilks, 1995) and were used in other studies including the Phillips Laboratory study (Nehrkorn *et al.*, 1994). The mean absolute error gives an indication of the magnitude of the average forecast error without regard to whether the model overforecasts or underforecasts. The root-mean-square error penalizes large forecast errors. That is, high RMSE values are indicative of a forecast that is wrong by a significant amount.

To illustrate the difference between MAE and RMSE, consider a sample of 4 points for which total FC forecasts were made using two different methods, method A and

method B. Suppose method A correctly forecasted 2 of the points but overforecasted the other two points by 100 percent while method B underforecasted all 4 points by 60 percent. For method A, the MAE is equal to 50 and the RMSE is roughly 71. For method B, however, the MAE and the RMSE are both equal to 60. Thus, as mentioned above, the high RMSE value for method A indicates that when it missed a forecast, it missed that forecast badly.

3.5.2 Sharpness as a Measure of Forecast Performance

An additional measure of a forecast's performance is its "sharpness". Sharpness is a measure of how often forecasts of extremes (clear or completely cloudy) are made without regard to the correct placement of these extreme forecasts. In this study, sharpness was calculated using an adapted version of the USAF Trapnell (1992) 20/20 score. The 20/20 score is the percentage of forecasts that are within 20 percent of clear (total FC amounts < 20 percent) or cloudy (total FC amounts > 80 percent). The 20/20 score, once calculated, was compared against the 20/20 score of the RTNEPH analysis to determine if the forecast methods produced forecasts with sharpness comparable to the analysis.

3.5.3 Contingency Table Statistics

In addition to the statistical techniques described above, forecasts of broken cloudiness (defined as total FC amounts ≥ 60 percent) produced by the ADVCLD model, the Kvamstø scheme, the Sundqvist scheme, the vertical column method, the layered method, and persistence were compared against the RTNEPH analysis by use of 2 x 2 contingency tables (see Figure 7). The decision to verify a scheme's ability to correctly forecast broken conditions was chosen because knowledge of whether the sky is broken or

scattered is extremely important to pilots whose procedures may change when there is broken cloud cover rather than scattered cloud cover.

		Broken Cloudiness Observed by RTNEPH		
		Yes	No	
Broken Cloudiness Forecasted	Yes	a	b	a + b
	No	c	d	c + d
		a + c	b + d	n

Figure 7. An example of a 2 x 2 contingency table.

Using the contingency tables, four other statistical measures of accuracy were calculated for each of the six forecasting methods listed above. These were the hit rate (HR), the critical success index (CSI), the probability of detection (POD), and the false alarm rate (FAR). Before describing these four statistics, the contingency table itself will be discussed.

In the 2 x 2 contingency table shown in Figure 7, a is the number of times that broken cloudiness was observed and forecasted, b is the number of times that broken cloudiness was forecasted but not observed, c is the number of times that broken cloudiness was observed but not forecasted, and d is the number of times that broken cloudiness was neither observed nor forecasted. Finally, n is equal to $a + b + c + d$, which

is the total number of observations/forecasts (i.e. the sample size). Note that n is equal to CNT from the previous section.

A perfect forecast would have b and c identically equal to 0. This means that every time broken cloudiness was forecasted it was also observed, and every time broken cloudiness was not forecasted it was not observed. For those forecasts which are not perfect, statistical measures of accuracy and skill are used to evaluate competing forecast methods (Wilks, 1995).

The hit rate (HR), one such statistical measure of accuracy, was used in this study and is given by the equation

$$HR = 100 \cdot \left(\frac{a + d}{n} \right), \quad (3.5)$$

where a , d , and n are defined as above. The hit rate defined by equation 3.5 is expressed as a percentage between 0 and 100, with 0 percent being the worst possible hit rate and 100 percent being the best possible hit rate. The HR weighs correct “yes” and “no” forecasts equally, and also weighs incorrect forecasts correctly (Wilks, 1995).

Another measure of accuracy used was the critical success index (CSI). This index is given by the formula

$$CSI = 100 \cdot \left(\frac{a}{a + b + c} \right), \quad (3.6)$$

where a , b , and c are defined as above. Again the best possible score is 100 percent, and the worst possible score is 0 percent. The CSI focuses only on the number of times broken cloudiness was forecasted and/or observed and does not include the number of times broken cloudiness was neither forecasted nor observed, d . The CSI can thus be

considered to be the hit rate after all correct “no” forecasts are removed from consideration. The CSI is especially effective in situations where the number of “yes” forecasts is significantly lower than the number of “no” forecasts (Wilks, 1995).

The probability of detection (POD), another statistical measure used in this study, is the ratio of correct “yes” forecasts to the total number of RTNEPH broken cloudiness observations. Mathematically, the probability of detection is given by

$$POD = 100 \cdot \left(\frac{a}{a + c} \right), \quad (3.7)$$

where a and c are defined as above. Here again, the best possible score is 100 percent and the worst possible score is 0 percent. The POD provides an indication of how likely it is that a particular forecast method detects broken cloudiness (Wilks, 1995).

The last statistical measure of accuracy that was used in conjunction with the contingency table in Figure 7 was the false alarm rate (FAR). The FAR is the ratio of incorrect “yes” forecasts to the total number of “yes” forecasts. The equation that defines the false alarm rate is

$$FAR = 100 \cdot \left(\frac{b}{a + b} \right), \quad (3.8)$$

where a and b are defined as above. In this case, the worst possible score is 100 percent and the best possible score is 0 percent (Wilks, 1995).

3.5.4 Forecast Skill

The skill of a forecast is the relative accuracy of that forecast when measured against some standard reference forecast. The skill score, once calculated, is expressed as a percentage. A positive skill score represents improvement over the reference forecast,

while a negative skill score indicates that the forecast method in question performed worse than the reference forecast. A skill score of zero indicates that the forecast method used and the reference forecast had equal skill.

In this study, skill scores were calculated for the hit rate and for the critical success index of the broken cloudiness forecasts of the ADVCLD, Kvamstø, Sundqvist, vertical column, and layered schemes. Persistence was used as the standard reference forecast against which the other forecast schemes were measured. Mathematically, the skill score used to compare the hit rates is given by the equation

$$SS_{pers} = 100 \cdot \left(\frac{HR - HR_{pers}}{HR_{perf} - HR_{pers}} \right), \quad (3.9)$$

where SS_{pers} is the skill score relative to persistence, HR_{pers} is the hit rate for persistence, HR_{perf} is a perfect hit rate (100 percent), and HR is the hit rate of the forecast scheme in question. All of the variables in equation 3.9 were expressed as percentages. A similar equation was used to compare the CSI for each method (Wilks, 1995).

3.5.5 Statistical Significance Testing

In order that the results of the statistical analysis can be considered meaningful, a dependence between the row classification (in this case broken cloudiness forecasted) and the column classification (in this case broken cloudiness observed) in the 2 x 2 contingency tables must be shown to exist. If this dependence cannot be demonstrated, a seemingly good relationship between observations and forecasts may be entirely due to chance (Kalbfleisch, 1979).

Two events, A and B, are considered to be independent if the occurrence or nonoccurrence of event B gives no information whatsoever about whether event A has

also occurred (Larson, 1982). Applied to the contingency table in Figure 7, independence of broken cloudiness observations and forecasts implies that the probability of observing broken cloudiness, given that broken cloudiness was forecast, equals the probability of observing broken cloudiness regardless of the forecast.

To show that the observations and forecasts are, in fact, dependent upon one another, a Pearson's chi-square (χ^2) test was performed using Statistix[®] software. A significance level of one tenth of one percent was used. That is, if the p-value computed in the test was less than 0.001, the notion of independence was rejected and the observance or non-observance of broken cloudiness was considered to be dependent upon the forecast. At this level of significance, there is only a 1 out of 1,000 probability that the forecast was made correctly by chance (Larson, 1982). Results of the χ^2 test, as well as the results from the rest of the statistical measures of accuracy and skill computed in this study and described above, are presented in detail in chapter 4.

3.6 Subjective Analysis

The subjective analysis done in this study was accomplished by visualizing the total FC forecasts from the various methods and comparing the forecasts against visualizations of the RTNEPH total FC analyses which were valid at the same time. In addition to comparing individual forecast hours, entire forecast cycles (0-hr through 36-hr in 3-hr increments) were animated and checked against an animation of the corresponding RTNEPH analyses. All visualizations were created using GrADS[®], as mentioned previously.

The primary objective for comparing the visualizations of an individual forecast hours against the visualizations of the corresponding RTNEPH analyses was to determine

if the methods were systematically underforecasting or overforecasting in certain geographical areas. For example, did the MM5 always underestimate cloudiness over the Adriatic Sea? Did the MM5 produce too much cloud cover over the mountainous regions in Italy?

Animations of forecast cycles were examined to determine if the models realistically reproduced the typical progression of synoptic scale cloud systems. That is, did large regions of cloudiness progress generally westward during the forecast cycle, as would be expected in the mid-latitudes? Did significant cloud areas appear, for example, in the 9-hr forecast and then disappear in the 12-hr forecast? The animations were also studied to determine if there were noticeable phase errors in either ADVCLD or MM5. Results of the subjective analysis, along with some of the visualizations examined, are presented in the next chapter.

IV. Results

This chapter presents the results of the statistical and subjective analyses performed in this study. The statistical results are presented graphically by month with each graph being discussed briefly. There are four graphs for each statistic, one for each month for which data was collected. The values plotted on each graph are average values of the statistic in question at each of the 12 forecast validation times (i.e. forecasts for the 3-hr, 6-hr, 9-hr, ..., 36-hr points). The subjective results are representative visualizations of forecasts from the various methods chosen to illustrate the major findings.

As an aid to interpreting the results of the individual statistical tests, it is useful to keep in mind the level of cloudiness for the months used in this study. Table 2 summarizes the average amount of cloud cover for each month in terms of the RTNEPH 20/20 scores. The mean RTNEPH 0-19 and 81-100 scores are shown as percentages. High 0-19 scores indicate a large percentage of clear skies for a particular month (i.e. a lack of cloudiness in that month). Large 81-100 scores indicate a high percentage of overcast skies for a particular month (i.e. a very cloudy month). An examination of Table 2 reveals that September was the driest month in this study. November was the cloudiest month.

The distribution of clear and conditions shown in Table 2 also indicates a seasonal change in the cloudiness pattern. The relatively high amount of clear skies in August and September is indicative of the fair weather that is usually present during the summer months. October, with lower 0-19 scores and higher 81-100 scores, is the transition month when cloudiness is usually associated with frontal systems and the arrival of colder air. By November, the transition to the winter cloudiness pattern is almost complete. In

winter, clouds tend to be quite persistent, especially in the mountains and valleys of Bosnia and in the Po Valley of Italy.

Table 2. Monthly average RTNEPH 20/20 scores given as percentages. Inspection of the values reveals that September was the month with the least cloudiness in this study while November was the cloudiest month in the study.

	0-19 RTNEPH Score	81-100 RTNEPH Score
August	53.7	15.6
September	64.2	13.6
October	41.9	30.0
November	21.3	54.8

4.1 Significance Testing Results

As mentioned in chapter 3, a Pearson's chi-square (χ^2) test was performed to determine the significance, or reliability, of the results of the 2 x 2 contingency table statistics. All forecast methods at all validation hours in all four months had contingency tables with p-values less than 0.001 except for the layered and vertical column methods at the 0-hr point and persistence after the 30-hr point.

The fact that the layered and vertical column methods failed the chi-square test is not surprising because of the fact that the total cloud condensate is initialized to zero in the MM5. No statistical results will be presented for the 0-hr analyses. The fact that persistence fails after the 30-hr point demonstrates that a forecast based on persistence eventually becomes no better than a forecast based on chance. Other than in these cases, dependence was shown to exist between the rows and columns of the contingency tables. Thus the results are statistically significant.

4.2 Scalar Measures of Accuracy Results

4.2.1 Mean Error Results

Figures 8-11 display the results of the mean error calculation for August-November respectively. Average hourly ME values are plotted. Tables 3-6 contain the descriptive statistics for Figures 8-11 respectively.

A large negative mean error is evident for all of the MM5 methods until the 12-hr point. The MM5 is finally fully “spun-up” at the 12-hr point. After that, the mean error remains roughly the same or tends slightly toward more positive values but still remains, with a few exceptions, negatively valued.

The mean error for ADVCLD at the 3-hr point is quite close to zero for all four months. The mean error then increases over time until there is a large positive ME by the 36-hr point. The mean error for persistence follows no particular pattern but does, on average, remain closer to zero than any of the other methods.

4.2.2 Mean Absolute Error Results

Figures 12-15 display the results of the mean absolute error calculation for August-November respectively. Average hourly MAE values are plotted. Tables 7-10 contain the descriptive statistics for Figures 12-15 respectively.

In general for the four months considered, the mean absolute error for the MM5 schemes decreases until the 12-hr point, and then the MAE increases slowly out to the 36-hr point. Again, as the model “spins-up” its forecasts get more accurate, and then, as the time scale for which the forecast is being made increases, the forecast accuracy decreases.

ADVCLD, on the other hand, generally shows a steady increase in MAE over the forecast period. It far outperforms any MM5 scheme until between the 9 and 12-hr

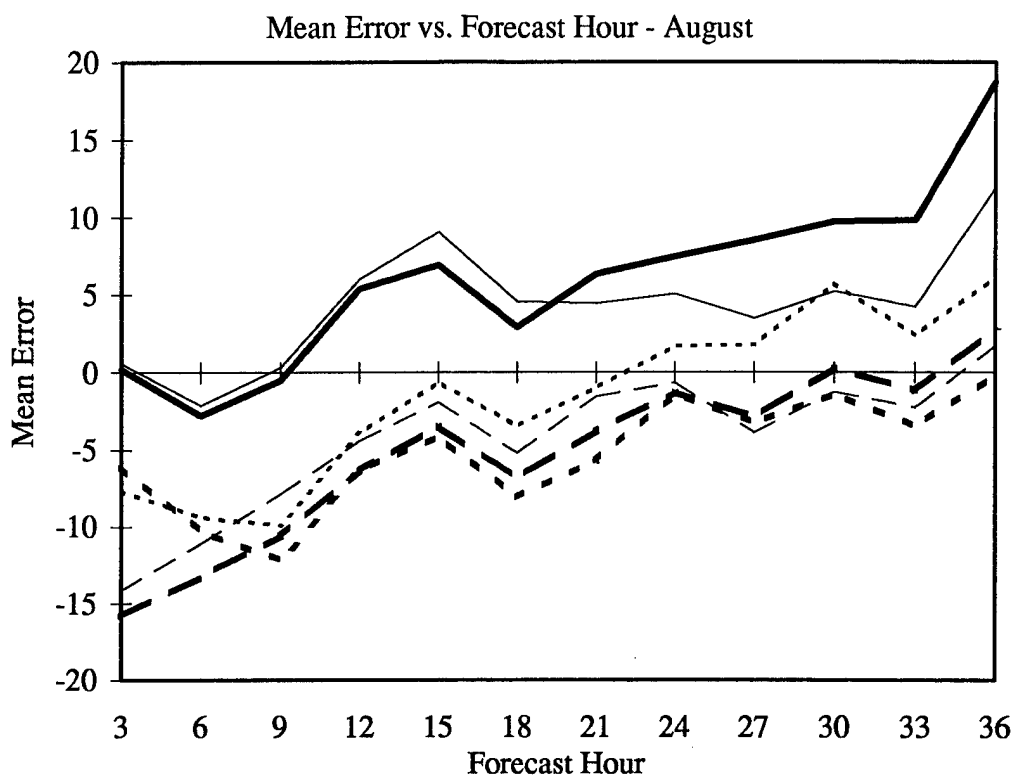


Figure 8. ME versus forecast hour for August 1997. The thick solid line represents ADVCLD, the thin solid line is persistence, the thick dotted line is the Kvamstø method, the thin dotted line is the Sundqvist method, the thick dashed line is the vertical column method, and the thin dashed line is the layered method. Average hourly ME values are plotted. See Table 3 for descriptive statistics.

Table 3. Descriptive statistics for Figure 8. Mean error for August 1997.

	ADVCLD	Kvamstø	Sundqvist	Persistence	Vertical Column	Layered
# of Forecasts	187	187	187	187	187	187
Mean	6.0	-5.2	-1.5	4.4	-5.2	-4.4
Std Deviation	15.8	13.6	15.3	15.4	14.5	15.1
Maximum	66.2	32.4	30.0	44.0	27.9	30.6
Median	6.6	-4.1	0.9	5.5	-2.4	-2.0
Minimum	-32.3	-49.0	-50.1	-35.3	-58.1	-55.2

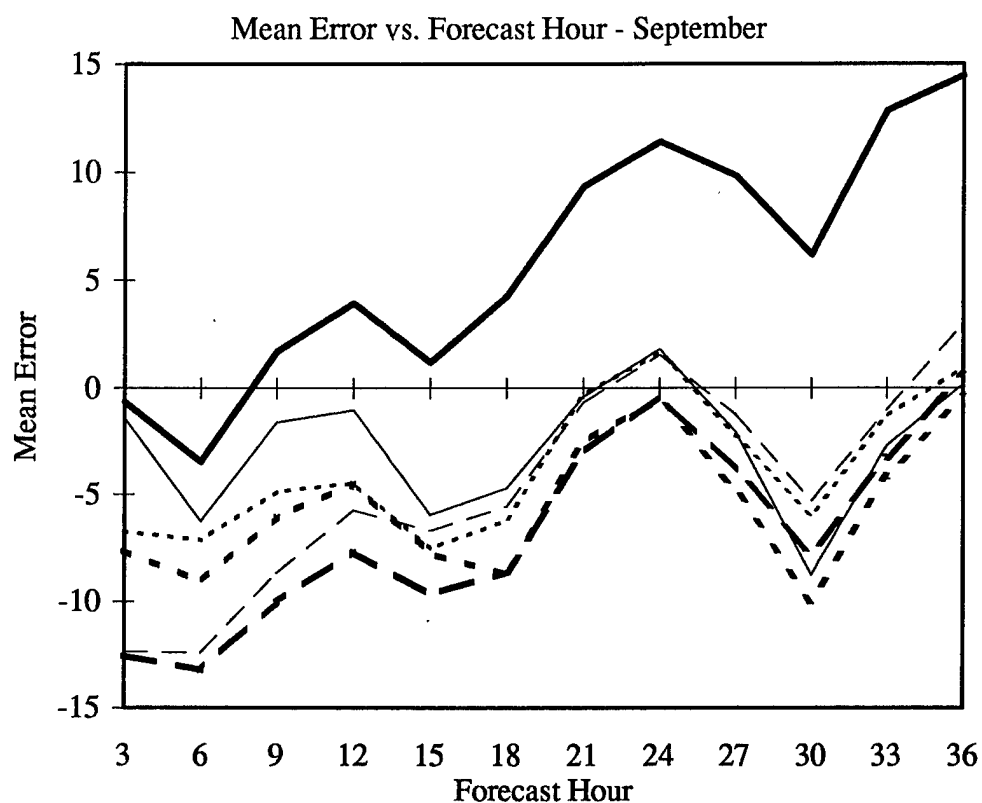


Figure 9. As in Figure 8 for September 1997. See Table 4 for descriptive statistics.

Table 4. Descriptive statistics for Figure 9. Mean error for September 1997.

	ADVCLD	Kvamstø	Sundqvist	Persistence	Vertical Column	Layered
# of Forecasts	445	445	445	445	445	445
Mean	5.9	-5.5	-3.7	-2.7	-6.6	-4.6
Std Deviation	15.7	12.3	14.2	17.3	13.3	13.2
Maximum	56.2	56.6	68.0	49.4	61.8	53.9
Median	4.5	-4.1	-2.4	-1.6	-5.6	-4.7
Minimum	-59.2	-43.2	-45.2	-59.2	-46.0	-46.3

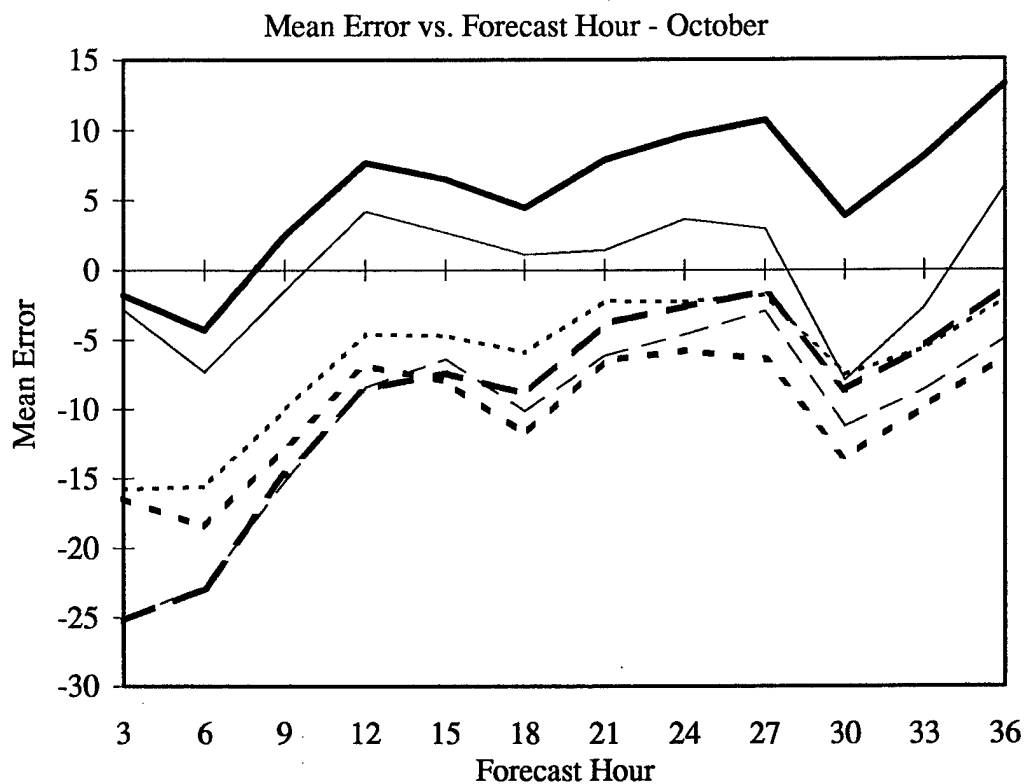


Figure 10. As in Figure 8 for October 1997. See Table 5 for descriptive statistics.

Table 5. Descriptive statistics for Figure 10. Mean error for October 1997.

	ADVCLD	Kvamstø	Sundqvist	Persistence	Vertical Column	Layered
# of Forecasts	390	390	390	390	390	390
Mean	5.7	-10.2	-6.5	-0.1	-9.3	-10.5
Std Deviation	20.1	16.2	16.9	25.5	18.0	17.7
Maximum	72.9	55.1	60.8	96.4	56.6	48.5
Median	5.0	-9.6	-5.5	3.7	-7.9	-9.8
Minimum	-41.7	-48.4	-47.0	-70.2	-56.1	-64.0

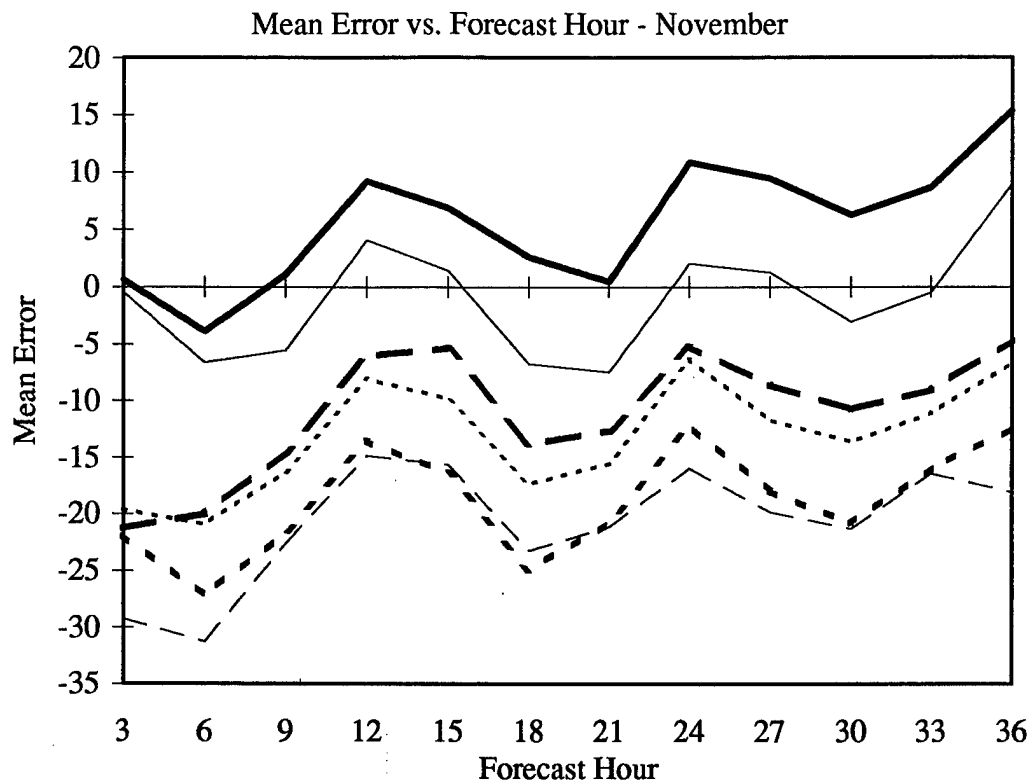


Figure 11. As in Figure 8 for November 1997. See Table 6 for descriptive statistics.

Table 6. Descriptive statistics for Figure 11. Mean error for November 1997.

	ADVCLD	Kvamstø	Sundqvist	Persistence	Vertical Column	Layered
# of Forecasts	112	112	112	112	112	112
Mean	5.6	-18.8	-13.1	-1.1	-11.0	-20.8
Std Deviation	16.8	16.2	15.8	18.0	14.6	14.8
Maximum	53.4	40.3	40.1	45.7	40.9	35.7
Median	9.2	-16.3	-9.9	3.5	-9.4	-16.8
Minimum	-32.2	-69.7	-71.4	-42.1	-69.0	-66.0

points. After that, the MAE for ADVCLD is similar to the mean absolute errors of the MM5 schemes until between the 33 and 36-hr points. By 36 hours, the MAE for ADVCLD is worse than all the MM5 schemes. However, in November ADVCLD outperformed all other methods for the entire forecast cycle.

Persistence had low mean absolute error values at the 3-hr point for each month. However, by the 9-hour point the MAE values for persistence were higher than the other methods and continued to increase for the rest of the period.

4.2.3 Root-Mean-Squared Error Results

Figures 16-19 display the results of the root-mean-squared error calculation for August-November respectively. Average hourly RMSE values are plotted. Tables 11-14 contain the descriptive statistics for Figures 16-19 respectively.

The RMSE values for the MM5 schemes decreased slightly, on average, until the 12-hr point. From the 15-hr point, they remained steady or increased just slightly until the 36-hr point.

The RMSE values for ADVCLD were almost all lower than the corresponding values for the MM5 schemes for all four months. The most notable exception was the 36-hr point in August when the MM5 performed well relative to ADVCLD. The RMSE values for ADVCLD were significantly lower than the corresponding values for the MM5 schemes until the 12-hr point.

Persistence had low RMSE values at the 3-hr point for each month. However, by the 9-hour point the RMSE values for persistence were higher than the other methods and continued to increase for the rest of the period.

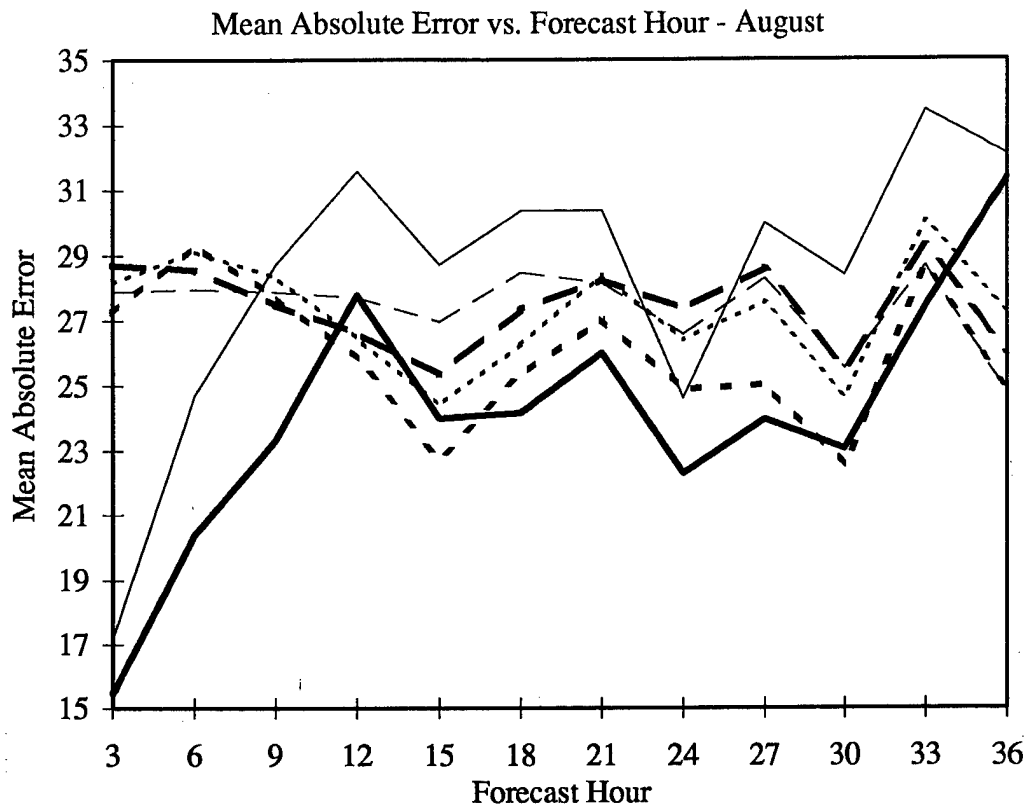


Figure 12. MAE versus forecast hour for August 1997. The thick solid line represents ADVCLD, the thin solid line is persistence, the thick dotted line is the Kvamstø method, the thin dotted line is the Sundqvist method, the thick dashed line is the vertical column method, and the thin dashed line is the layered method. Average hourly MAE values are plotted. See Table 7 for descriptive statistics.

Table 7. Descriptive statistics for Figure 12. MAE for August 1997.

	ADVCLD	Kvamstø	Sundqvist	Persistence	Vertical Column	Layered
# of Forecasts	187	187	187	187	187	187
Mean	24.1	25.9	27.3	28.4	27.4	27.4
Std Deviation	9.8	9.7	9.7	9.3	9.3	8.6
Maximum	66.2	54.5	53.6	52.1	58.8	56.2
Median	22.9	23.9	25.6	27.8	25.9	26.9
Minimum	7.1	4.8	3.8	6.8	6.5	6.1

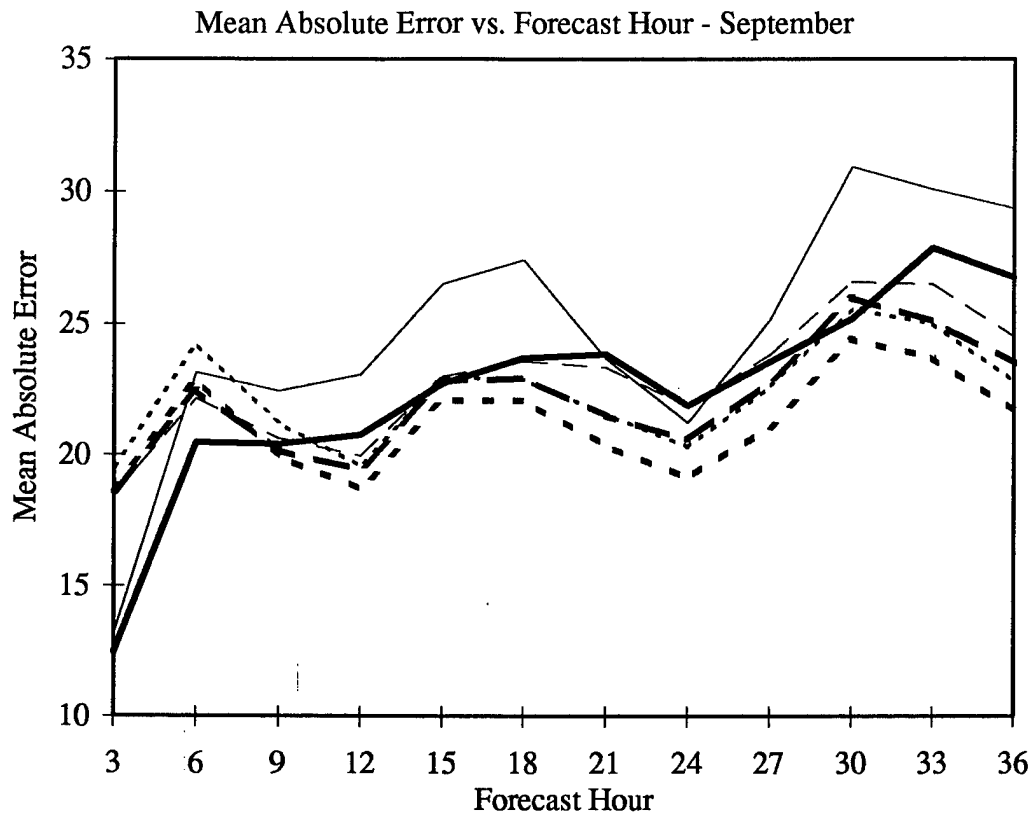


Figure 13. As in Figure 12 for September 1997. See Table 8 for descriptive statistics.

Table 8. Descriptive statistics for Figure 13. MAE for September 1997.

	ADVCLD	Kvamstø	Sundqvist	Persistence	Vertical Column	Layered
# of Forecasts	445	445	445	445	445	445
Mean	22.5	21.2	22.3	24.7	22.2	22.9
Std Deviation	10.7	10.3	10.6	12.2	11.0	10.8
Maximum	59.2	62.5	70.5	68.0	66.3	59.4
Median	21.8	19.2	20.1	23.1	20.5	21.3
Minimum	0.9	1.0	1.0	0.9	0.9	0.9

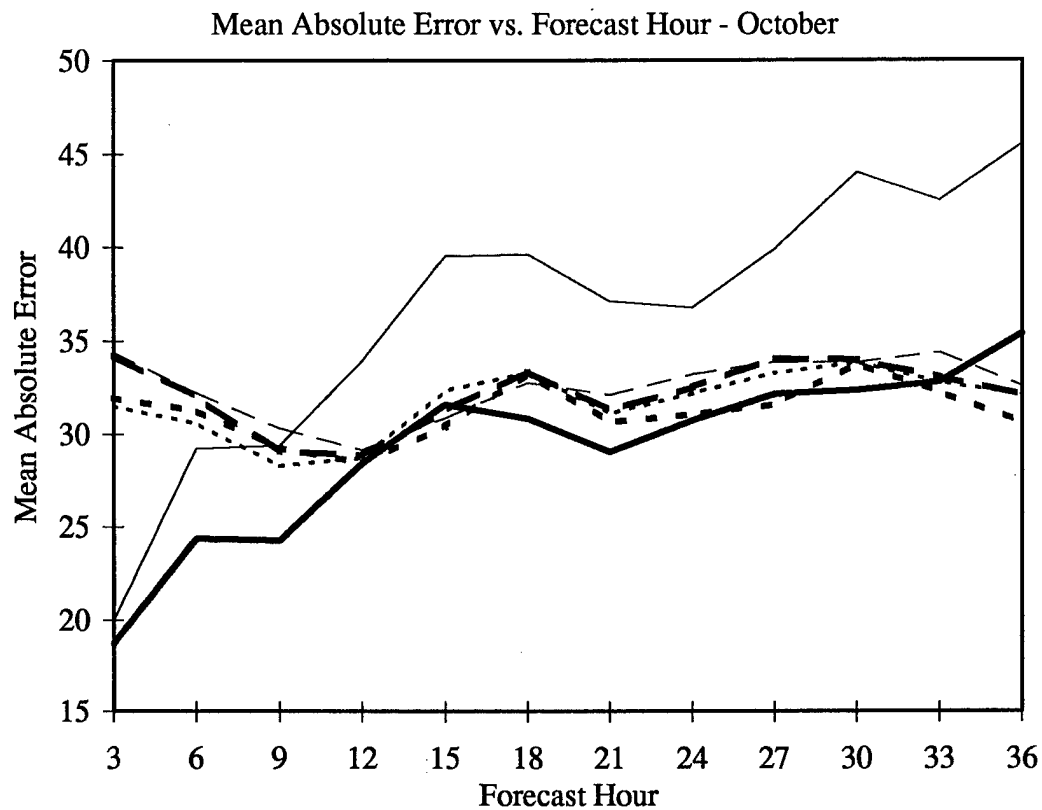


Figure 14. As in Figure 12 for October 1997. See Table 9 for descriptive statistics.

Table 9. Descriptive statistics for Figure 14. MAE for October 1997.

	ADVCLD	Kvamstø	Sundqvist	Persistence	Vertical Column	Layered
# of Forecasts	390	390	390	390	390	390
Mean	29.2	31.2	31.7	36.5	32.2	32.5
Std Deviation	12.4	9.4	9.0	14.3	9.8	9.8
Maximum	73.0	63.0	64.6	96.4	62.4	64.9
Median	29.8	30.8	30.5	36.1	32.1	33.1
Minimum	0.0	0.0	0.0	1.4	0.0	0.1

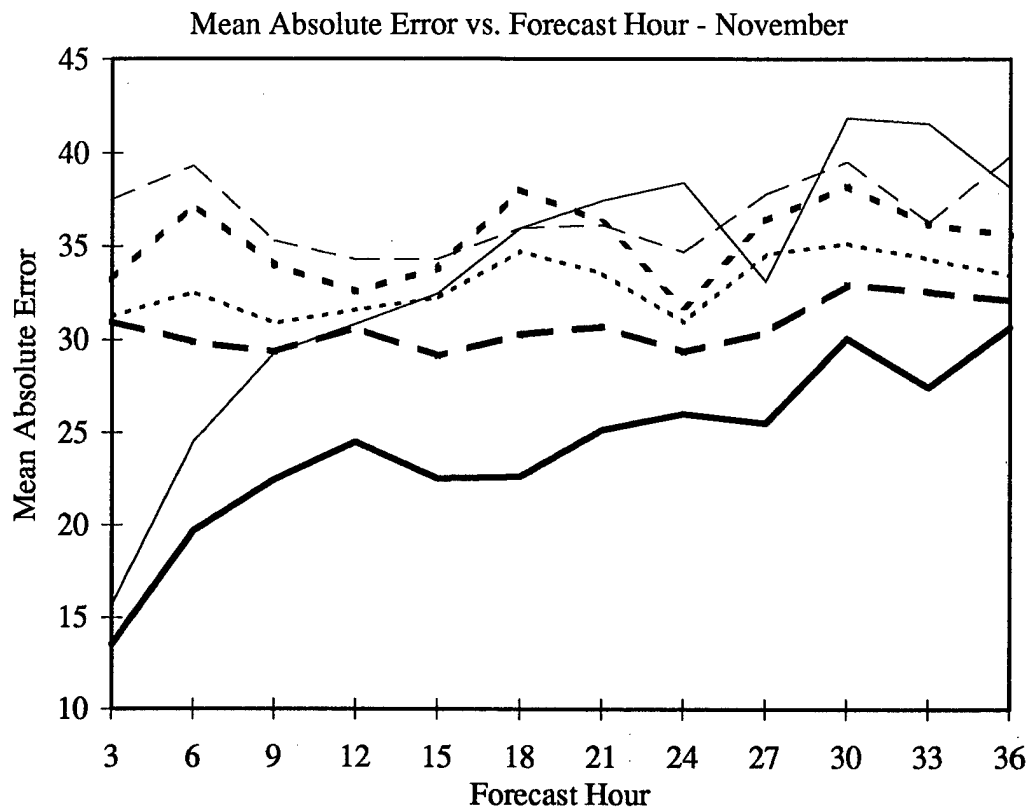


Figure 15. As in Figure 12 for November 1997. See Table 10 for descriptive statistics.

Table 10. Descriptive statistics for Figure 15. MAE for November 1997.

	ADVCLD	Kvamstø	Sundqvist	Persistence	Vertical Column	Layered
# of Forecasts	112	112	112	112	112	112
Mean	24.2	35.3	32.9	33.2	30.7	36.7
Std Deviation	10.5	8.0	7.2	11.1	7.6	9.5
Maximum	53.4	69.7	71.4	61.4	69.0	66.0
Median	26.2	35.6	32.6	32.4	31.3	36.8
Minimum	5.8	11.2	11.2	9.1	7.5	9.7

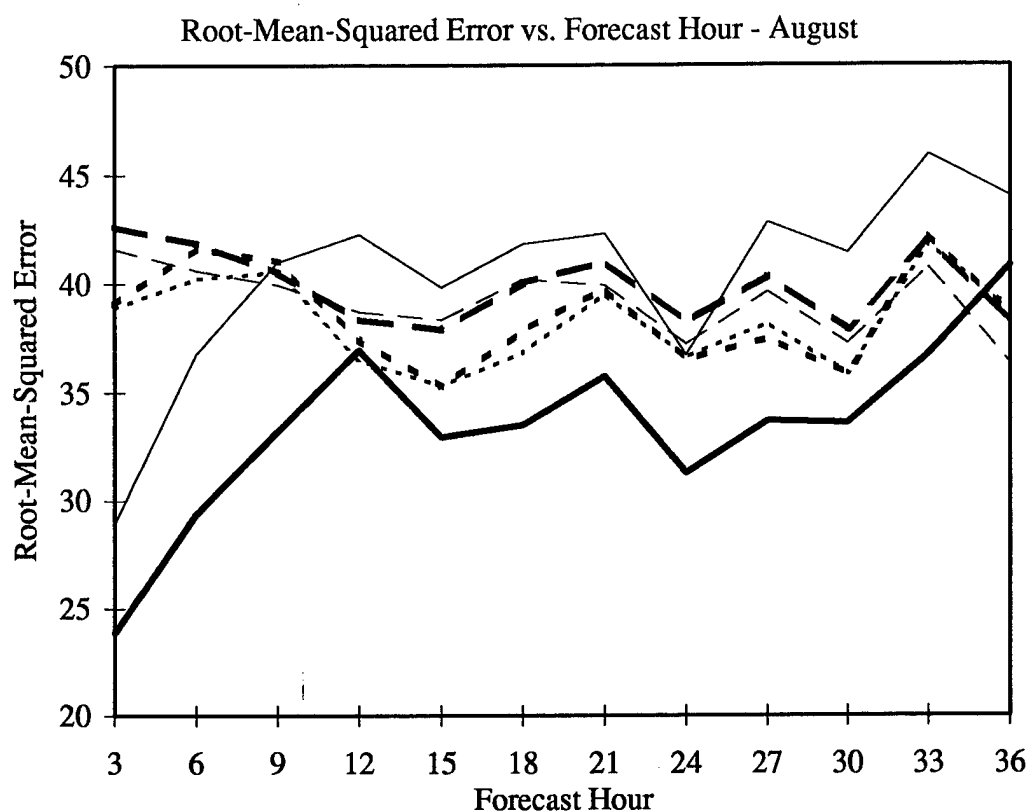


Figure 16. RMSE versus forecast hour for August 1997. The thick solid line represents ADVCLD, the thin solid line is persistence, the thick dotted line is the Kvamstø method, the thin dotted line is the Sundqvist method, the thick dashed line is the vertical column method, and the thin dashed line is the layered method. Average hourly RMSE values are plotted. See Table 11 for descriptive statistics.

Table 11. Descriptive statistics for Figure 16. RMS error for August 1997.

	ADVCLD	Kvamstø	Sundqvist	Persistence	Vertical Column	Layered
# of Forecasts	187	187	187	187	187	187
Mean	33.5	38.5	38.2	40.3	39.9	39.2
Std Deviation	10.0	9.6	9.8	9.4	9.6	8.9
Maximum	72.5	63.1	62.1	62.2	68.2	66.5
Median	32.3	36.8	37.4	39.9	38.0	37.7
Minimum	12.6	12.5	9.7	14.6	12.9	13.3

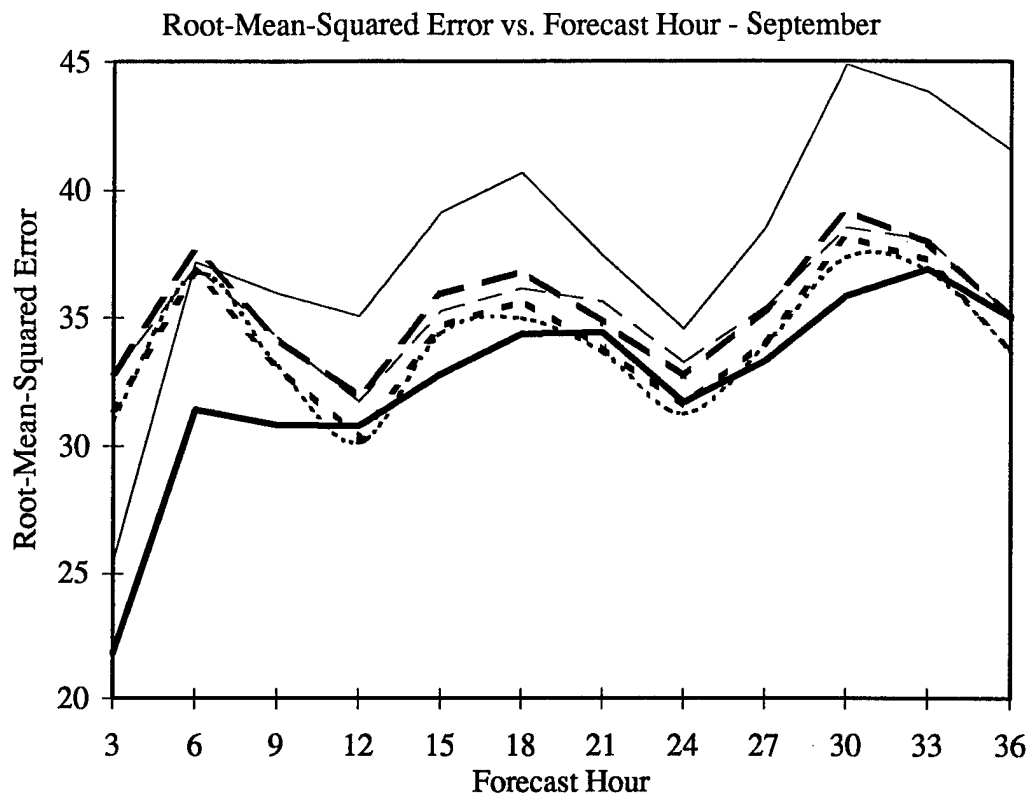


Figure 17. As in Figure 16 for September 1997. See Table 12 for descriptive statistics.

Table 12. Descriptive statistics for Figure 17. RMS error for September 1997.

	ADVCLD	Kvamstø	Sundqvist	Persistence	Vertical Column	Layered
# of Forecasts	445	445	445	445	445	445
Mean	32.4	34.2	33.9	37.8	35.4	35.3
Std Deviation	11.2	10.9	11.1	12.5	11.7	11.4
Maximum	75.1	71.6	76.8	76.0	75.6	70.3
Median	31.9	33.2	32.5	37.0	34.3	33.7
Minimum	5.6	5.6	5.6	5.6	5.0	5.0

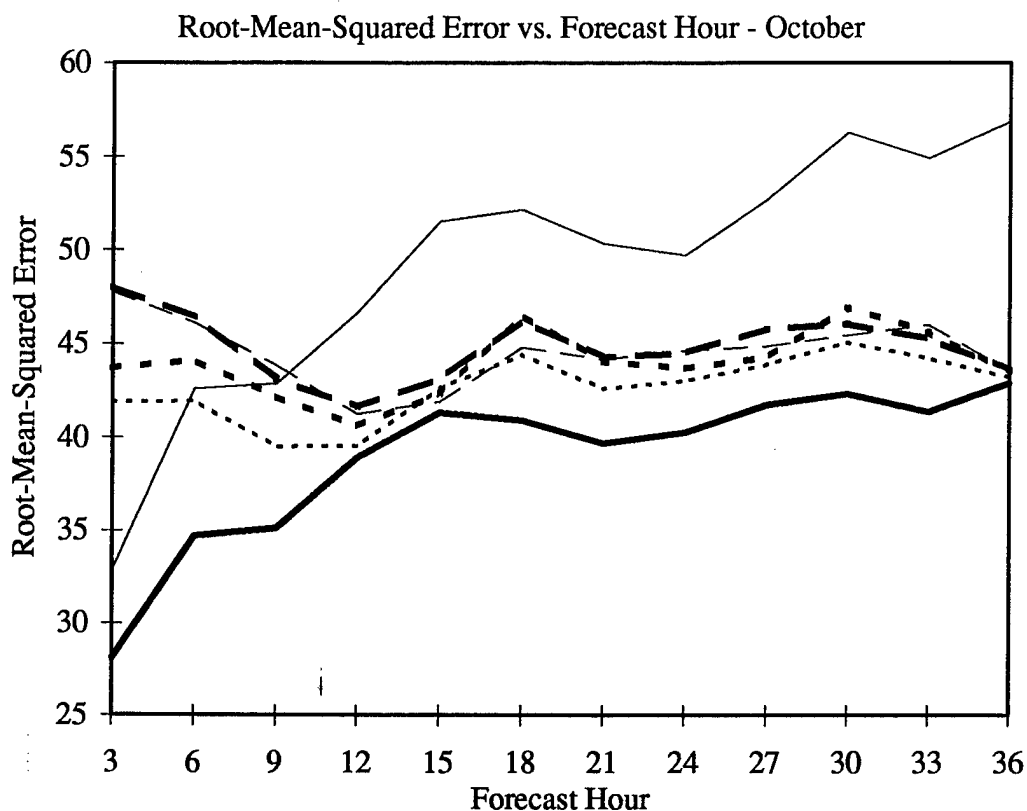


Figure 18. As in Figure 16 for October 1997. See Table 13 for descriptive statistics.

Table 13. Descriptive statistics for Figure 18. RMS error for October 1997.

	ADVCLD	Kvamstø	Sundqvist	Persistence	Vertical Column	Layered
# of Forecasts	390	390	390	390	390	390
Mean	38.9	43.9	42.7	49.1	44.8	44.5
Std Deviation	12.4	9.7	9.6	13.6	10.0	10.0
Maximum	81.7	73.5	73.3	96.7	72.0	75.5
Median	38.7	43.7	41.6	48.6	44.1	44.5
Minimum	0.0	0.0	0.2	5.9	0.6	2.7

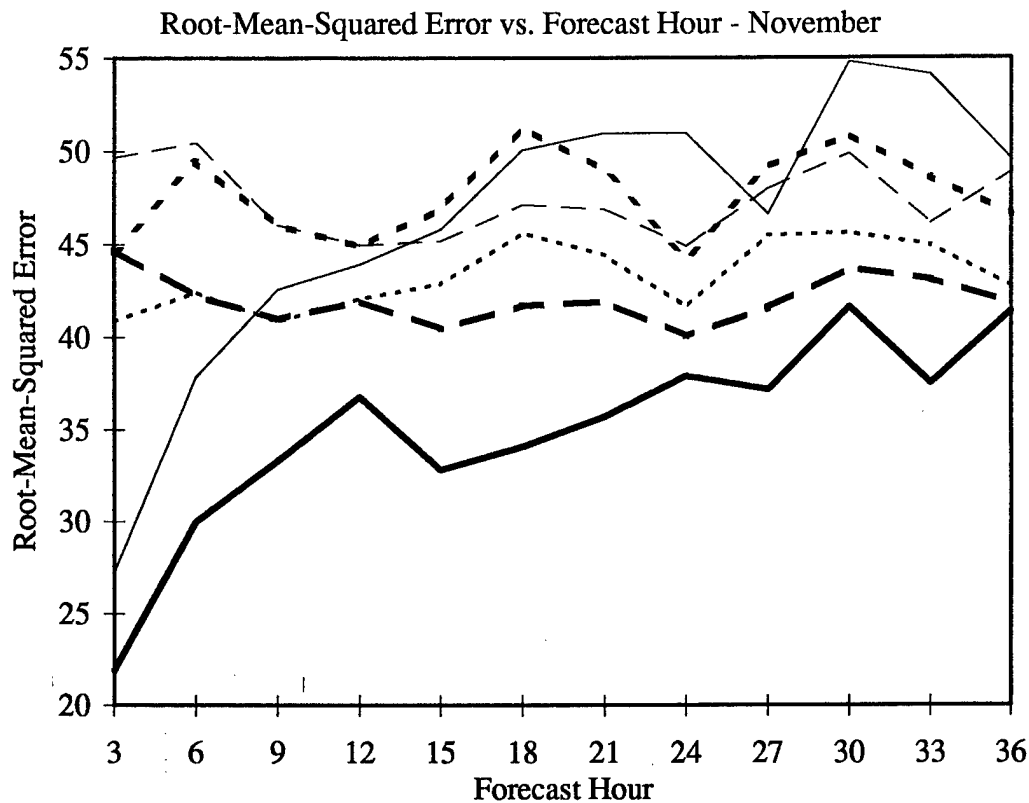


Figure 19. As in Figure 16 for November 1997. See Table 14 for descriptive statistics.

Table 14. Descriptive statistics for Figure 19. RMS error for November 1997.

	ADVCLD	Kvamstø	Sundqvist	Persistence	Vertical Column	Layered
# of Forecasts	112	112	112	112	112	112
Mean	35.0	47.6	43.3	46.2	42.0	47.3
Std Deviation	10.7	8.3	7.5	11.3	7.8	9.2
Maximum	66.4	74.2	75.2	69.9	74.1	71.9
Median	36.3	47.8	43.0	46.0	42.3	46.9
Minimum	15.2	14.1	16.5	19.2	13.5	19.7

4.3 Sharpness (20/20 Score) Results

4.3.1 Sharpness for Clear Skies (0-19 Score) Results

Figures 20-23 display the results of the clear (0-19 score) sharpness calculation for August-November respectively. Average hourly 0-19 scores are plotted. Tables 15-18 contain the descriptive statistics for Figures 20-23 respectively.

The MM5 schemes consistently forecasted more clear conditions than were observed for the first 18 hours of the forecast cycle in all four months. Of the MM5 schemes evaluated, the Sundqvist scheme best mirrored the clear conditions analyzed by the RTNEPH. The next best scheme was the vertical column method. The Kvamstø scheme and the layered method more clear conditions than were observed at almost every validation hour for all four months.

ADVCLD, again, did quite well initially, but by the 9-hr point ADVCLD began significantly underforecasting clear conditions. The underforecasting became progressively worse until 36 hours, at which point the average underforecast for the four months was 25 percent (i.e. ADVCLD forecasted clear skies 25 percent less than it was analyzed by the RTNEPH). Persistence performed better than any method except the Sundqvist method at forecasting the correct percentage of clear skies. It did, however, exhibit a tendency to slightly underforecast the amount of clear skies. Some underforecast is desirable as the RTNEPH analysis has a clear bias (mentioned earlier).

4.3.2 Sharpness for Overcast Skies (81-100 Score) Results

Figures 24-27 display the results of the clear (81-100 score) sharpness calculation for August-November respectively. Average hourly 81-100 scores are plotted. Tables 19-22 contain the descriptive statistics for Figures 24-27 respectively.

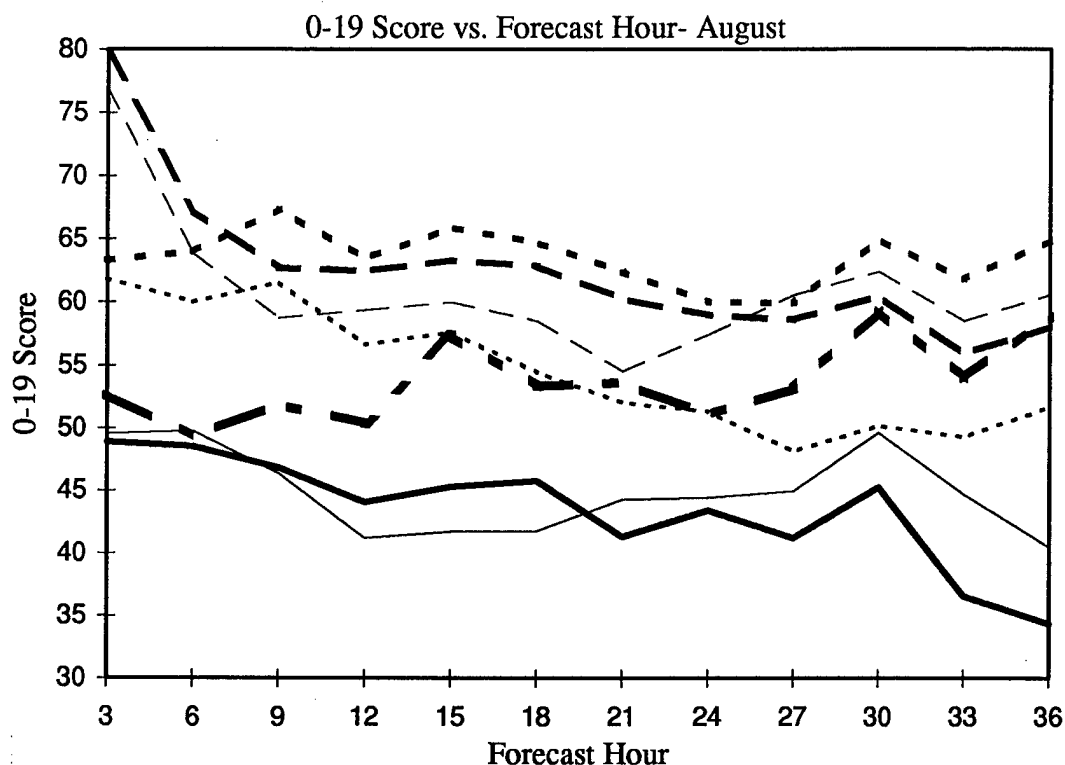


Figure 20. 0-19 score versus forecast hour for August 1997. The thick solid line represents ADVCLD, the thin solid line is persistence, the thick dotted line is the Kvamstø method, the thin dotted line is the Sundqvist method, the thick dashed line is the vertical column method, and the thin dashed line is the layered method. RTNEPH is the thick dashed/dotted line. Average hourly 0-19 scores are plotted. See Table 15 for descriptive statistics.

Table 15. Descriptive statistics for Figure 1. 0-19 score for August 1997.

	ADVCLD	Kvamstø	Sundqvist	Persistence	Vertical Column	Layered	RTNEPH
# of Forecasts	187	187	187	187	187	187	187
Mean	43.5	63.5	54.5	44.9	62.5	60.9	53.7
Std Deviation	19.3	15.0	18.5	19.2	16.6	17.5	21.5
Maximum	83.2	93.6	96.2	87.9	96.7	96.1	96.7
Median	47.0	64.8	54.9	49.7	63.7	64.0	58.5
Minimum	0.0	22.6	8.3	9.9	2.7	13.2	4.5

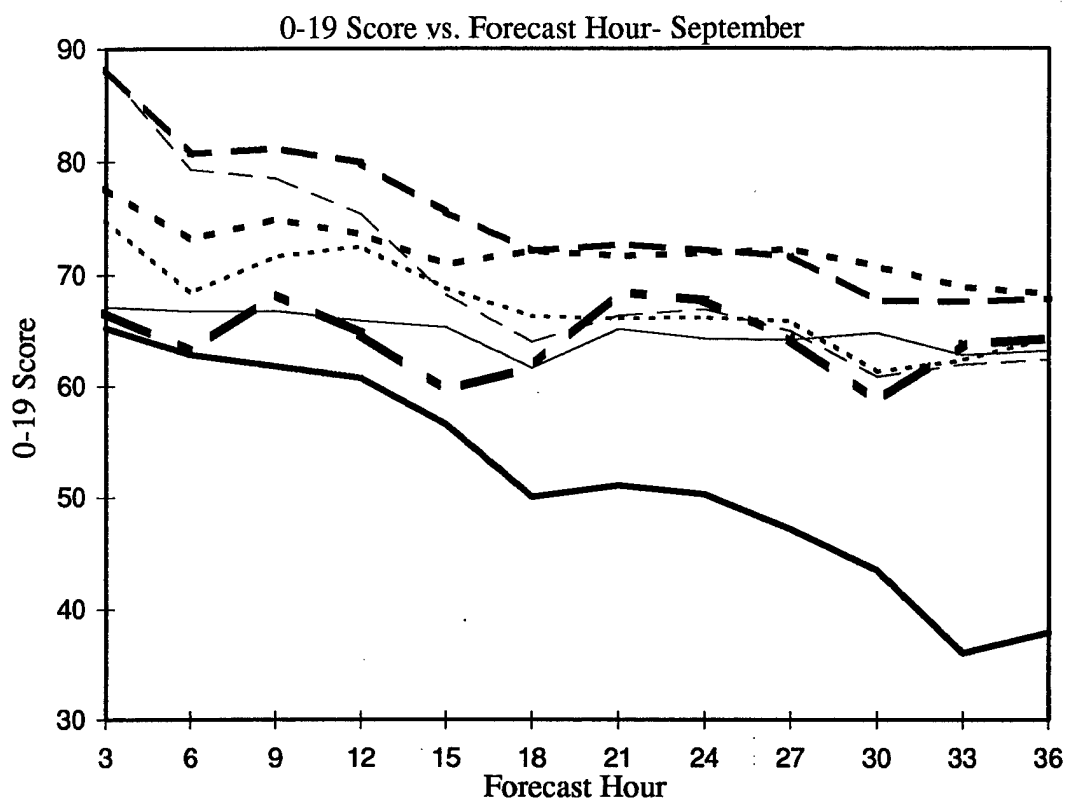


Figure 21. As in Figure 20 for September 1997. See Table 16 for descriptive statistics.

Table 16. Descriptive statistics for Figure 2. 0-19 score for September 1997.

	ADVCLD	Kvamstø	Sundqvist	Persistence	Vertical Column	Layered	RTNEPH
# of Forecasts	445	445	445	445	445	445	445
Mean	51.9	72.2	67.4	64.8	74.8	69.7	64.2
Std Deviation	29.6	19.6	20.7	22.8	21.1	22.8	22.9
Maximum	100.0	100.0	100.0	100.0	100.0	100.0	100.0
Median	51.0	76.9	71.2	68.2	81.0	74.8	71.2
Minimum	0.0	0.0	2.4	4.6	16.1	14.7	7.6

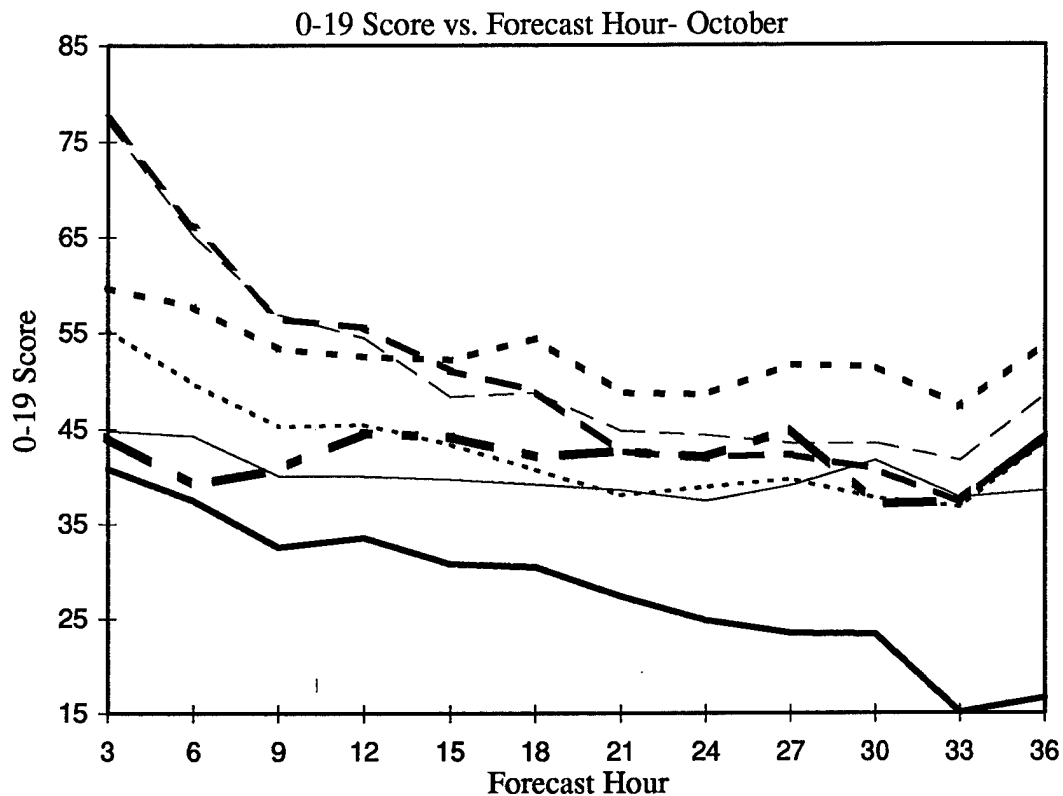


Figure 22. As in Figure 20 for October 1997. See Table 17 for descriptive statistics.

Table 17. Descriptive statistics for Figure 3. 0-19 score for October 1997.

	ADVCLD	Kvamstø	Sundqvist	Persistence	Vertical Column	Layered	RTNEPH
# of Forecasts	390	390	390	390	390	390	390
Mean	28.0	52.6	42.9	40.1	50.4	51.4	41.9
Std Deviation	25.5	23.0	22.6	23.7	25.7	26.2	24.4
Maximum	100.0	100.0	100.0	100.0	100.0	100.0	100.0
Median	23.2	52.1	40.4	34.1	47.8	48.5	41.3
Minimum	0.0	1.2	0.0	0.0	0.0	0.0	0.0

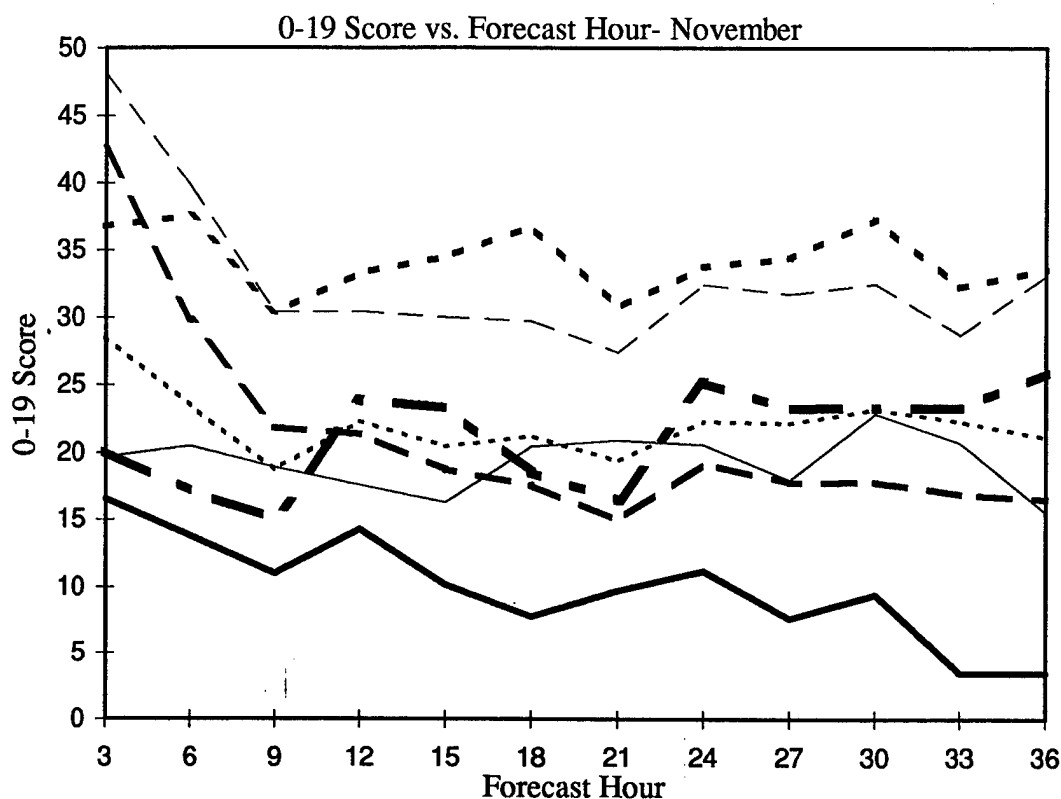


Figure 23. As in Figure 20 for November 1997. See Table 18 for descriptive statistics.

Table 18. Descriptive statistics for Figure 4. 0-19 score for November 1997.

	ADVCLD	Kvamstø	Sundqvist	Persistence	Vertical Column	Layered	RTNEPH
# of Forecasts	112	112	112	112	112	112	112
Mean	9.9	34.3	22.1	19.3	21.2	32.8	21.3
Std Deviation	15.6	14.5	13.5	14.4	15.7	15.6	18.6
Maximum	58.3	88.3	90.2	62.5	89.0	84.3	78.2
Median	3.0	36.2	22.0	17.3	19.2	33.2	19.4
Minimum	0.0	6.2	3.7	2.6	4.5	6.5	0.0

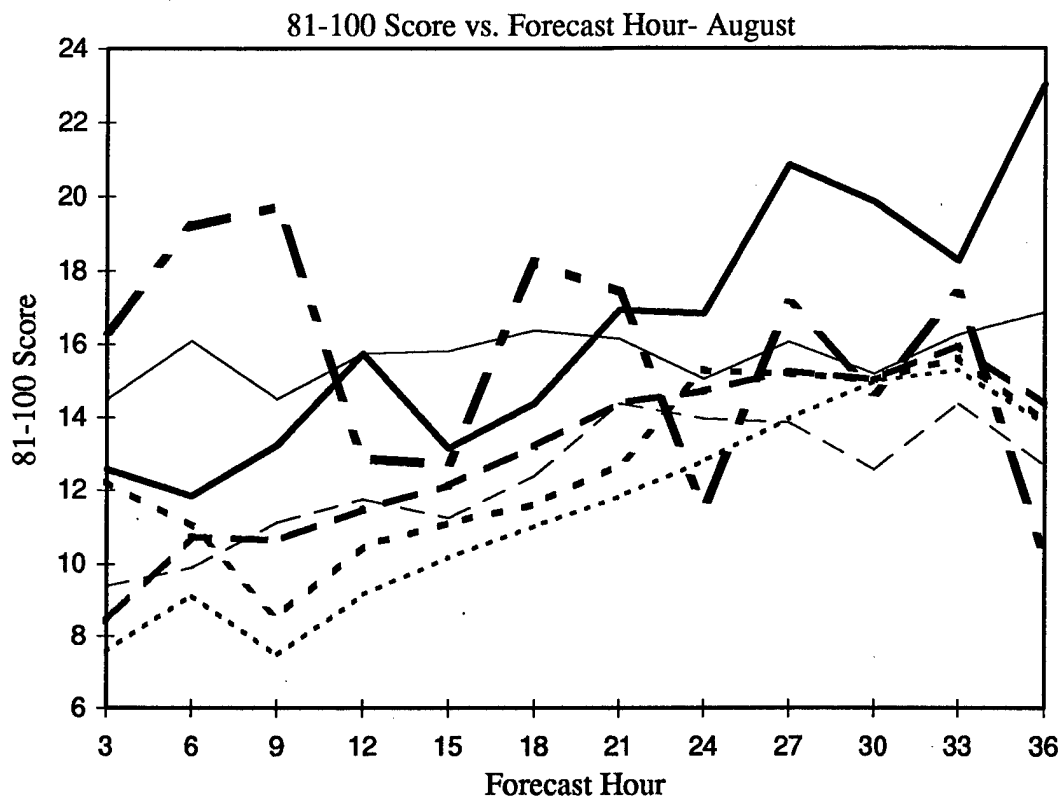


Figure 24. 81-100 score versus forecast hour for August 1997. The thick solid line represents ADVCLD, the thin solid line is persistence, the thick dotted line is the Kvamstø method, the thin dotted line is the Sundqvist method, the thick dashed line is the vertical column method, and the thin dashed line is the layered method. RTNEPH is the thick dashed/dotted line. Average hourly 81-100 scores are plotted. See Table 19 for descriptive statistics.

Table 19. Descriptive statistics for Figure 24. 81-100 score for August 1997.

	ADVCLD	Kvamstø	Sundqvist	Persistence	Vertical Column	Layered	RTNEPH
# of Forecasts	187	187	187	187	187	187	187
Mean	16.4	12.7	11.4	15.7	13.0	12.3	15.6
Std Deviation	14.5	9.3	8.4	8.8	8.2	11.3	11.4
Maximum	73.3	48.9	45.2	45.4	51.0	47.4	53.6
Median	12.3	10.0	9.5	13.6	10.8	10.5	10.5
Minimum	0.0	0.1	0.0	0.0	0.0	0.0	0.0

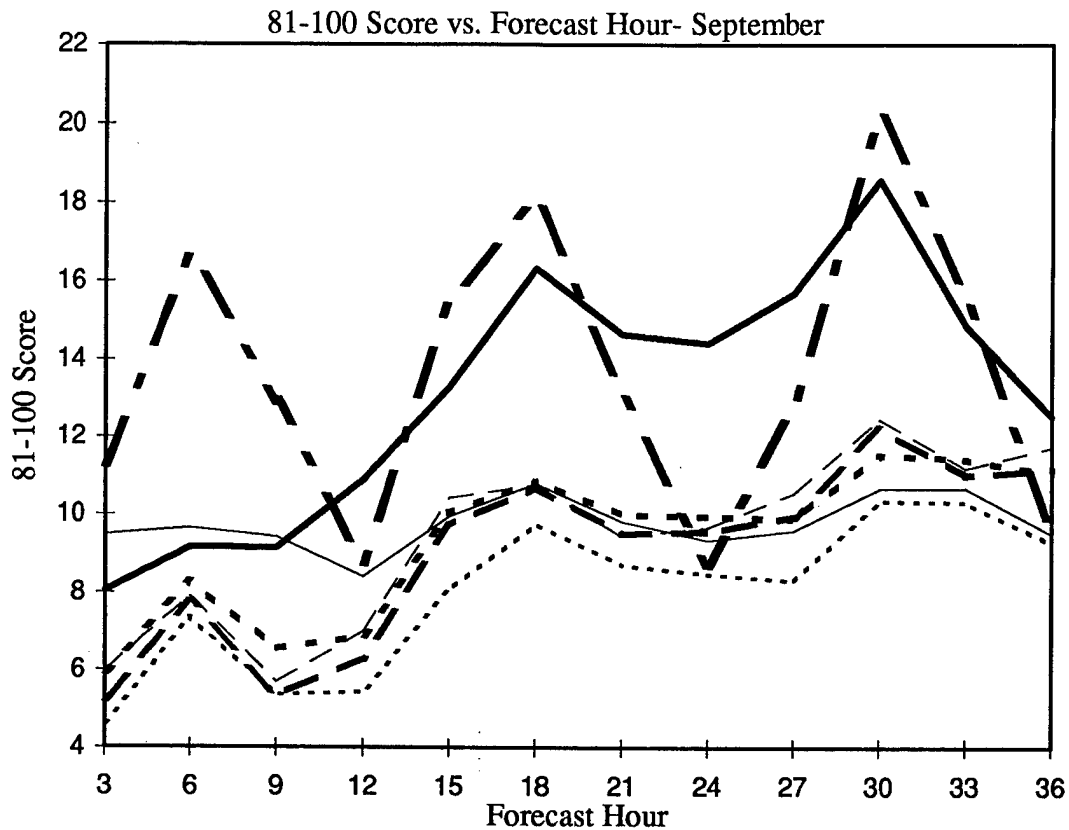


Figure 25. As in Figure 24 for September 1997. See Table 20 for descriptive statistics.

Table 20. Descriptive statistics for Figure 25. 81-100 score for September 1997.

	ADVCLD	Kvamstø	Sundqvist	Persistence	Vertical Column	Layered	RTNEPH
# of Forecasts	445	445	445	445	445	445	445
Mean	13.1	9.4	8.0	9.8	9.0	9.4	13.6
Std Deviation	16.8	11.7	10.6	12.1	11.0	11.8	15.4
Maximum	74.8	53.2	58.2	64.9	63.4	53.5	66.1
Median	5.6	3.7	3.0	5.9	4.2	3.3	6.5
Minimum	0.0	0.0	0.0	0.0	0.0	0.0	0.0

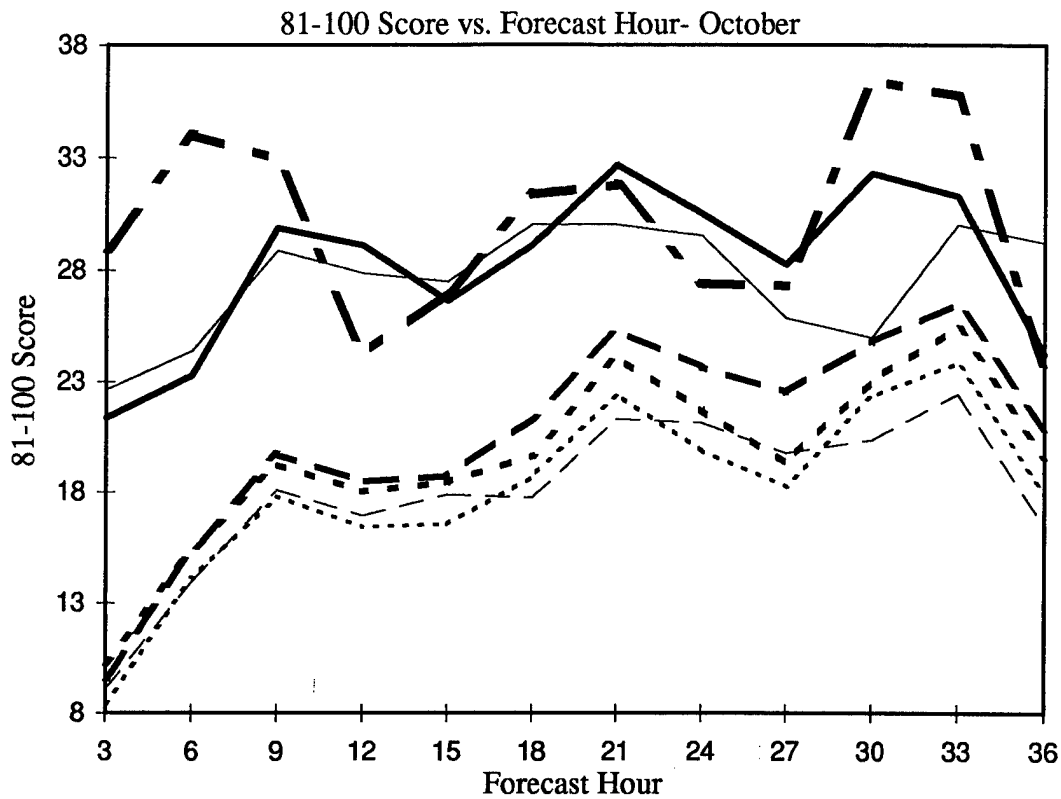


Figure 26. As in Figure 24 for October 1997. See Table 21 for descriptive statistics.

Table 21. Descriptive statistics for Figure 26. 81-100 score for October 1997.

	ADVCLD	Kvamstø	Sundqvist	Persistence	Vertical Column	Layered	RTNEPH
# of Forecasts	390	390	390	390	390	390	390
Mean	28.2	19.5	18.1	27.6	20.6	17.9	30.0
Std Deviation	26.1	16.3	15.2	21.2	17.2	16.6	21.3
Maximum	100.0	77.5	73.5	100.0	88.0	78.8	82.4
Median	25.2	14.7	13.1	23.6	15.3	14.0	23.6
Minimum	0.0	0.0	0.0	0.0	0.0	0.0	0.0

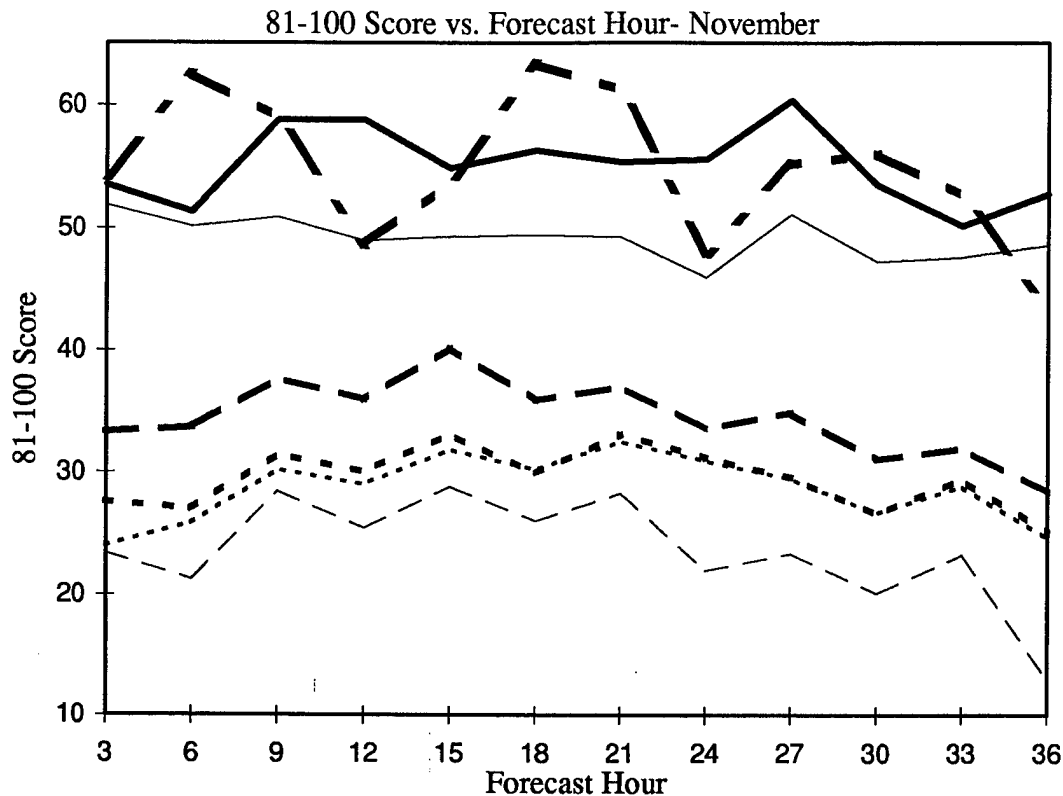


Figure 27. As in Figure 24 for November 1997. See Table 22 for descriptive statistics.

Table 22. Descriptive statistics for Figure 27. 81-100 score for November 1997.

	ADVCLD	Kvamstø	Sundqvist	Persistence	Vertical Column	Layered	RTNEPH
# of Forecasts	112	112	112	112	112	112	112
Mean	55.1	29.5	28.7	49.2	34.5	23.6	54.8
Std Deviation	22.1	13.3	13.1	13.2	15.5	18.4	23.1
Maximum	96.8	63.0	57.7	82.6	70.7	71.0	90.1
Median	53.7	25.6	25.8	46.9	31.6	15.1	47.9
Minimum	3.9	0.0	0.0	1.0	0.0	0.0	0.0

The MM5 schemes significantly underforecasted the amount of overcast conditions. This is especially true in October and November which, with RTNEPH average 81-100 scores of 30 percent and 55 percent respectively, were the cloudiest months. The tendency to significantly underforecast is also evident in August and September during the first 9 hours, or "spin-up" time, of the forecast cycle.

ADVCLD did an excellent job of producing overcast percentages similar to those analyzed by the RTNEPH. It outperformed all of the MM5 schemes and persistence.

Persistence, too, outperformed all of the MM5 schemes at producing the correct overcast percentages. Persistence did, however, exhibit a tendency to slightly underforecast overcast skies when compared against the RTNEPH analyses.

4.4 Contingency Table Results

4.4.1 Hit Rate Results

Figures 28-31 display the results of the hit rate calculation for a broken cloudiness forecast for August-November respectively. Average hourly hit rate values are plotted. Tables 23-26 contain the descriptive statistics for Figures 28-31 respectively.

For August-October, the MM5 schemes generally outperform ADVCLD after the 12-hr point, with the Kvamstø scheme performing the best. In November, the vertical column method had higher hit rate scores than any other MM5 scheme but did worse than ADVCLD.

The hit rate values for the MM5 schemes for the months of August and September ranged from 74-81. These were the driest two months of the study (RTNEPH 81-100 scores of 15 and 13 respectively). The hit rate values for October and November, however, ranged from 60-69. Again, the dry bias in MM5 is evident.

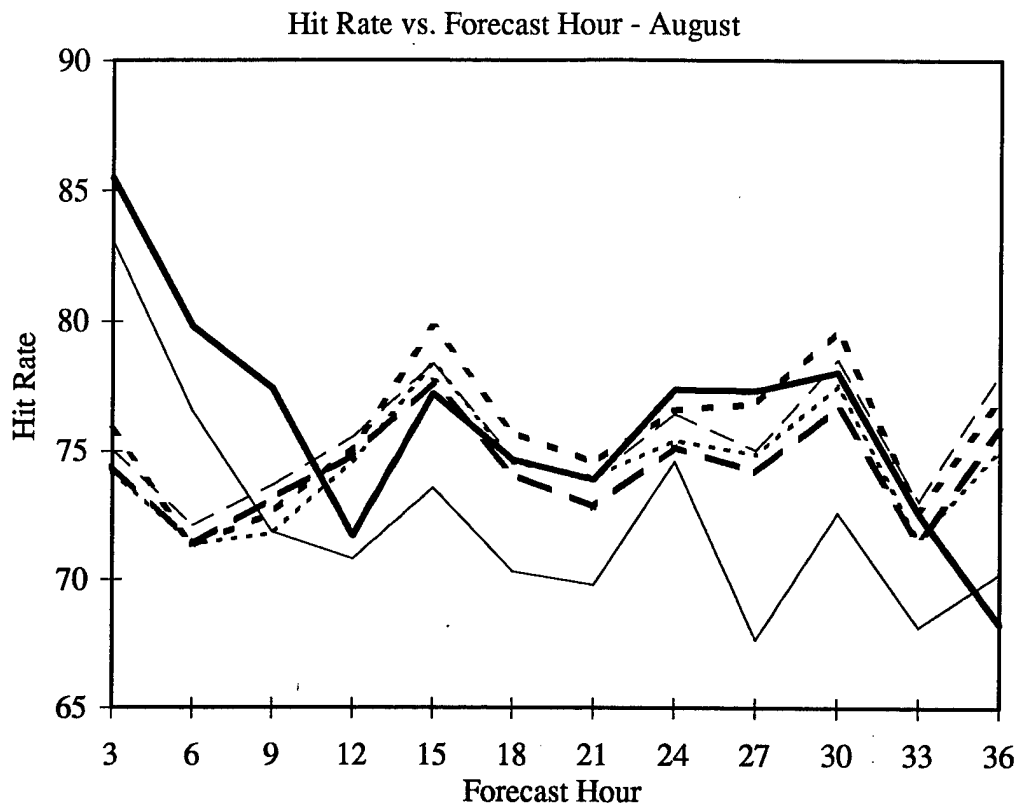


Figure 28. Hit rate for a broken cloudiness forecast versus forecast hour for August 1997. The thick solid line represents ADVCLD, the thin solid line is persistence, the thick dotted line is the Kvamstø method, the thin dotted line is the Sundqvist method, the thick dashed line is the vertical column method, and the thin dashed line is the layered method. Average hourly hit rate values are plotted. See Table 23 for descriptive statistics.

Table 23. Descriptive statistics for Figure 28. Hit rate for August 1997.

	ADVCLD	Kvamstø	Sundqvist	Persistence	Vertical Column	Layered
# of Forecasts	187	187	187	187	187	187
Mean	76.1	75.6	74.4	72.4	74.3	75.4
Std Deviation	13.3	11.9	12.3	11.9	11.5	11.3
Maximum	100.0	99.2	99.8	99.6	99.7	100.0
Median	79.3	79.0	77.5	75.2	76.3	77.5
Minimum	19.8	43.3	43.3	31.3	43.2	48.5

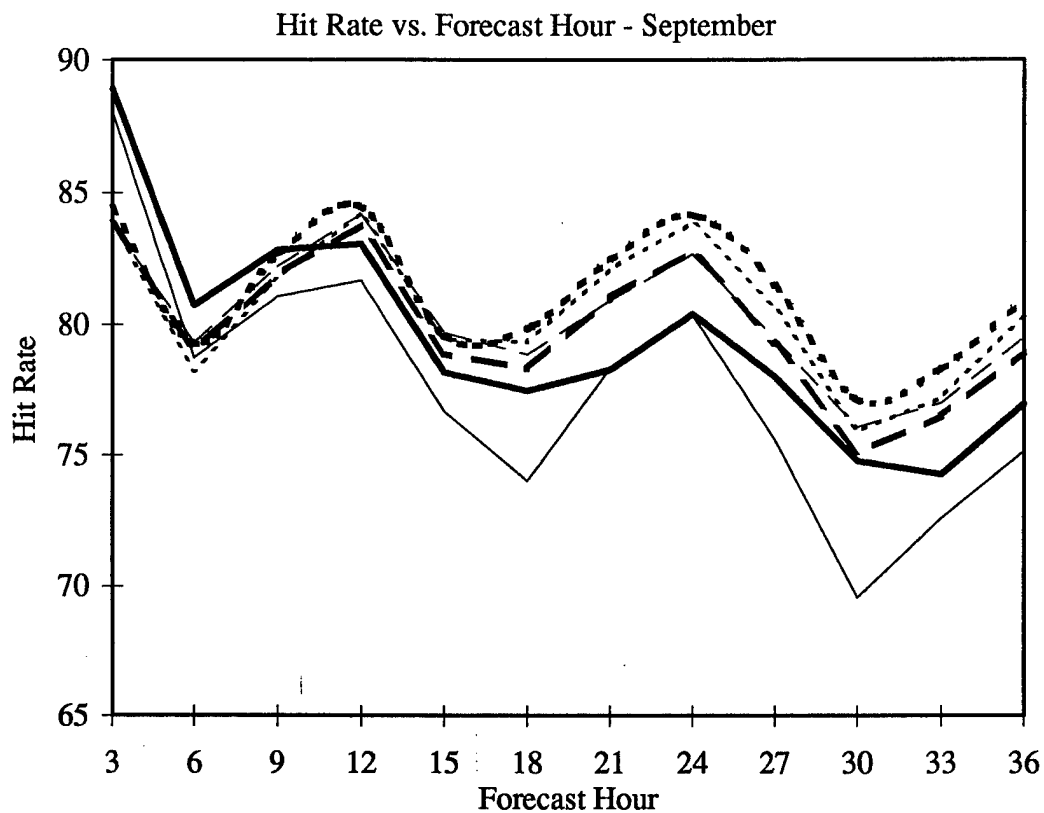


Figure 29. As in Figure 28 for September 1997. See Table 24 for descriptive statistics.

Table 24. Descriptive statistics for Figure 29. Hit rate for September 1997.

	ADVCLD	Kvamstø	Sundqvist	Persistence	Vertical Column	Layered
# of Forecasts	445	445	445	445	445	445
Mean	79.5	81.2	80.6	77.6	79.9	80.3
Std Deviation	13.1	12.2	13.2	14.6	13.1	13.3
Maximum	100.0	100.0	100.0	100.0	100.0	100.0
Median	81.8	84.7	83.6	80.1	82.8	83.9
Minimum	35.7	40.7	26.4	23.9	31.0	41.5

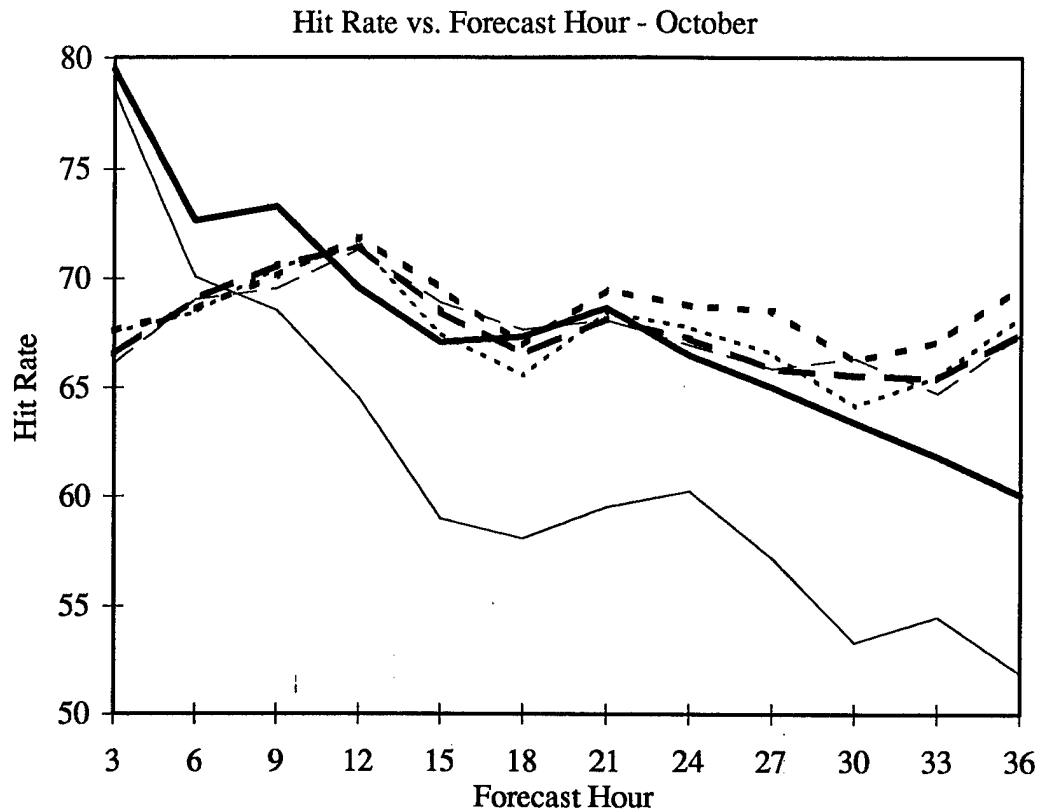


Figure 30. As in Figure 28 for October 1997. See Table 25 for descriptive statistics.

Table 25. Descriptive statistics for Figure 30. Hit rate for October 1997.

	ADVCLD	Kvamstø	Sundqvist	Persistence	Vertical Column	Layered
# of Forecasts	390	390	390	390	390	390
Mean	67.9	68.7	67.6	61.3	67.7	67.7
Std Deviation	18.2	13.6	13.9	17.6	13.2	13.7
Maximum	100.0	100.0	100.0	100.0	100.0	100.0
Median	67.7	68.6	68.7	61.8	67.9	66.7
Minimum	10.0	0.0	0.0	0.1	0.0	3.9

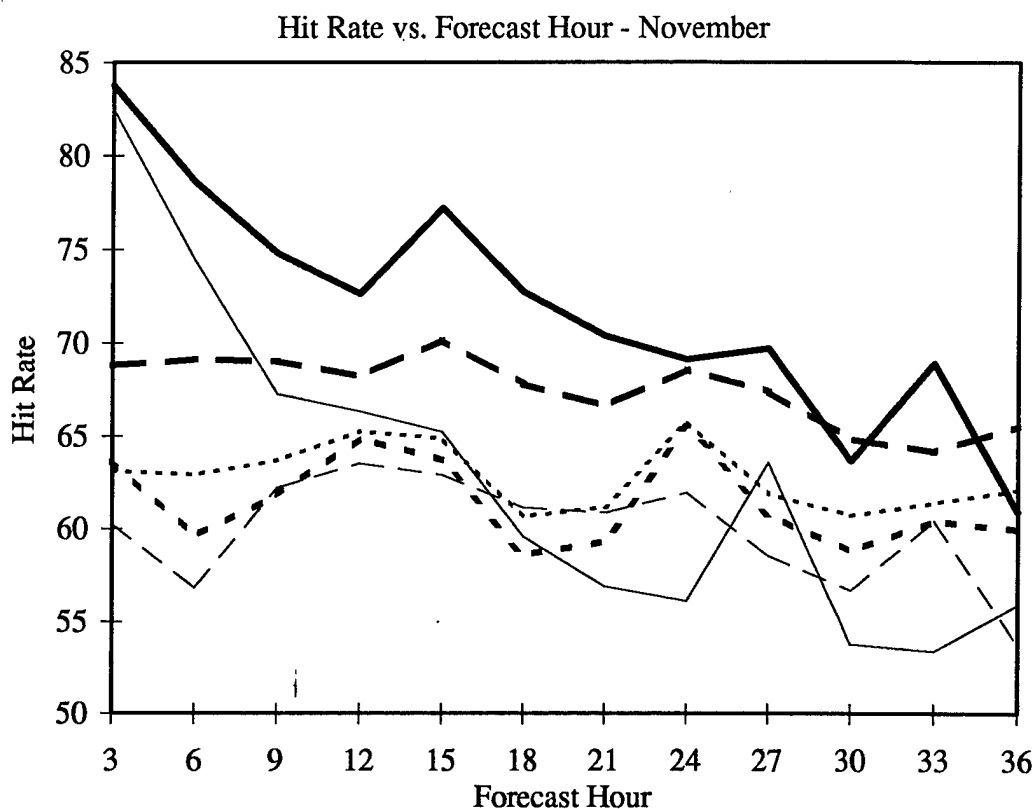


Figure 31. As in Figure 28 for November 1997. See Table 26 for descriptive statistics.

Table 26. Descriptive statistics for Figure 31. Hit rate for November 1997.

	ADVCLD	Kvamstø	Sundqvist	Persistence	Vertical Column	Layered
# of Forecasts	112	112	112	112	112	112
Mean	71.9	61.4	62.8	62.9	67.5	59.9
Std Deviation	14.1	10.7	10.0	13.7	9.5	13.7
Maximum	97.4	98.8	97.8	92.3	97.6	91.5
Median	70.7	61.1	63.1	64.0	66.9	60.7
Minimum	35.6	33.0	29.9	25.5	34.0	34.4

ADVCLD, as mentioned above, outperformed all other schemes in November and also during the first 9 hours of the forecast cycle in August-October. From the 12-hr to 30-hr points in these months, ADVCLD was competitive with the other schemes, however, by the 36-hr point, ADVCLD had lower hit rates than all the MM5 schemes.

Persistence had high hit rates at the 3-hr and 6-hr points, but by the 9-hr point it had lower hit rates than any other scheme for August-October. In November, by the 18-hr point persistence was consistently the worst forecast.

4.4.2 Critical Success Index Results

Figures 32-35 display the results of the critical success index calculation for a broken cloudiness forecast for August-November respectively. Average hourly CSI values are plotted. Tables 27-30 contain the descriptive statistics for Figures 32-35 respectively.

The CSI scores for the MM5 schemes showed improvement over the first 9-12 hours of the forecast model as the moisture “spun-up”. After the 12-hr point, the CSI values remained steady or improved just slightly for the four months considered in this study.

ADVCLD outperformed all other forecasts at all validation hours. The only exception was the 3-hr point where persistence had the highest critical success index scores.

For August-October persistence contended with ADVCLD as the best method until the 12-hr point, but by the 27-hr point it was the worst method. In November, persistence consistently remained one of the best three methods along with ADVCLD and the vertical column method.

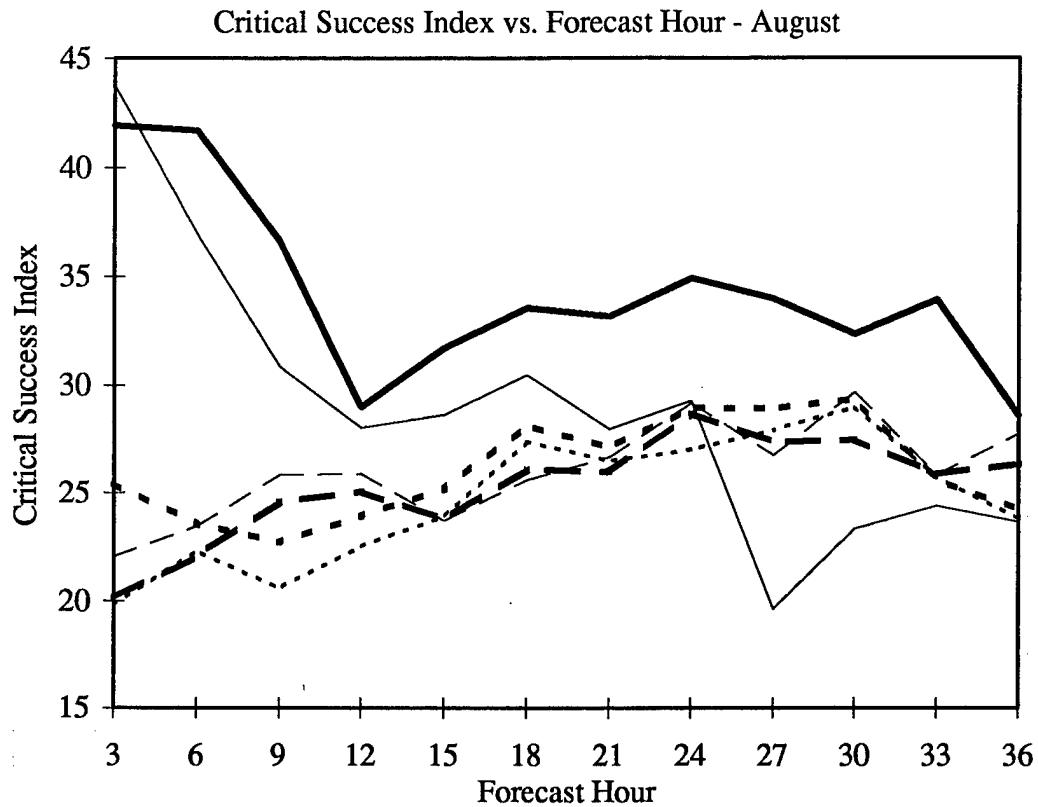


Figure 32. Critical success index versus forecast hour for August 1997. The thick solid line represents ADVCLD, the thin solid line is persistence, the thick dotted line is the Kvamstø method, the thin dotted line is the Sundqvist method, the thick dashed line is the vertical column method, and the thin dashed line is the layered method. Average hourly CSI values are plotted. See Table 27 for descriptive statistics.

Table 27. Descriptive statistics for Figure 32. Critical success index for August 1997.

	ADVCLD	Kvamstø	Sundqvist	Persistence	Vertical Column	Layered
# of Forecasts	187	187	187	187	187	187
Mean	34.3	26.1	24.7	28.9	25.3	26.0
Std Deviation	19.8	16.2	15.5	15.7	13.9	14.9
Maximum	100.0	71.2	71.5	74.7	59.1	100.0
Median	31.6	22.7	22.8	25.8	23.0	23.3
Minimum	0.0	0.0	0.0	0.0	0.0	0.0

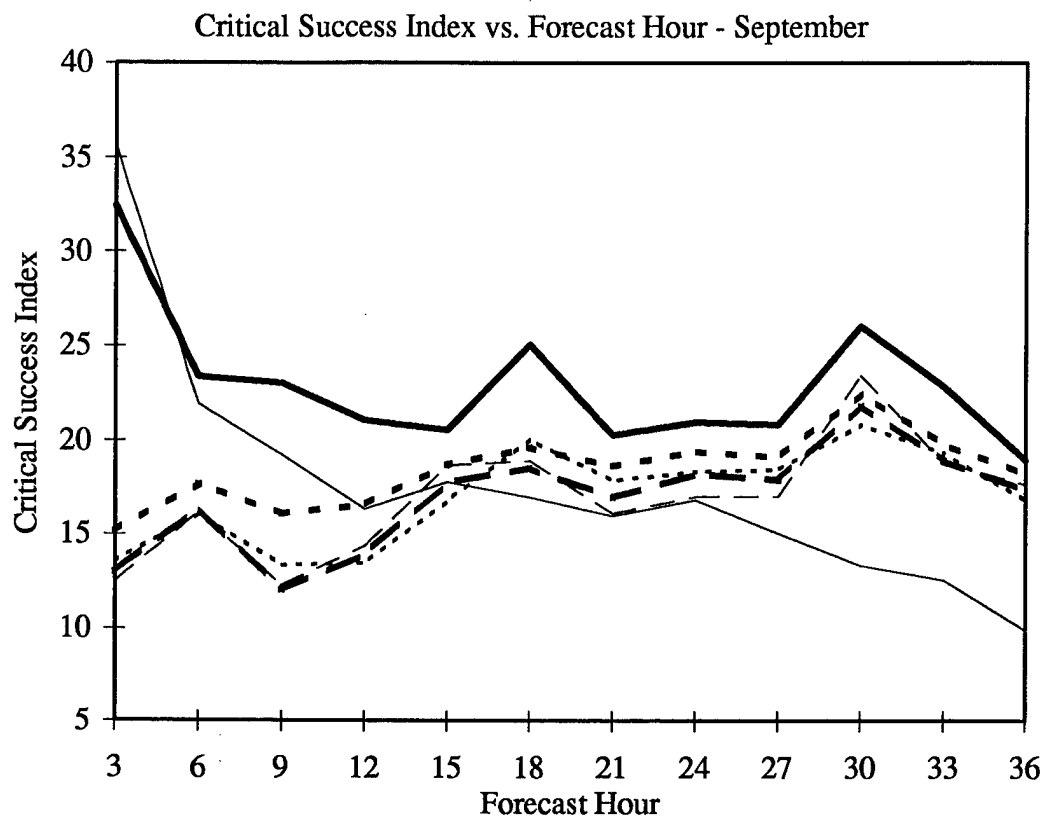


Figure 33. As in Figure 32 for September 1997. See Table 28 for descriptive statistics.

Table 28. Descriptive statistics for Figure 33. Critical success index for September 1997.

	ADVCLD	Kvamstø	Sundqvist	Persistence	Vertical Column	Layered
# of Forecasts	445	445	445	445	445	445
Mean	23.0	18.5	17.1	17.6	16.9	16.9
Std Deviation	22.7	19.4	18.3	17.0	18.5	19.5
Maximum	100.0	100.0	100.0	100.0	100.0	100.0
Median	17.2	11.7	11.0	13.0	10.7	9.8
Minimum	0.0	0.0	0.0	0.0	0.0	0.0

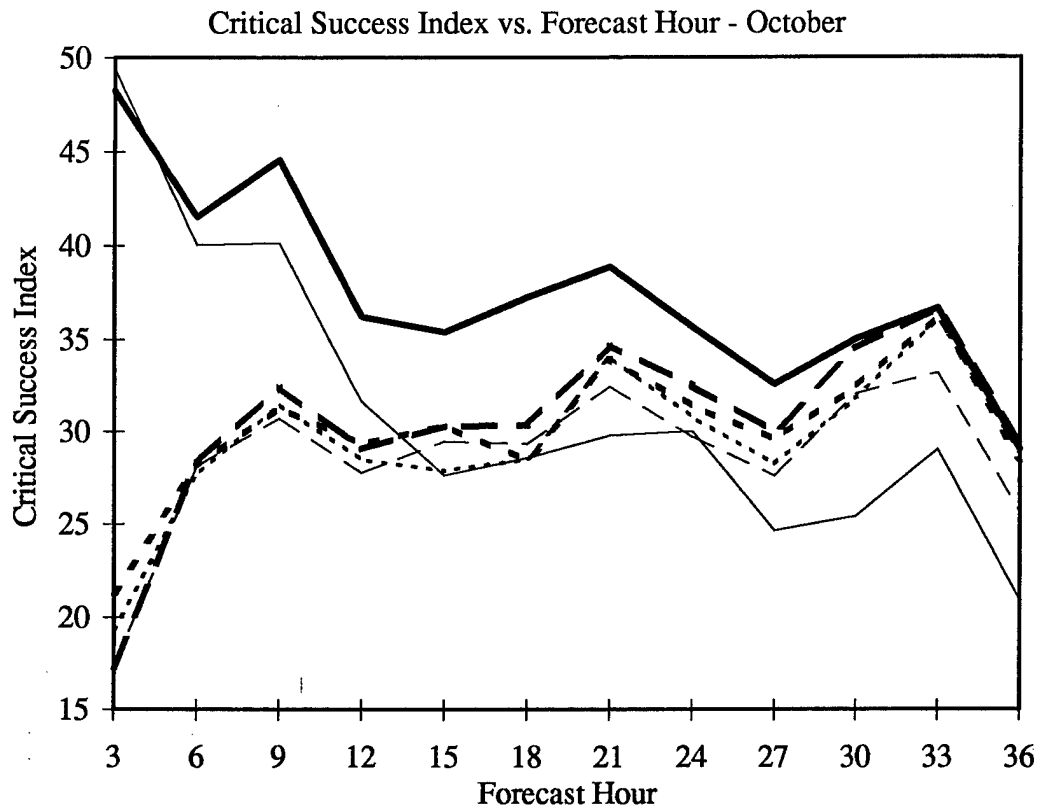


Figure 34. As in Figure 32 for October 1997. See Table 29 for descriptive statistics.

Table 29. Descriptive statistics for Figure 34. Critical success index for October 1997.

	ADVCLD	Kvamstø	Sundqvist	Persistence	Vertical Column	Layered
# of Forecasts	390	390	390	390	390	390
Mean	37.6	30.1	29.4	31.4	30.5	28.6
Std Deviation	24.9	23.7	23.5	22.0	23.7	23.5
Maximum	100.0	100.0	100.0	100.0	100.0	100.0
Median	34.9	27.2	25.5	27.4	25.7	24.2
Minimum	0.0	0.0	0.0	0.0	0.0	0.0

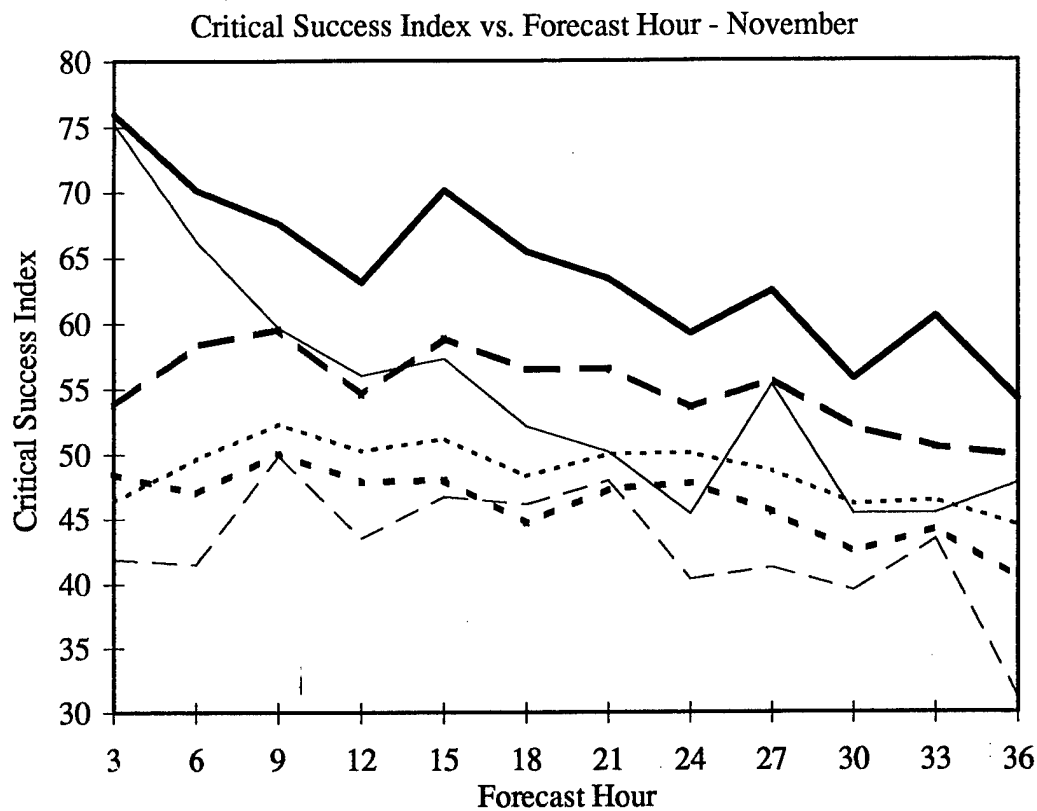


Figure 35. As in Figure 32 for November 1997. See Table 30 for descriptive statistics.

Table 30. Descriptive statistics for Figure 35. Critical success index for November 1997.

	ADVCLD	Kvamstø	Sundqvist	Persistence	Vertical Column	Layered
# of Forecasts	112	112	112	112	112	112
Mean	64.0	46.1	48.6	54.7	55.0	42.8
Std Deviation	21.7	16.7	16.1	19.2	17.9	21.6
Maximum	97.4	93.8	74.2	89.9	88.2	89.1
Median	59.8	43.7	46.8	52.4	52.9	35.0
Minimum	0.0	0.0	0.0	0.0	0.0	0.0

4.4.3 Probability of Detection Results

Figures 36-39 display the results of the probability of detection calculation for a broken cloudiness forecast for August-November respectively. Average hourly POD values are plotted. Tables 31-34 contain the descriptive statistics for Figures 36-39 respectively.

The MM5 schemes, although displaying improvement throughout the forecast cycle, performed poorly when compared against ADVCLD and even persistence. The MM5 schemes could not consistently beat persistence which was the best method at the 3-hr point. After the 3-hr point, ADVCLD was the best method.

4.4.4 False Alarm Rate Results

Figures 40-43 display the results of the false alarm rate calculation for a broken cloudiness forecast for August-November respectively. Average hourly FAR values are plotted. Tables 35-38 contain the descriptive statistics for Figures 40-43 respectively.

The MM5 methods, ADVCLD, and persistence all exhibited increasing false alarm rates with increasing forecast length. For the cloudiest months (October and November), the MM5 schemes had lower false alarm rates than both ADVCLD and persistence after the 12-hr point. For August and September, ADVCLD consistently had the lowest false alarm rates. In general, persistence had the highest false alarm rates after the 6-hr point.

The false alarm rates for all six forecasting methods were higher in September (the driest month) than in any other month and were lower in November (the cloudiest month) than in any other month.

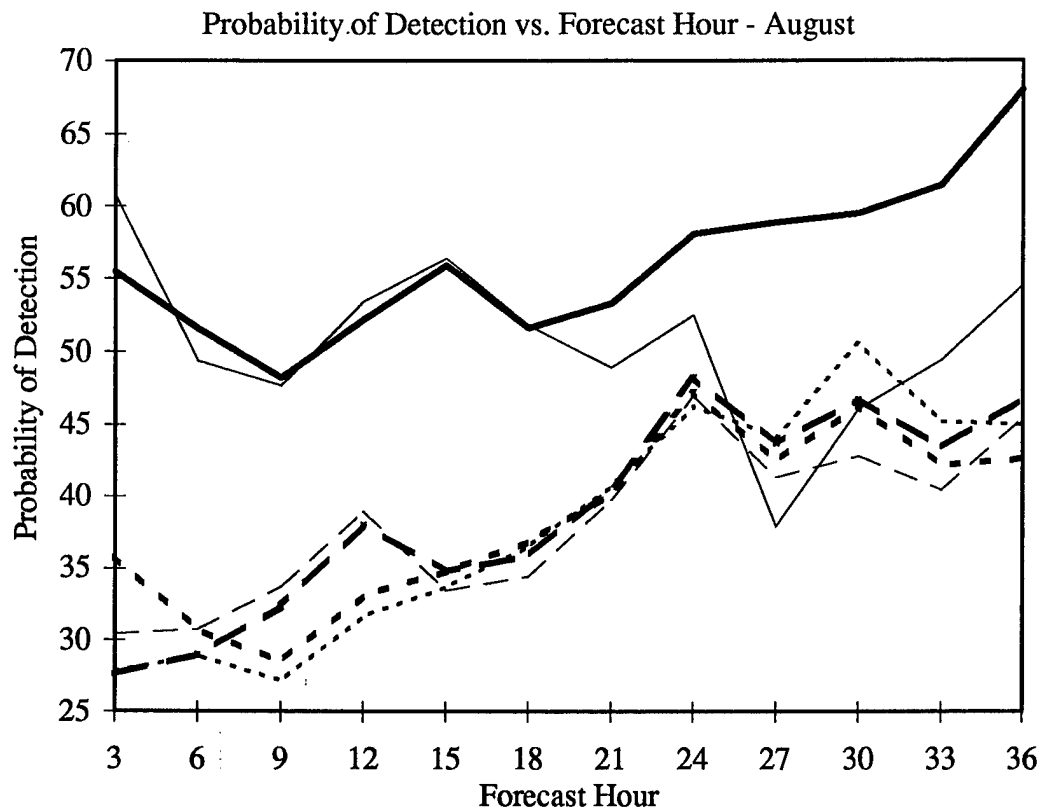


Figure 36. Probability of detection versus forecast hour for August 1997. The thick solid line represents ADVCLD, the thin solid line is persistence, the thick dotted line is the Kvamstø method, the thin dotted line is the Sundqvist method, the thick dashed line is the vertical column method, and the thin dashed line is the layered method. Average hourly POD values are plotted. See Table 31 for descriptive statistics.

Table 31. Descriptive statistics for Figure 36. Probability of detection for August 1997.

	ADVCLD	Kvamstø	Sundqvist	Persistence	Vertical Column	Layered
# of Forecasts	187	187	187	187	187	187
Mean	56.2	38.4	38.1	50.7	38.9	38.2
Std Deviation	25.2	22.9	23.5	23.4	19.2	18.1
Maximum	100.0	100.0	100.0	100.0	88.9	81.2
Median	59.9	35.7	38.0	51.9	38.6	37.4
Minimum	0.0	0.0	0.0	0.0	0.0	0.0

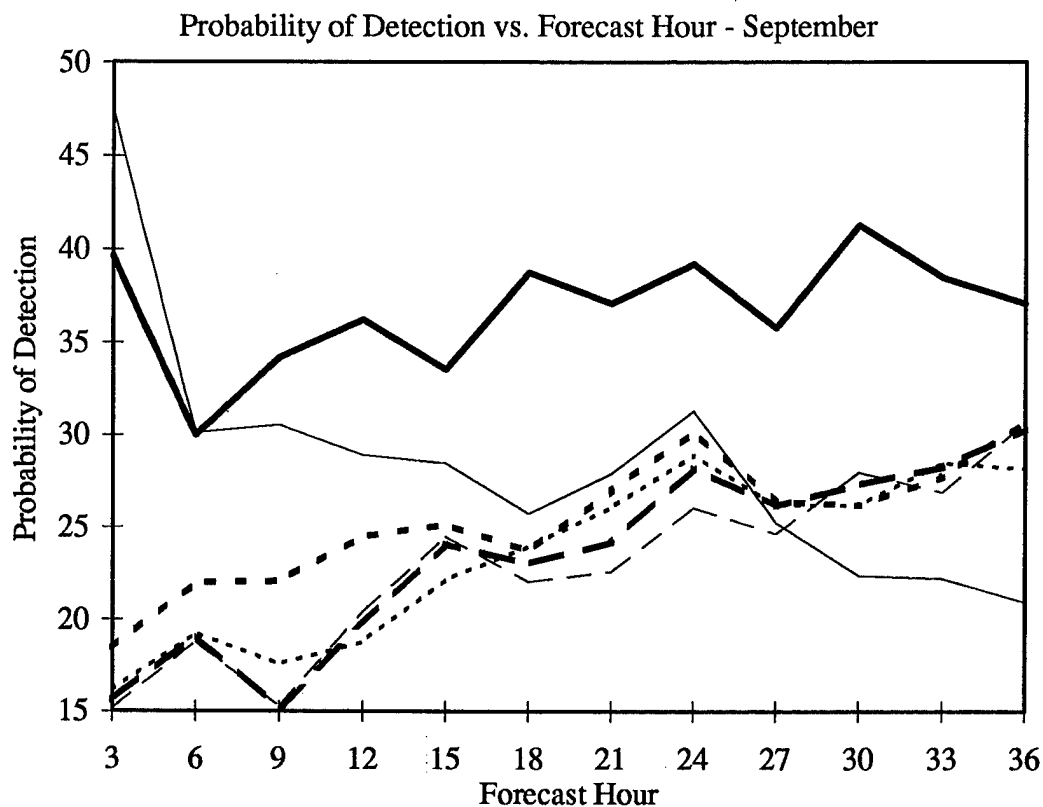


Figure 37. As in Figure 36 for September 1997. See Table 32 for descriptive statistics.

Table 32. Descriptive statistics for Figure 37. Probability of detection for September 1997.

	ADVCLD	Kvamstø	Sundqvist	Persistence	Vertical Column	Layered
# of Forecasts	445	445	445	445	445	445
Mean	36.8	25.3	23.5	28.4	23.4	22.9
Std Deviation	30.9	23.2	22.0	23.5	21.9	22.5
Maximum	100.0	81.4	93.0	100.0	97.2	100.0
Median	33.8	18.1	17.5	24.8	16.8	15.8
Minimum	0.0	0.0	0.0	0.0	0.0	0.0

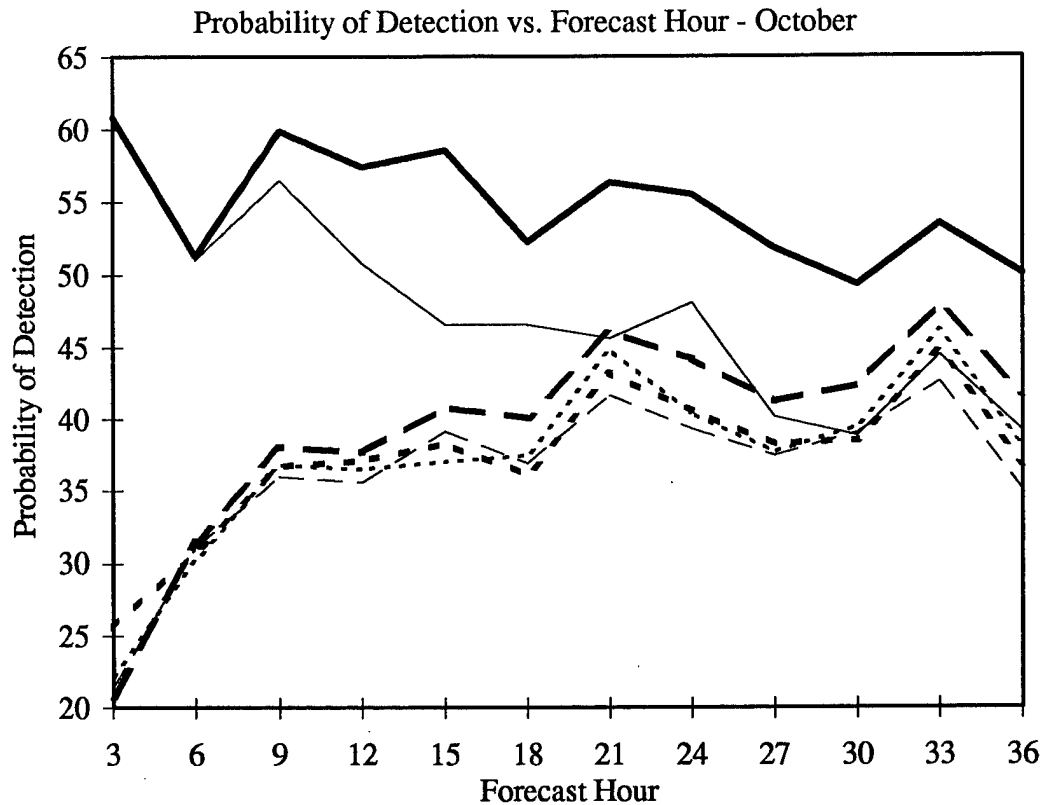


Figure 38. As in Figure 36 for October 1997. See Table 33 for descriptive statistics.

Table 33. Descriptive statistics for Figure 38. Probability of detection for October 1997.

	ADVCLD	Kvamstø	Sundqvist	Persistence	Vertical Column	Layered
# of Forecasts	390	390	390	390	390	390
Mean	54.7	37.2	37.2	47.4	39.3	36.3
Std Deviation	24.3	24.3	24.1	25.2	25.6	26.1
Maximum	100.0	98.9	94.5	100.0	98.5	96.1
Median	59.8	39.4	38.7	53.6	39.2	37.6
Minimum	0.0	0.0	0.0	0.0	0.0	0.0

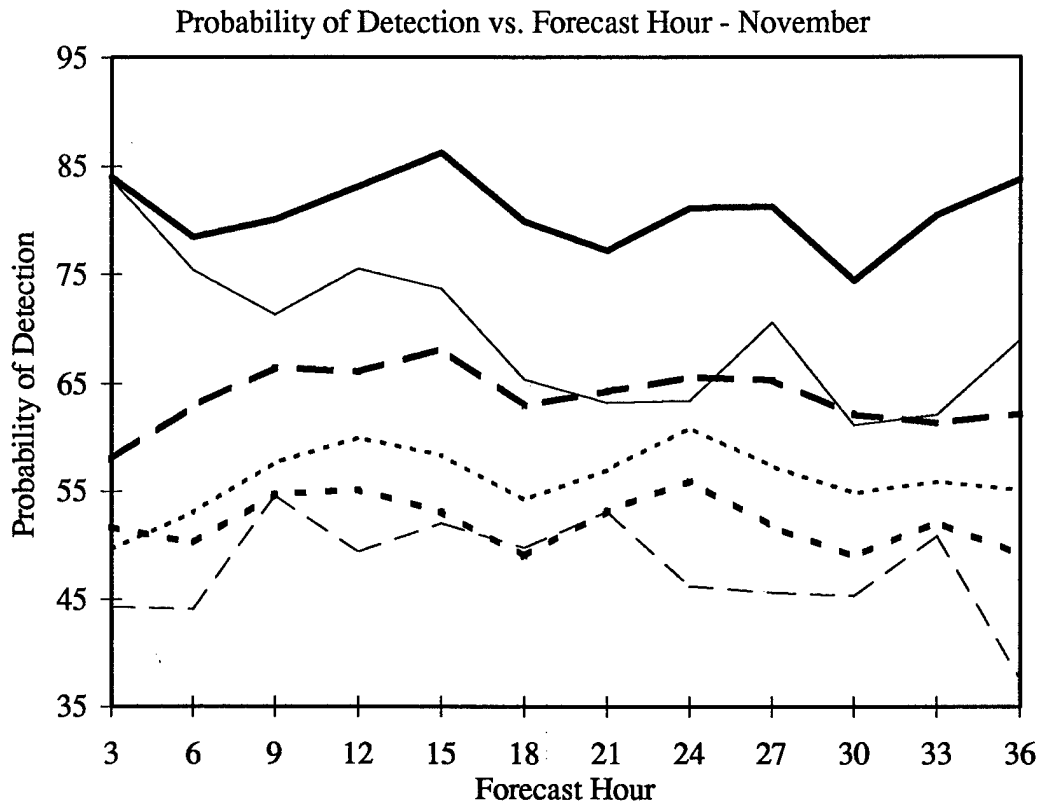


Figure 39. As in Figure 36 for November 1997. See Table 34 for descriptive statistics.

Table 34. Descriptive statistics for Figure 39. Probability of detection for November 1997.

	ADVCLD	Kvamstø	Sundqvist	Persistence	Vertical Column	Layered
# of Forecasts	112	112	112	112	112	112
Mean	80.8	52.1	56.1	69.5	63.8	47.7
Std Deviation	18.0	14.7	15.1	16.3	14.6	21.0
Maximum	100.0	93.8	82.4	100.0	93.8	92.0
Median	87.4	51.9	56.0	71.8	63.0	41.9
Minimum	28.9	0.0	3.1	31.6	8.8	5.9

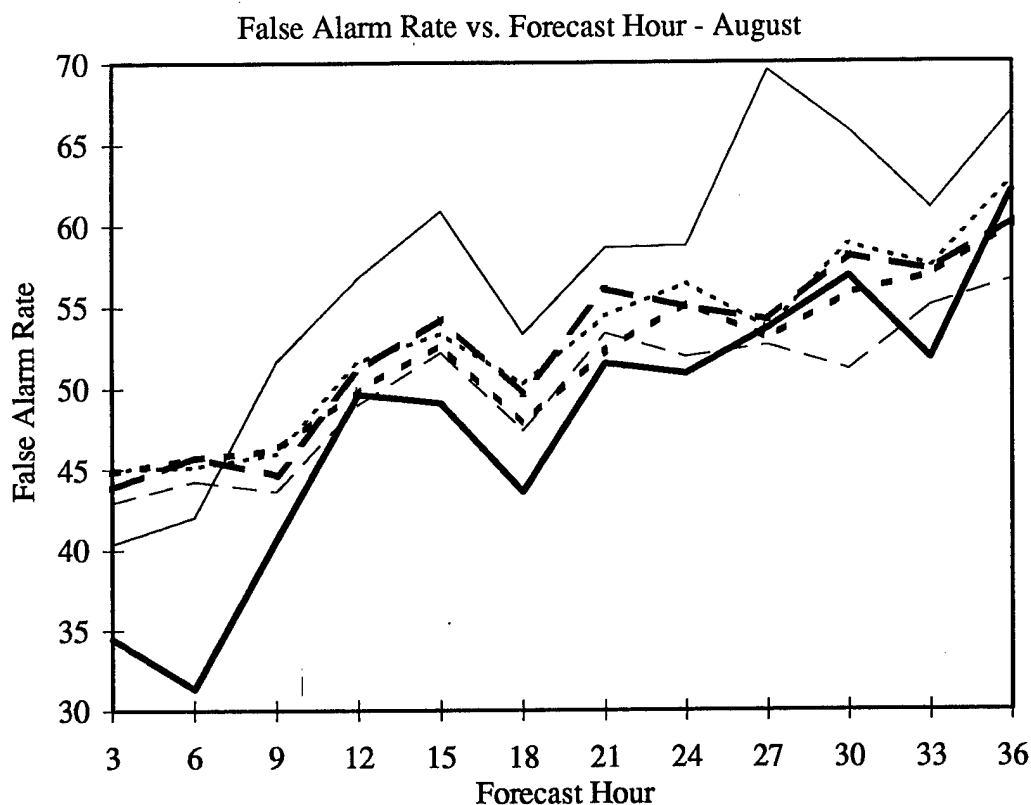


Figure 40. False alarm rate versus forecast hour for August 1997. The thick solid line represents ADVCLD, the thin solid line is persistence, the thick dotted line is the Kvamstø method, the thin dotted line is the Sundqvist method, the thick dashed line is the vertical column method, and the thin dashed line is the layered method. Average hourly FAR values are plotted. See Table 35 for descriptive statistics.

Table 35. Descriptive statistics for Figure 40. False alarm rate for August 1997.

	ADVCLD	Kvamstø	Sundqvist	Persistence	Vertical Column	Layered
# of Forecasts	187	187	187	187	187	187
Mean	47.9	51.7	52.9	57.2	52.5	50.0
Std Deviation	26.4	26.6	26.8	21.9	25.5	25.9
Maximum	100.0	100.0	100.0	100.0	100.0	100.0
Median	48.7	53.5	57.9	60.8	56.0	51.3
Minimum	0.0	1.2	0.0	10.7	0.0	0.0

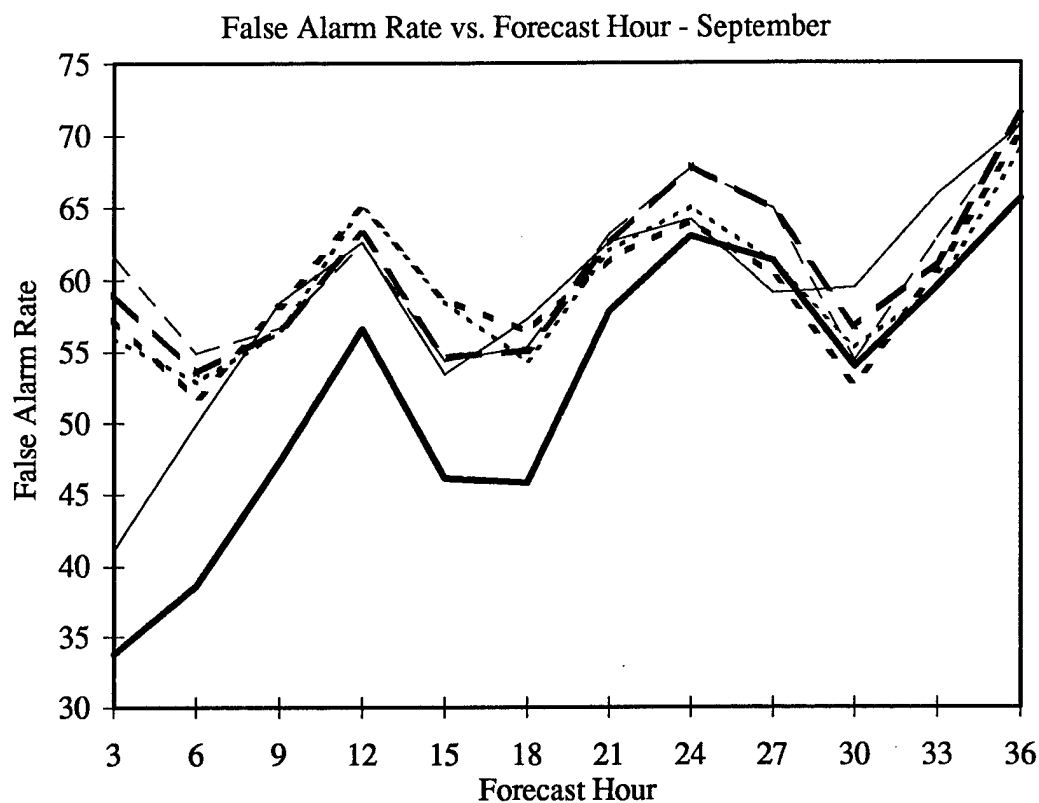


Figure 41. As in Figure 40 for September 1997. See Table 36 for descriptive statistics.

Table 36. Descriptive statistics for Figure 41. False alarm rate for September 1997.

	ADVCLD	Kvamstø	Sundqvist	Persistence	Vertical Column	Layered
# of Forecasts	445	445	445	445	445	445
Mean	52.4	59.7	59.6	58.7	60.5	60.8
Std Deviation	33.8	30.5	31.1	30.9	30.9	31.3
Maximum	100.0	100.0	100.0	100.0	100.0	100.0
Median	53.7	64.4	63.6	64.2	67.2	65.1
Minimum	0.0	0.0	0.0	0.0	0.0	0.0

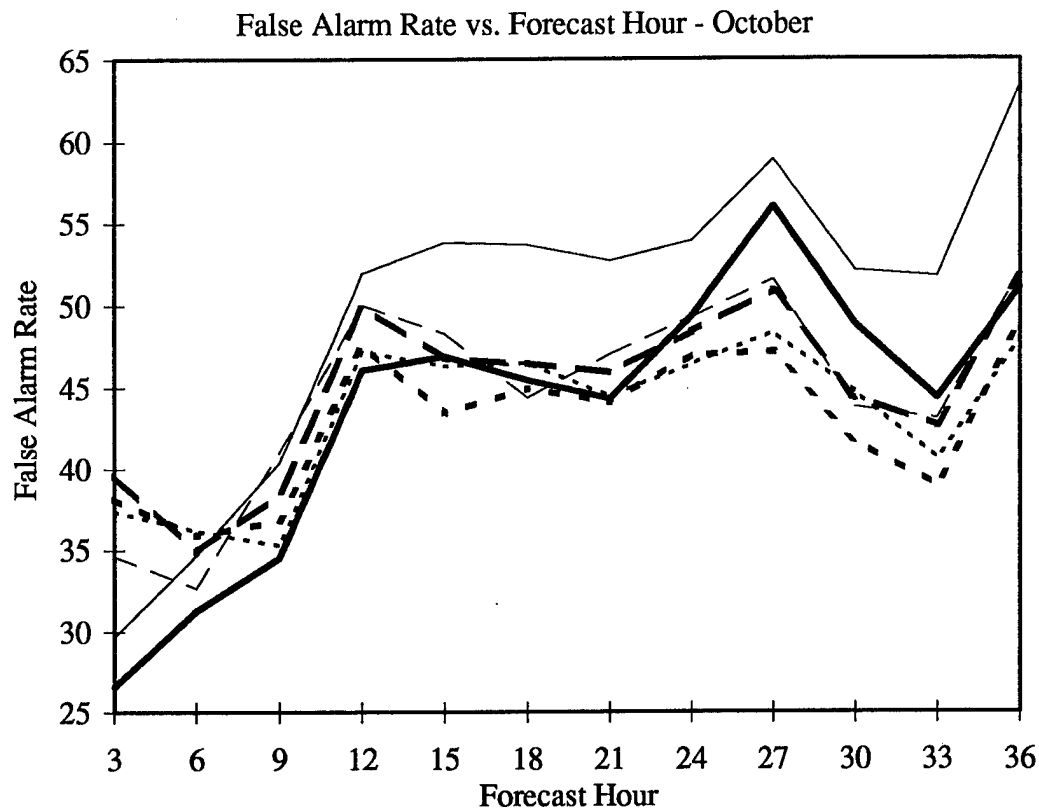


Figure 42. As in Figure 40 for October 1997. See Table 37 for descriptive statistics.

Table 37. Descriptive statistics for Figure 42. False alarm rate for October 1997.

	ADVCLD	Kvamstø	Sundqvist	Persistence	Vertical Column	Layered
# of Forecasts	390	390	390	390	390	390
Mean	43.7	42.9	43.4	49.7	45.0	44.8
Std Deviation	28.7	31.0	30.8	27.5	30.0	30.4
Maximum	100.0	100.0	100.0	100.0	100.0	100.0
Median	45.1	37.8	38.8	51.3	42.4	40.9
Minimum	0.0	0.0	0.0	0.0	0.0	0.0

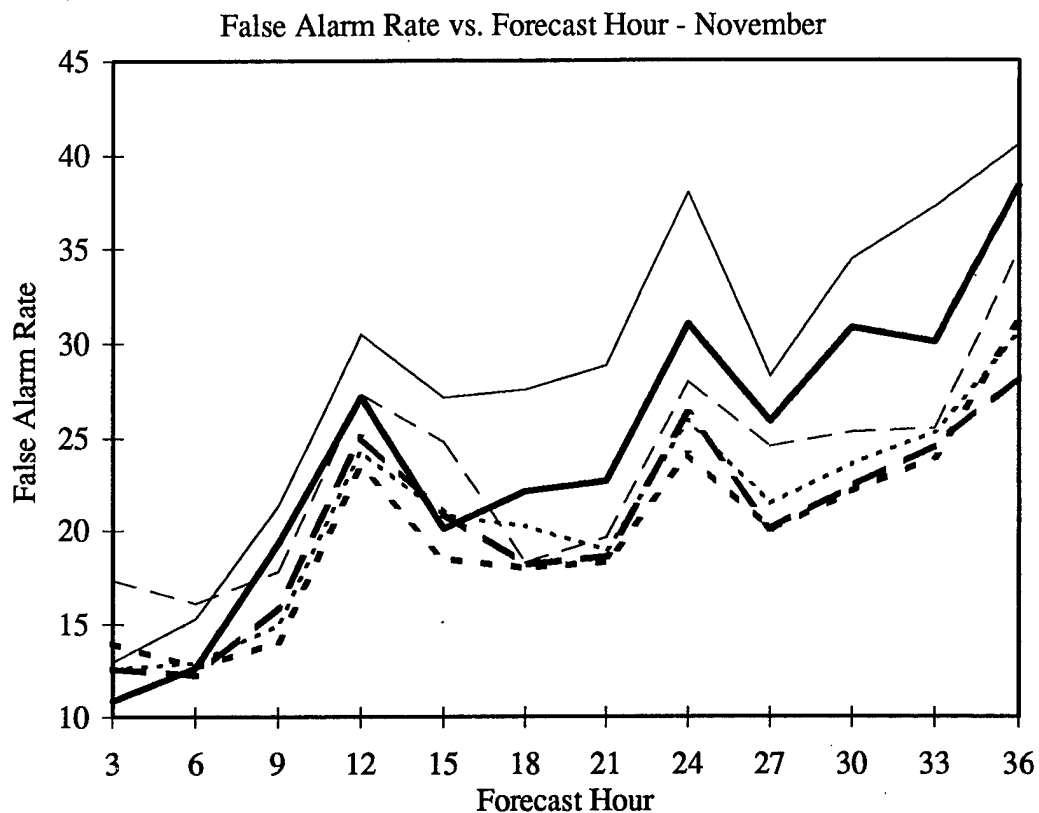


Figure 43. As in Figure 40 for November 1997. See Table 38 for descriptive statistics.

Table 38. Descriptive statistics for Figure 43. False alarm rate for November 1997.

	ADVCLD	Kvamstø	Sundqvist	Persistence	Vertical Column	Layered
# of Forecasts	112	112	112	112	112	112
Mean	24.3	20.0	20.9	28.5	20.4	23.9
Std Deviation	22.7	26.3	22.3	23.5	21.8	24.4
Maximum	100.0	100.0	100.0	100.0	100.0	100.0
Median	27.8	21.5	22.6	28.9	20.6	23.5
Minimum	0.0	0.0	0.0	0.2	0.0	0.0

4.5 Skill Score Results

4.5.1 Hit Rate Skill Score Results

Figures 44-47 display the results of the hit rate skill score calculation for a broken cloudiness forecast for August-November respectively. Average hourly hit rate skill score values are plotted as percentages. Tables 39-42 contain the descriptive statistics for Figures 44-47 respectively. The entries in tables 39-42 are descriptive statistics calculated using only the 12 values plotted in Figures 44-47.

All of the hit rates for the MM5 schemes represented an improvement over persistence from the 9-hr point until the 36-hr point for the months of August-October. At the 3-hr and 6-hr points, persistence performed better. In November, the vertical column method had positive skill scores from the 9-hr point to the 36-hr point, while the other three schemes had positive skill scores only from 18-24 hours and 30-36 hours.

The hit rate for ADVCLD represented an improvement over persistence at all forecast times for all four months. The only exceptions were the 36-hr point in August and the 21-hr point in September.

4.5.2 Critical Success Index Skill Score Results

Figures 48-51 display the results of the hit rate skill score calculation for a broken cloudiness forecast for August-November respectively. Average hourly hit rate skill score values are plotted as percentages. Tables 43-46 contain the descriptive statistics for Figures 48-51 respectively. The entries in tables 43-46 are descriptive statistics calculated using only the 12 values plotted in Figures 48-51.

In August the critical success indices for the MM5 schemes represented an improvement over persistence only from the 27-hr point to the 36-hr point. In

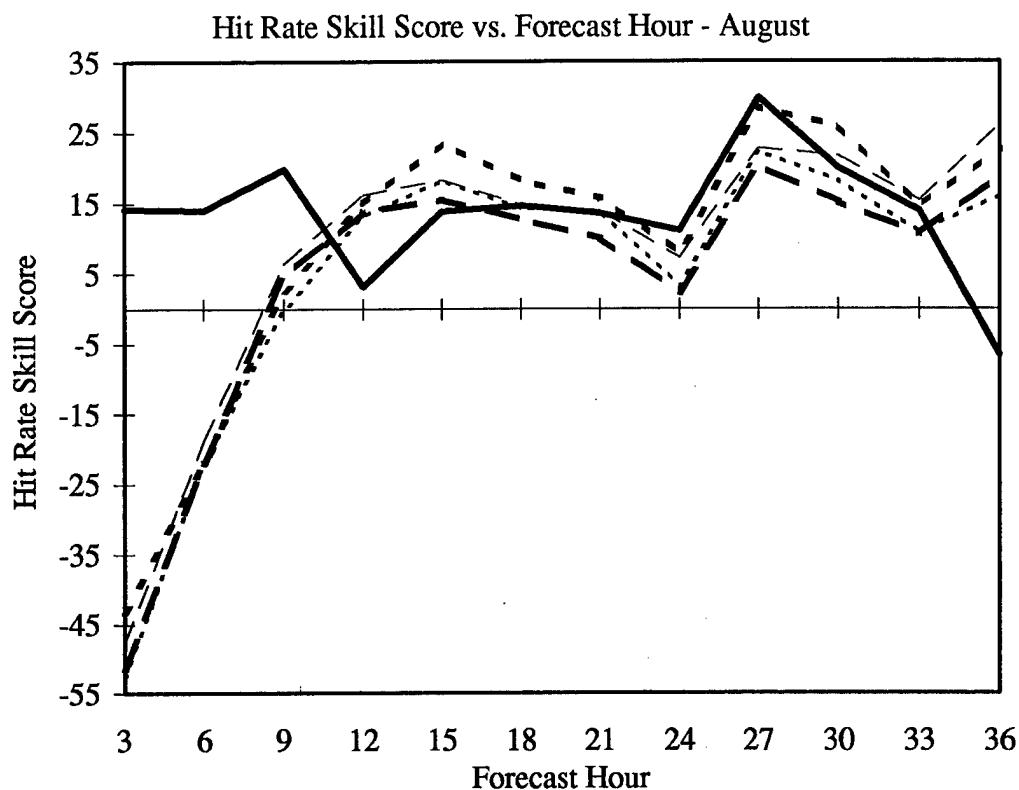


Figure 44. HR skill score versus forecast hour for August 1997. The thick solid line represents ADVCLD, the thick dotted line is the Kvamstø method, the thin dotted line is the Sundqvist method, the thick dashed line is the vertical column method, and the thin dashed line is the layered method. Average hourly HR skill score values against a reference persistence forecast are plotted as percentages. See Table 39 for descriptive statistics.

Table 39. Descriptive statistics for Figure 44. Hit rate skill score for August 1997.

	ADVCLD	Kvamstø	Sundqvist	Vertical Column	Layered
N	12	12	12	12	12
Mean	13.4	9.0	4.6	4.1	8.0
Std Deviation	8.9	21.3	21.5	20.8	21.0
Maximum	29.9	28.4	22.2	20.1	26.1
Median	13.9	15.3	13.4	11.6	15.1
Minimum	-6.6	-43.2	-52.7	-51.5	-47.7

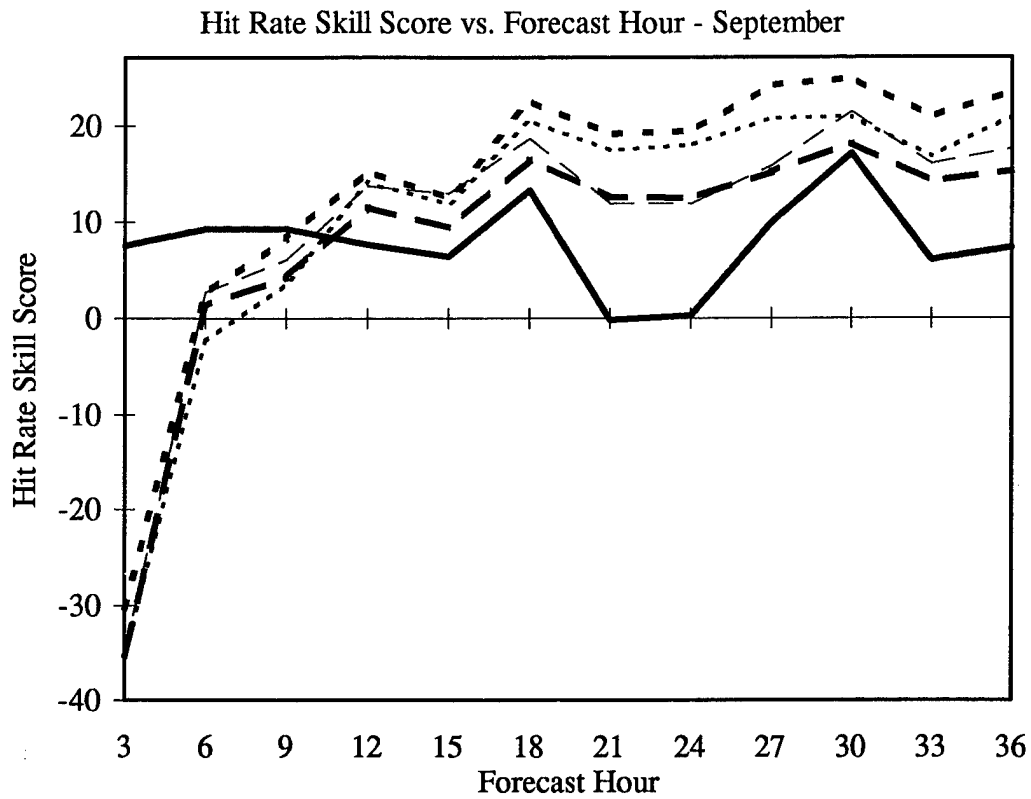


Figure 45. As in Figure 44 for September 1997. See Table 40 for descriptive statistics.

Table 40. Descriptive statistics for Figure 45. Hit rate skill score for September 1997.

	ADVCLD	Kvamstø	Sundqvist	Vertical Column	Layered
N	12	12	12	12	12
Mean	7.8	13.5	10.6	7.9	9.5
Std Deviation	4.8	15.4	16.2	14.5	15.0
Maximum	17.1	24.8	20.9	18.1	21.4
Median	7.6	19.2	17.1	12.5	13.3
Minimum	-0.2	-30.3	-35.3	-35.3	-35.1

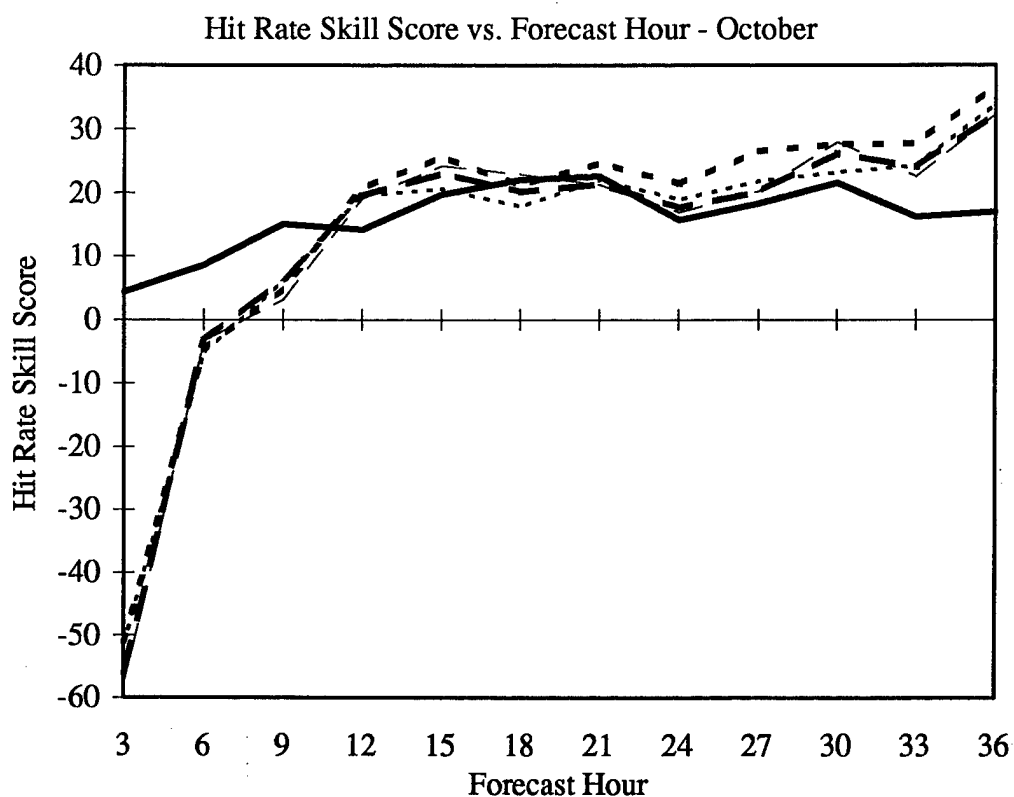


Figure 46. As in Figure 44 for October 1997. See Table 41 for descriptive statistics.

Table 41. Descriptive statistics for Figure 46. Hit rate skill score for October 1997.

	ADVCLD	Kvamstø	Sundqvist	Vertical Column	Layered
N	12	12	12	12	12
Mean	16.2	15.1	12.6	12.6	12.4
Std Deviation	5.4	23.5	22.4	23.5	24.3
Maximum	22.6	36.8	33.9	32.4	32.2
Median	16.5	23.0	20.1	20.1	20.7
Minimum	4.3	-51.0	-51.4	-56.1	-58.1

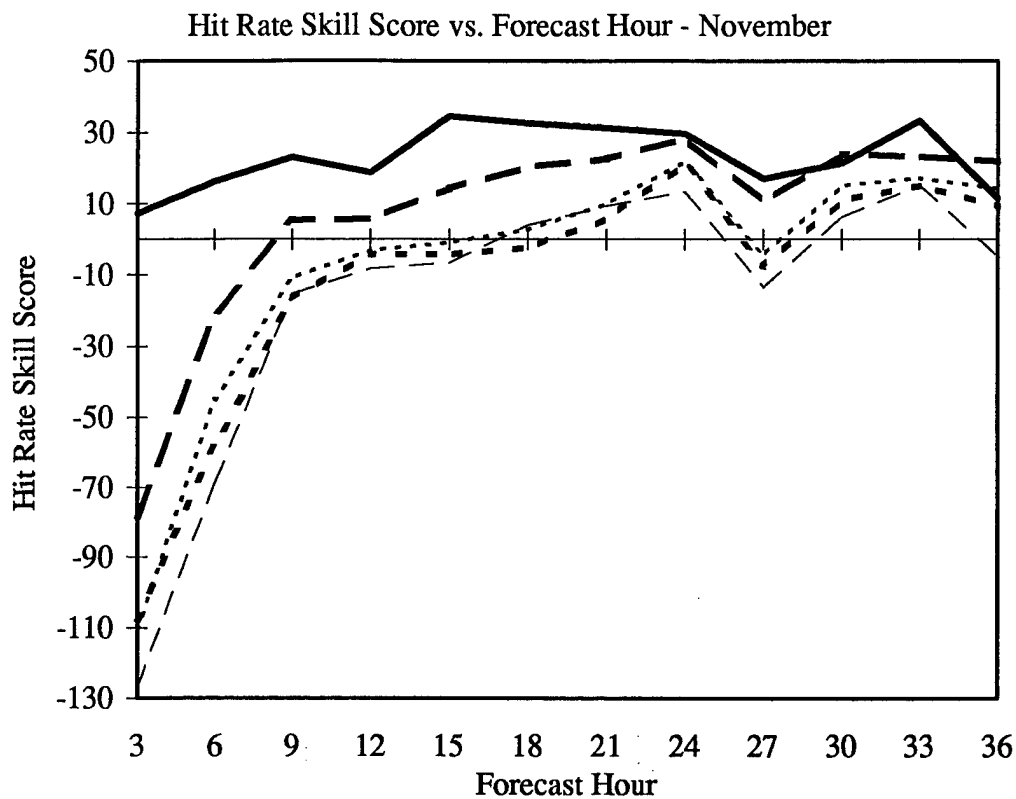


Figure 47. As in Figure 44 for November 1997. See Table 42 for descriptive statistics.

Table 42. Descriptive statistics for Figure 47. Hit rate skill score for November 1997.

	ADVCLD	Kvamstø	Sundqvist	Vertical Column	Layered
N	12	12	12	12	12
Mean	23.0	-11.6	-7.9	6.4	-16.4
Std Deviation	9.2	36.5	36.9	29.8	41.3
Maximum	34.5	21.3	21.9	28.3	15.1
Median	22.2	-3.4	0.8	17.2	-5.7
Minimum	7.2	-107.7	-110.7	-78.3	-127.1

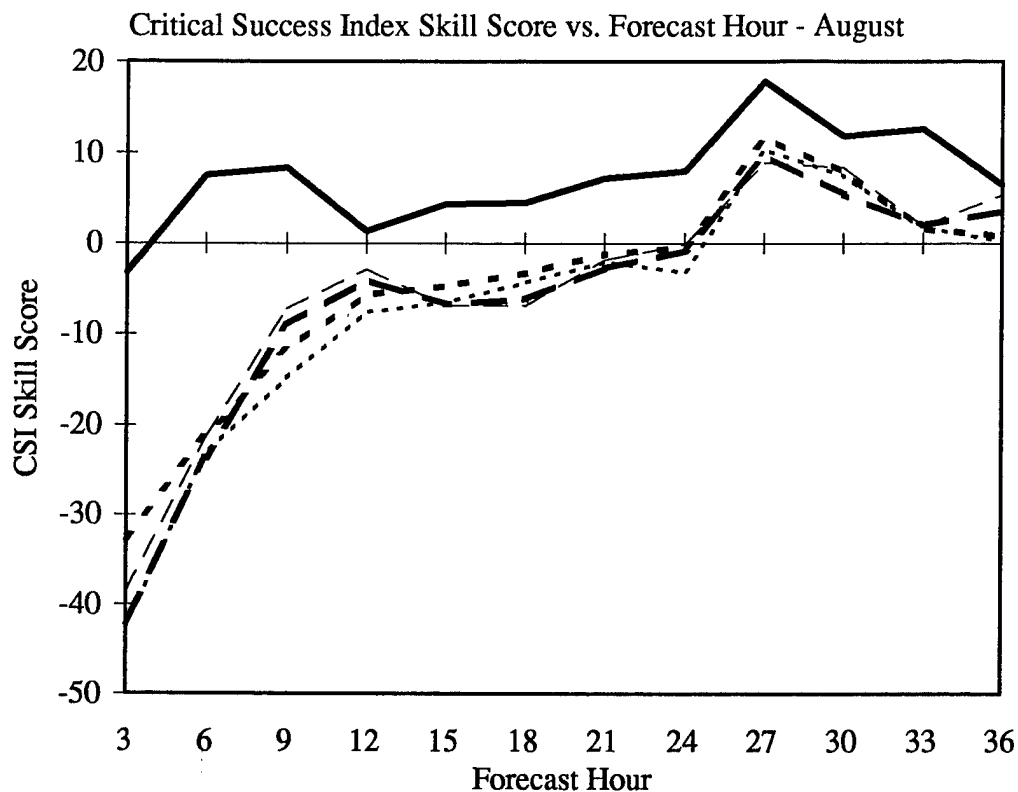


Figure 48. CSI skill score versus forecast hour for August 1997. The thick solid line represents ADVCLD, the thick dotted line is the Kvamstø method, the thin dotted line is the Sundqvist method, the thick dashed line is the vertical column method, and the thin dashed line is the layered method. Average hourly CSI skill score values against a reference persistence forecast are plotted as percentages. See Table 43 for descriptive statistics.

Table 43. Descriptive statistics for Figure 48. CSI skill score for August 1997.

	ADVCLD	Kvamstø	Sundqvist	Vertical Column	Layered
N	12	12	12	12	12
Mean	7.2	-4.9	-7.1	-6.3	-5.1
Std Deviation	5.4	12.2	14.4	14.1	13.4
Maximum	17.8	11.6	10.3	9.6	8.9
Median	7.3	-2.3	-3.8	-3.4	-2.4
Minimum	-3.3	-32.6	-42.6	-42.0	-38.6

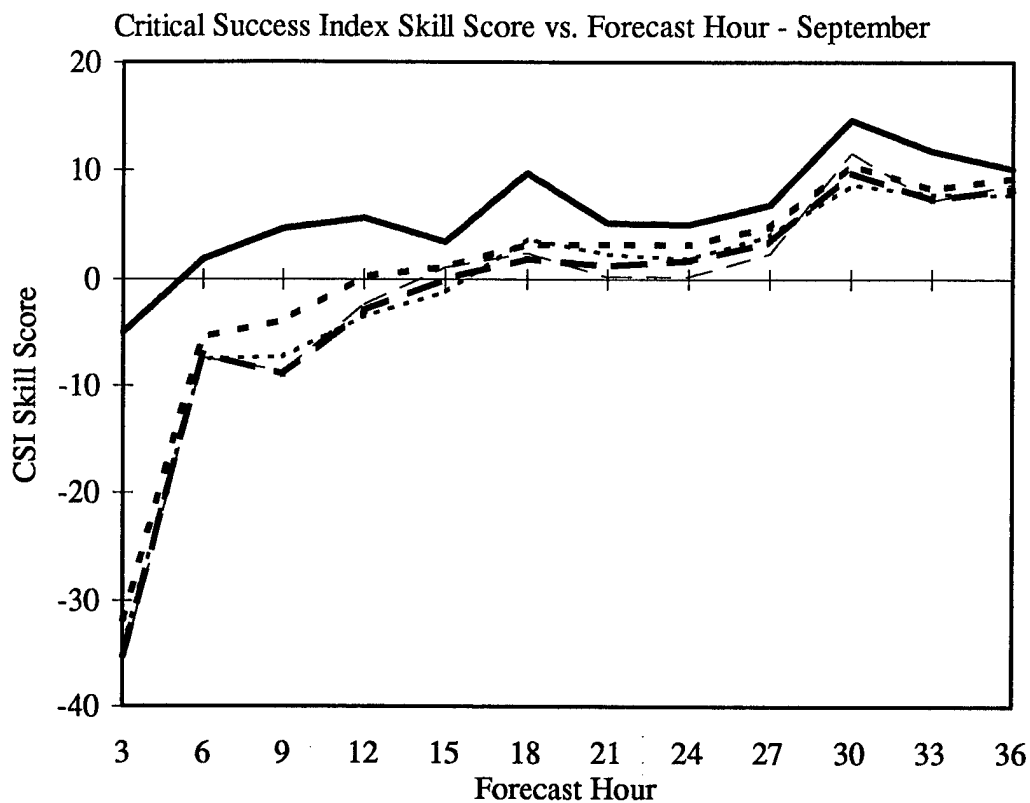


Figure 49. As in Figure 48 for September 1997. See Table 44 for descriptive statistics.

Table 44. Descriptive statistics for Figure 49. CSI skill score for September 1997.

	ADVCLD	Kvamstø	Sundqvist	Vertical Column	Layered
N	12	12	12	12	12
Mean	6.1	0.2	-1.5	-1.7	-1.7
Std Deviation	5.1	11.2	11.7	12.0	12.3
Maximum	14.6	10.5	8.6	9.8	11.6
Median	5.4	3.1	2.0	1.4	0.7
Minimum	-5.0	-31.8	-34.3	-35.2	-35.9

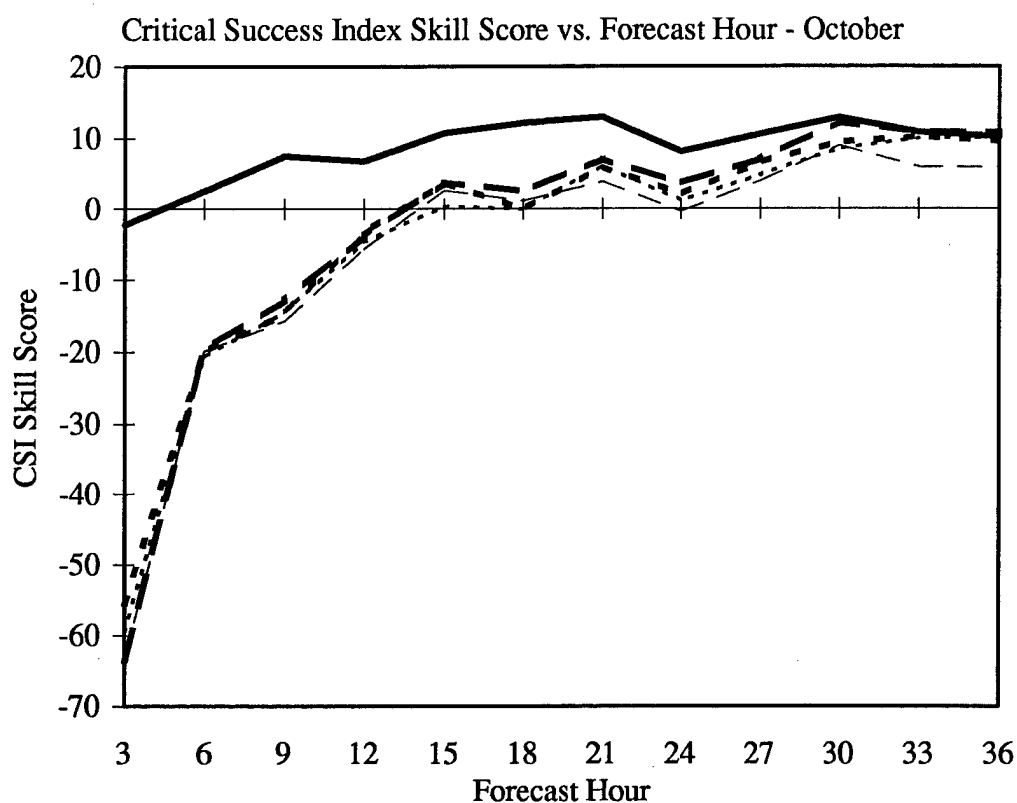


Figure 50. As in Figure 48 for October 1997. See Table 45 for descriptive statistics.

Table 45. Descriptive statistics for Figure 50. CSI skill score for October 1997.

	ADVCLD	Kvamstø	Sundqvist	Vertical Column	Layered
N	12	12	12	12	12
Mean	8.5	-3.9	-4.9	-3.5	-6.1
Std Deviation	4.6	18.8	19.7	21.2	20.1
Maximum	13.0	10.2	10.0	12.1	8.9
Median	10.3	2.8	0.7	3.6	1.8
Minimum	-2.4	-55.5	-59.5	-63.6	-63.6

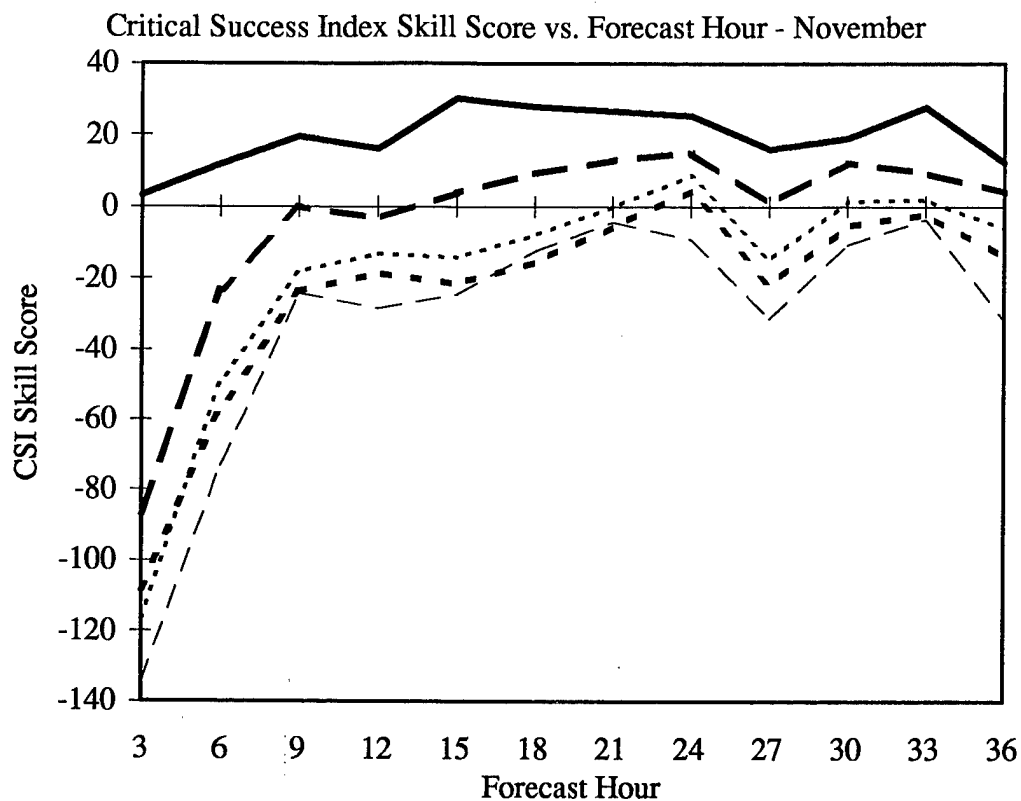


Figure 51. As in Figure 48 for November 1997. See Table 46 for descriptive statistics.

Table 46. Descriptive statistics for Figure 51. CSI skill score for November 1997.

	ADVCLD	Kvamstø	Sundqvist	Vertical Column	Layered
N	12	12	12	12	12
Mean	19.6	-24.2	-19.1	-3.9	-32.4
Std Deviation	8.2	30.7	34.1	28.0	37.3
Maximum	30.1	4.3	8.5	14.9	-3.7
Median	19.3	-17.1	-10.6	3.8	-24.6
Minimum	3.0	-108.2	-116.7	-86.8	-134.8

September and October, the MM5 schemes outperformed persistence from the 18-hr point until the end of the forecast cycle. In November, the only MM5 method that had a CSI which consistently represented an improvement over persistence was the vertical column method after the 12-hr point.

As with the hit rate skill score, ADVCLD had a better CSI than persistence for all validation hours in all four months with the exception of the 3-hr points in August, September, and October.

4.6 Subjective Analysis Results

As mentioned previously, every forecast cycle for all six forecast methods was visualized and animated. Figures 52-59 are examples of the visualizations that were examined. These figures were chosen because they illustrate the most important results of the subjective analysis. These are that the MM5 consistently underestimates the amount of cloudiness over the Adriatic Sea and overestimates the amount of cloudiness over the mountains in Italy and the mountains in Croatia and Bosnia. No systematic phase errors were detected for either ADVCLD or MM5.

Figures 52-56 are 24-hr total FC forecasts from the Kvamstø method, the Sundqvist method, the vertical column method, the layered method, and ADVCLD respectively. These figures are all valid for 8 October 1997 at 12 UTC, which is the same valid time as the satellite image displayed in Figure 4.

By comparing Figures 52-55 against Figure 4, one notes that all of the MM5 schemes underforecasted over the Adriatic Sea. Each MM5 scheme did forecast non-zero total FC amounts over the central and southern Adriatic, however, they were invariably too low. ADVCLD certainly did not underforecast the cloudiness in the Adriatic, but

ADVCLD's quarter-mesh resolution at this validation hour cannot capture the detail in the cloud formations that is evident in the infrared satellite picture in Figure 4.

Figures 57-59 are all valid for 9 September 1997 at 15 UTC. Figure 57 is the RTNEPH analysis, while Figures 58 and 59 are 15-hr total FC forecasts from the Kvamstø method and the layered method respectively.

By comparing Figures 58 and 59 against the RTNEPH analysis, it is evident that the two MM5 schemes overestimated the cloud cover over the mountains along the length of the boot of Italy and just inland from the Adriatic Sea into Croatia and Bosnia. The Kvamstø and layered methods were chosen for display, however, both the Sundqvist and vertical column methods exhibited the same tendency to overforecast cloudiness in mountainous areas.

An examination of the animation of the entire forecast cycle revealed that the tendency to overforecast over the mountains was related to mesoscale (or smaller) features. The synoptic scale cloudiness in Figure 57 is in the northeast corner of the image, and it intensified and moved southward from the 15-hr point to the 36-hr point. The MM5 handled the amount and movement of this synoptic scale cloudiness quite well. The cloudiness over the mountains, however, continued to be overestimated, was not advected by the wind and thus remained over the mountains, and dissipated by the 24-hr point of the forecast. In general, the MM5 produced too much convective cumulus over the mountains.

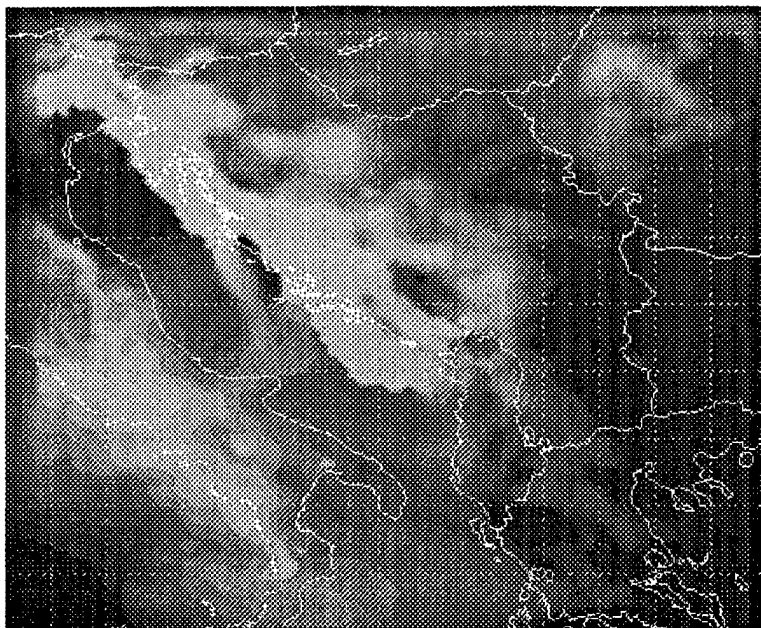


Figure 52. 24-hour total FC forecast valid 8 October at 12 UTC obtained from the Kvamstø method. This is the same valid time as Figures 4 and 5 shown in chapter 3. Black corresponds to total FC amounts of zero percent and white corresponds to 100 percent.

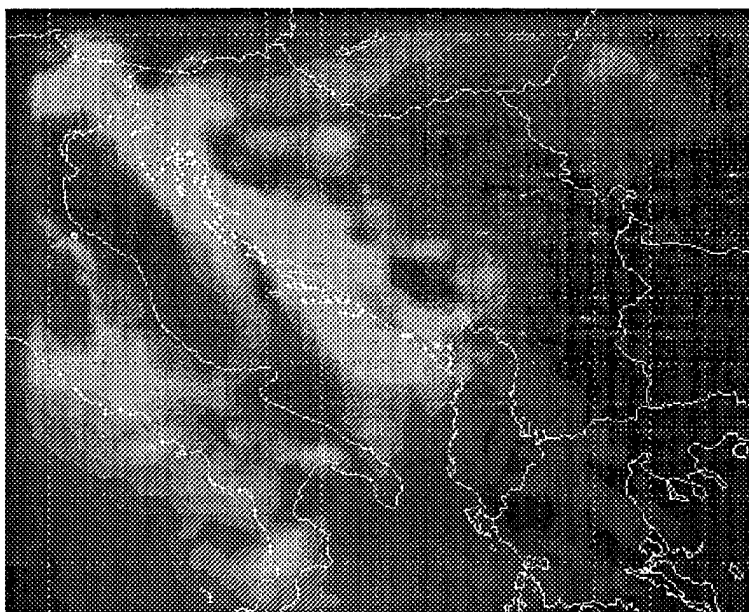


Figure 53. As in Figure 52 for the 24-hr forecast using the Sundqvist method.

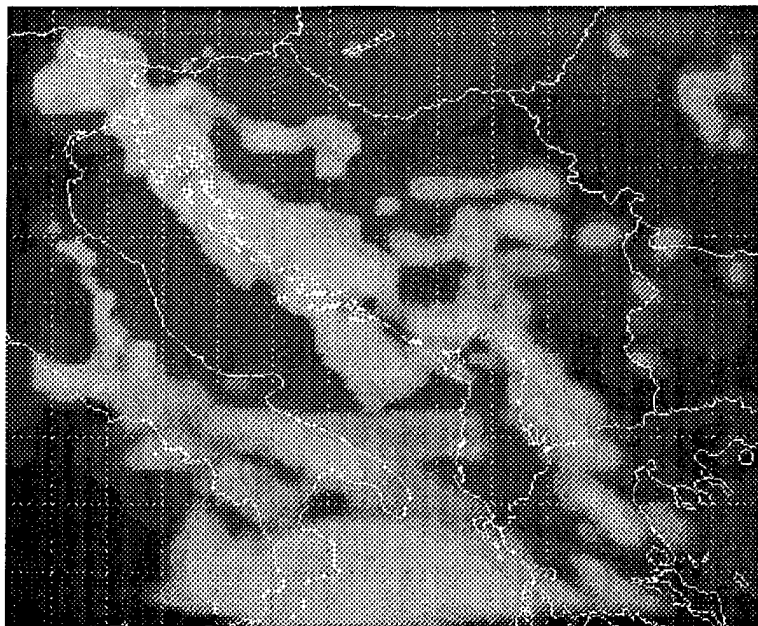


Figure 54. As in Figure 52 for the 24-hr forecast using the vertical column method.

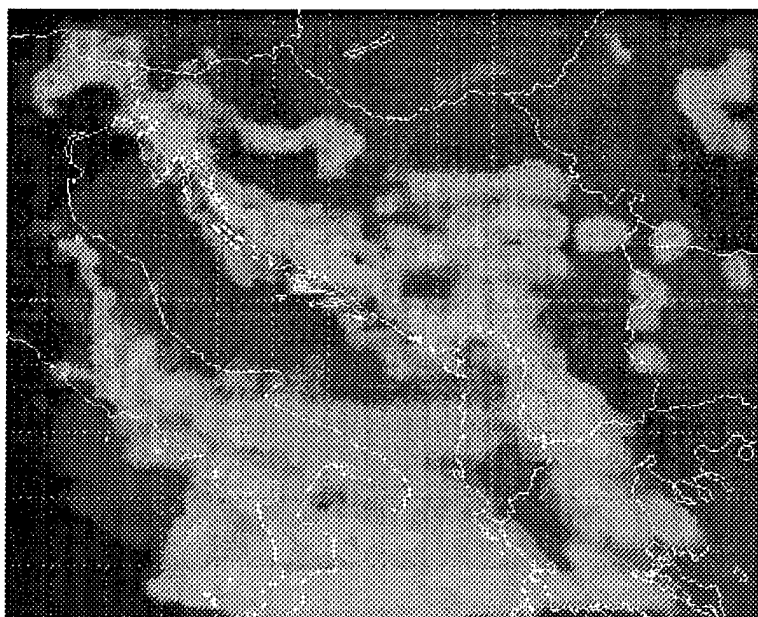


Figure 55. As in Figure 52 for the 24-hr forecast using the layered method.

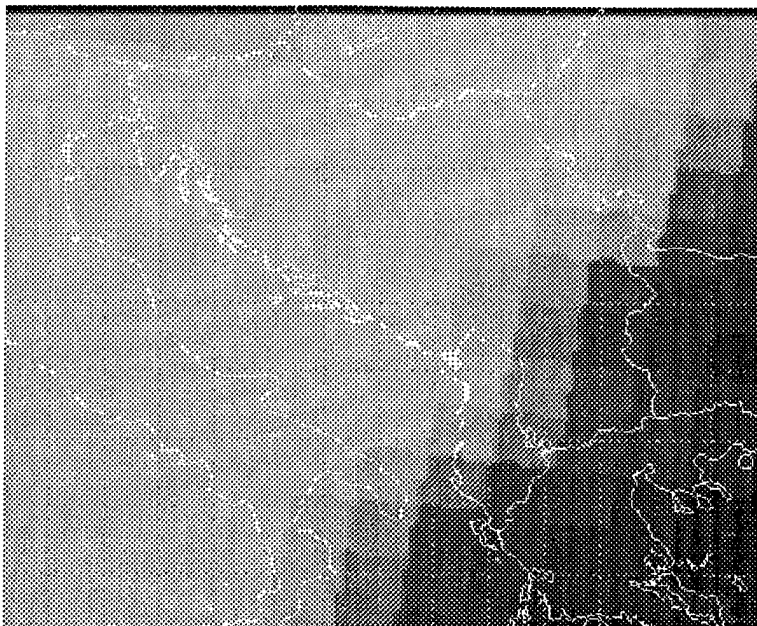


Figure 56. As in Figure 52 for the 24-hr ADVCLD forecast.

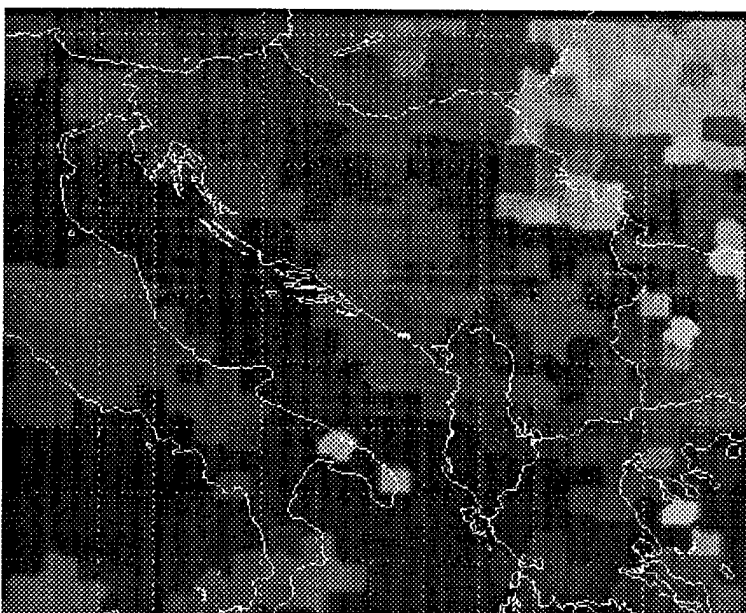


Figure 57. RTNEPH analysis valid for 9 September at 15 UTC. Grayscale as in Figure 52.

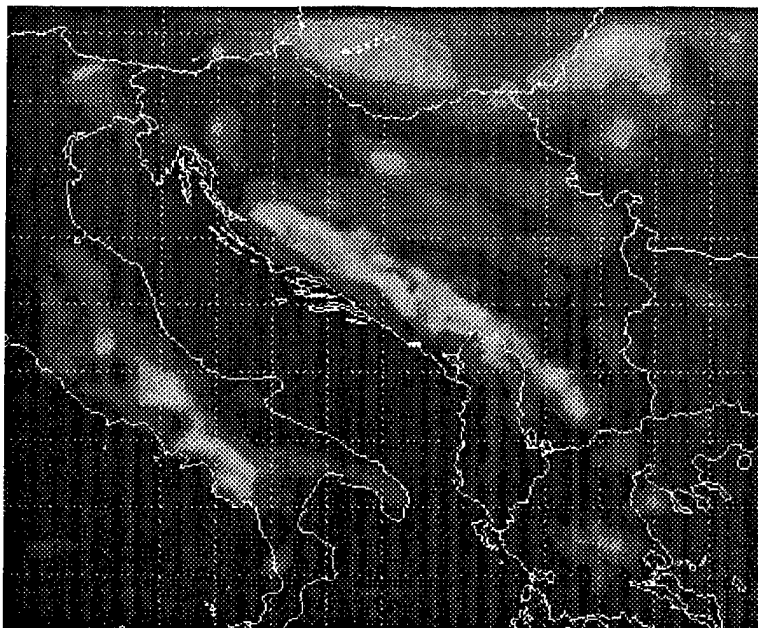


Figure 58. 15-hour total FC forecast valid 9 September at 15 UTC obtained from the Kvamstø method. This is the same valid time as the RTNEPH analysis shown in Figure 57. Grayscale as in Figure 52.

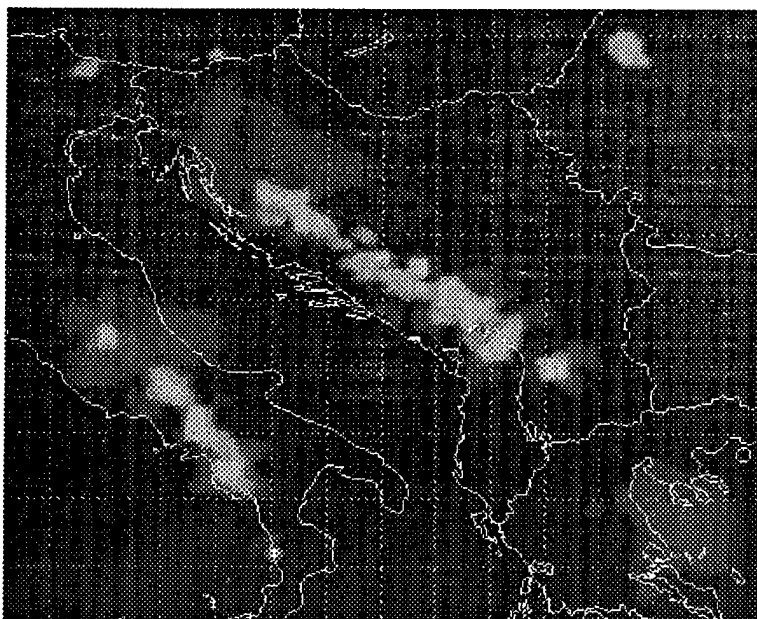


Figure 59. As in Figure 58 for a 15-hr forecast using the layered method.

V. Conclusions and Recommendations

5.1 Conclusions

5.1.1 Conclusions From Comparisons of ADVCLD and MM5

Based upon the results displayed in the previous chapter, the following conclusions are made. ADVCLD, while it displayed a tendency to overforecast late in the forecast period, outperformed all of the MM5 schemes until the 36-hr point in the forecast. At the 36-hr point, the quality of the ADVCLD forecast was reduced, and all four MM5 schemes produced total FC forecasts that were competitive with ADVCLD. In the first 9 hours of the forecast cycle, ADVCLD's superiority is clearly evident in almost every statistic calculated.

The most notable weakness in the ADVCLD total FC forecasts revealed by the statistical analysis was its lack of sharpness in forecasting clear conditions. ADVCLD, from the 15-hr point in the forecast until the 36-hr point, significantly underforecast the amount of clear skies observed by RTNEPH. This weakness is not, however, a major one when the fact that the RTNEPH (as mentioned in chapter 2) tends to overanalyze clear skies is taken into consideration. The major weakness of the MM5 schemes was the negative forecast bias (underforecast) that all four schemes displayed. The MM5 did not produce enough moisture.

Thus in September, the driest month in this study, the MM5 schemes, and the Kvamstø method in particular, had better hit rates for a broken cloudiness forecast than did ADVCLD from the 12-hr point until the end of the forecast period. However,

ADVCLD still had better critical success index and probability of detection scores than every MM5 scheme for all forecast validation hours in September. The false alarm rate for ADVCLD in September was also lower than the MM5 schemes' false alarm rates at almost every forecast hour.

ADVCLD had greater sharpness than any other method in forecasting overcast conditions. This fact combined with the negative forecast bias of the MM5 made the superiority of ADVCLD quite evident in the cloudiest months, October and November. In these months, the underforecasting bias of the MM5 was quite pronounced. In fact, ADVCLD in November had better hit rates at all forecast hours than all of the MM5 schemes except at the 36-hr point. The only exception was the 30-hr point, where the vertical column method had a slightly better hit rate than ADVCLD. As was the case with the driest month, in the cloudiest months ADVCLD's CSI and POD scores were consistently the best.

ADVCLD's forecast accuracy, as measured in terms of RMSE and MAE, was also clearly superior to the forecast accuracy of every MM5 method. In August, October, and November, the RMSE for ADVCLD was the lowest at all forecast hours except the 36-hr point. ADVCLD's mean absolute error for these months was also consistently lower than the other methods. In September, ADVCLD's MAE was in general higher than the mean absolute errors of the MM5 schemes after the 9-hr point, however, its RMSE was still consistently among the lowest.

From the above discussion, it is clear that ADVCLD did a better job of estimating total FC in the first 33 hours of the forecast. The MM5 hit rate scores are somewhat inflated by the fact that MM5 underforecasted and thus correctly forecasted scattered

conditions. The MM5, however, did not handle either the placement or the amount of broken cloudiness well as is evidenced by the low (compared to ADVCLD) CSI and POD scores for all four MM5 schemes in all four months.

5.1.2 Conclusions From Comparisons of MM5 Schemes

In comparing the MM5 total fractional cloudiness schemes, it should be kept in mind that both the Kvamstø and Sundqvist schemes were modified to produce more cloudiness. Both Kvamstø and Sundqvist used 75 percent as their critical value for relative humidity. As mentioned in chapter 3, in this study critical relative humidities of 70, 65, and 60 percent were used for the low, middle, and high levels of the atmosphere respectively. The Kvamstø and Sundqvist methods were initially implemented without this modification, however, they were not competitive compared to the total cloud condensate schemes in any month because they did not produce enough cloud cover. As a result, the critical relative humidities were lowered to produce more cloudiness.

The subjective analysis revealed that the primary explanation for the negative forecast bias in the MM5 was its treatment of cloudiness over the Adriatic Sea. Over the water, the MM5 consistently underforecasted total FC amounts. Underforecasting over the Adriatic, certainly reduced the POD scores for the MM5 schemes. The tendency to overforecast over mountainous regions, although less pronounced than the underforecast over the water, tended to lower the MM5 CSI scores, as broken cloudiness was forecasted where none was actually observed.

Among the MM5 schemes for the months of August through October, there was not a great difference evident in the values of the various statistics that were calculated.

Keeping this in mind, the Kvamstø method did perform slightly better than the other three. This is especially apparent in the MAE, RMSE, and hit rate scores.

In the cloudiest month (November), however, the vertical column method performed far better than any of the other MM5 schemes. In November, the vertical column method had the best scores for every statistic calculated except the sharpness score for clear skies (where it was a close second to the Sundqvist method) and the false alarm rate (where it was essentially the same as the Kvamstø method).

5.1.3 Conclusions Based on Persistence

Persistence performed as may be expected. At the 3-hr point it vied with ADVCLD as the best method in all categories. By the 12-hr point, however, the MAE, RMSE, hit rate, and false alarm rate scores for persistence were already worse than the corresponding scores for any other forecast method.

Persistence actually outperformed all other methods in all months at all forecast hours at demonstrating sharpness (except for ADVCLD's sharpness at forecasting overcast skies). Persistence consistently produced a total FC distribution that closely matched the RTNEPH analysis. As a result, persistence mean error scores were also among the best for all forecast hours. This is not surprising as a persistence forecast has a total FC distribution based on conditions that actually existed in the atmosphere. Hence, one would expect it to be realistic, and this is particularly true for November which, as mentioned in section 4.1, was the most winter-like month.

Notwithstanding the fact that persistence had a total FC distribution that closely matched the total FC distribution of the RTNEPH analysis, persistence did have problems placing the clouds in the correct locations, as is evidenced by the high RMSE values for

persistence after the 12-hr point. Despite this difficulty, it still had consistently better POD scores than all of the MM5 schemes until the 27-hr point of the forecast cycle. The negative bias of the MM5 is again evident.

5.1.4 Summary of Conclusions

In summary, there are three major findings from this study that are valid for the months of August through November. The first is that ADVCLD produced the best total FC forecasts for the first 33 hours of the forecast period and should be used to make total FC forecasts that are shorter than 36 hours.

The second major finding is that the MM5 had a significant negative bias in both the relative humidity and total cloud condensate fields. That is, it did not produce enough moisture (primarily over the water). As a consequence, it consistently forecasted total FC amounts that were lower than those analyzed by the RTNEPH.

The last major finding is that persistence, although it thoroughly outperformed the MM5 schemes in the first 6 hours of the forecast, should not be used to make total FC forecasts that are at least three hours into the future. ADVCLD's total FC forecasts, even at the 3-hr point, demonstrated skill when compared against total FC forecasts based on persistence (note especially the MAE and RMSE scores).

5.2 Recommendations

5.2.1 Recommendations for Operational Implementation

ADVCLD should be used to make total FC forecasts through the 33-hr point in the forecast cycle. If data from ADVCLD is unavailable, the Kvamstø method should be used to make total FC forecasts during the summer and early autumn months, and the vertical column method should be used in the late autumn and winter months.

5.2.2 Recommendations for Further Research

Ideally, the statistical comparisons performed in this study should be applied to data for an entire year. In this way, any seasonal variations and biases of the MM5 and ADVCLD may be better identified.

In order to remove the tendency of ADVCLD to underforecast clear conditions, more research is needed into the conversion of low fractional cloudiness amounts into condensation pressure spread values, and vice versa. If this conversion could be slightly improved, the positive bias evident now in ADVCLD would be removed.

Perhaps the most promising area of potential research has to do with the initialization of moisture, and in particular the cloud condensate fields, in the MM5. The main advantage ADVCLD had over the MM5 was the fact that it was initialized with actual total FC values. The time required to “spin-up” moisture in the MM5 could be eliminated if the RTNEPH analysis were used to initialize the cloud condensate fields.

To do this, the 12-hr forecast from the previous MM5 forecast cycle could be used as a “first guess”. This would ensure that the correct ratios between snow, ice, cloud water, and rain water were maintained. This “first guess” could then be nudged towards the RTNEPH analysis in order to place the cloud condensate in the correct location. The cloud condensate amounts from the “first guess” could also be proportionally reduced or increased as they, too, get nudged towards the RTNEPH analysis.

Finally, in order to implement this technique, more research would be necessary into correctly transforming cloud condensate amounts into fractional cloudiness amounts. Perhaps each cloud condensate variable (snow, ice, rain water, and cloud water) could be treated separately with threshold values being determined for each. Instead of creating

thresholds based on pressure levels, the thresholds could be made to vary based directly on the temperature at the level where the moisture variable is forecasted. By doing this, a set of thresholds that will work consistently well throughout the seasons may perhaps be discovered. The role of vertical velocity in establishing thresholds between cloud condensate amounts and FC amounts should also be examined.

Appendix A: Tables used in ADVCLD to relate CPS and FC amounts.

Tables A1-A4 are used by ADVCLD to convert from fractional cloudiness amounts in percent to condensation pressure spread values in millibars for 850mb, 700mb, 500mb, and 300mb respectively. Tables A5-A8 are used by ADVCLD to convert from CPS values in millibars to FC in percent for 850mb, 700mb, 500mb, and 300mb respectively. All tables are as presented in Crum (1987).

Table A1. Conversion from fractional cloudiness to CPS for 850 mb. Units of cloud percent form the abscissa and tens of cloud percent form the ordinate. CPS values are located in the interior of the table.

	0	1	2	3	4	5	6	7	8	9	10
0	120.0	114.0	111.0	108.2	106.0	103.2	100.5	98.0	95.7	93.7	90.6
10	90.6	88.4	86.0	83.0	81.0	77.7	75.5	73.4	71.0	69.6	68.2
20	68.2	66.8	66.0	64.0	62.6	61.0	59.6	58.0	56.6	55.8	55.0
30	55.0	53.7	52.5	51.6	50.6	49.0	48.2	47.4	46.6	45.8	45.0
40	45.0	44.2	43.4	42.6	41.8	41.0	40.2	39.4	38.6	37.8	37.0
50	37.0	36.2	35.4	34.8	34.4	34.1	33.7	33.4	33.0	32.6	32.3
60	32.3	31.9	31.6	31.2	30.7	30.3	29.7	29.2	28.8	28.3	27.9
70	27.9	27.5	27.0	26.6	26.1	25.7	25.2	24.7	24.2	23.7	23.2
80	23.2	22.5	21.9	21.2	20.4	19.5	18.6	17.7	16.8	15.6	14.5
90	14.5	13.5	12.4	11.3	10.1	9.0	7.6	6.0	4.2	2.6	1.0

Table A2. Conversion from fractional cloudiness to CPS for 700 mb. Units of cloud percent form the abscissa and tens of cloud percent form the ordinate. CPS values are located in the interior of the table.

	0	1	2	3	4	5	6	7	8	9	10
0	109.0	107.0	105.0	102.8	100.8	99.2	96.7	95.6	94.5	93.4	92.2
10	92.2	91.0	90.2	89.4	87.0	86.0	85.0	83.2	81.0	79.0	77.0
20	77.0	75.2	73.3	71.5	70.0	68.3	66.9	65.3	63.9	62.4	61.0
30	61.0	59.8	58.7	57.5	56.2	55.1	54.0	52.9	51.8	50.7	49.8
40	49.8	48.8	48.0	47.1	46.2	45.3	44.5	43.7	42.8	41.9	41.0
50	41.0	40.7	40.3	40.0	39.6	39.3	38.9	38.6	38.2	37.9	37.6
60	37.6	37.2	36.8	36.4	36.0	35.6	35.2	34.8	34.3	33.6	33.3
70	33.3	32.8	32.2	31.8	31.3	30.7	30.2	29.6	29.0	28.4	27.9
80	27.9	27.3	26.7	26.2	25.6	25.0	24.2	23.4	22.4	21.4	20.0
90	20.0	18.4	17.3	16.0	14.5	13.2	11.4	9.6	7.2	4.7	1.0

Table A3. Conversion from fractional cloudiness to CPS for 500 mb. Units of cloud percent form the abscissa and tens of cloud percent form the ordinate. CPS values are located in the interior of the table.

	0	1	2	3	4	5	6	7	8	9	10
0	101.0	100.2	99.4	98.6	97.8	97.1	96.2	95.4	94.5	93.7	92.9
10	92.9	92.1	91.4	90.6	89.8	89.0	88.0	87.0	85.0	83.0	81.0
20	81.0	79.3	77.7	76.0	74.3	72.7	71.0	70.2	69.3	68.4	67.5
30	67.5	66.7	65.8	64.9	64.0	63.2	62.3	61.5	60.0	58.3	56.4
40	56.4	54.7	52.0	51.0	50.3	49.6	48.9	48.3	47.6	46.9	46.1
50	46.1	45.5	44.8	44.1	43.4	42.7	42.0	41.3	40.8	40.4	40.0
60	40.0	39.6	39.2	38.8	38.4	38.0	37.6	37.2	36.8	36.3	35.9
70	35.9	35.5	35.0	34.6	34.2	33.7	33.3	32.8	32.1	31.5	30.7
80	30.7	29.7	28.8	28.0	27.2	26.2	25.1	24.0	23.0	21.9	20.7
90	20.7	19.6	18.3	16.9	15.3	13.4	11.4	9.4	7.4	5.0	1.0

Table A4. Conversion from fractional cloudiness to CPS for 300 mb. Units of cloud percent form the abscissa and tens of cloud percent form the ordinate. CPS values are located in the interior of the table.

	0	1	2	3	4	5	6	7	8	9	10
0	97.0	96.2	95.4	94.6	93.8	93.2	92.2	91.4	90.5	89.7	88.9
10	88.9	88.1	87.4	86.6	85.8	85.0	84.5	84.0	83.5	83.0	81.0
20	81.0	79.3	77.7	76.0	74.3	72.7	71.0	70.2	69.3	68.4	67.5
30	67.5	66.7	65.8	64.9	64.0	63.2	62.3	61.5	60.0	58.3	56.4
40	56.4	54.7	52.0	51.0	50.3	49.6	48.9	48.3	47.6	46.9	46.1
50	46.1	45.5	44.8	44.1	43.4	42.7	42.0	41.3	40.8	40.4	40.0
60	40.0	39.6	39.2	38.8	38.4	38.0	37.6	37.2	36.8	36.3	35.9
70	35.9	35.5	35.0	34.6	34.2	33.7	33.3	32.8	32.1	31.5	30.7
80	30.7	29.7	28.8	28.0	27.2	26.2	25.1	24.0	23.0	21.9	20.7
90	20.7	19.6	18.3	16.9	15.3	13.4	11.4	9.4	7.4	5.0	1.0

Table A5. Conversion from CPS to fractional cloudiness for 850 mb. Units of CPS form the abscissa and tens of CPS form the ordinate. Cloud percent values are located in the interior of the table.

	0	1	2	3	4	5	6	7	8	9	10
0	100.0	100.0	99.4	98.7	98.1	97.6	97.0	96.4	95.7	95.0	94.1
10	94.1	93.3	92.4	91.5	90.5	89.5	88.7	87.8	86.7	85.5	84.4
20	84.4	83.3	81.8	80.3	78.4	76.4	74.3	72.1	69.8	67.5	65.5
30	65.5	63.5	60.8	58.0	55.2	52.5	51.2	50.0	48.7	47.5	46.2
40	46.2	45.0	43.7	42.5	41.2	40.0	38.7	37.5	36.2	35.0	34.3
50	34.3	33.7	32.6	31.5	30.8	30.0	28.7	27.5	27.0	26.5	25.7
60	25.7	25.0	24.4	23.7	23.0	22.2	22.0	20.8	20.1	19.5	18.7
70	18.7	18.0	17.6	17.2	16.7	16.2	15.8	15.3	14.9	14.5	14.2
80	14.2	14.0	13.5	13.0	12.7	12.5	12.0	11.6	11.2	10.7	10.3
90	10.3	9.8	9.6	9.4	8.8	8.2	7.9	7.5	7.0	6.6	6.2
100	6.2	5.8	5.4	5.1	4.7	4.4	4.0	3.6	3.1	2.7	2.3
110	2.3	2.0	1.6	1.2	1.0	0.8	0.7	0.5	0.4	0.2	0

Table A6. Conversion from CPS to fractional cloudiness for 700 mb. Units of CPS form the abscissa and tens of CPS form the ordinate. Cloud percent values are located in the interior of the table.

	0	1	2	3	4	5	6	7	8	9	10
0	100.0	100.0	99.9	99.7	99.3	98.9	98.5	98.1	97.7	97.3	96.8
10	96.8	96.2	95.7	95.2	94.4	93.6	93.0	92.3	91.4	90.5	90.0
20	90.0	89.4	88.4	87.5	86.2	85.0	83.3	81.5	79.8	78.0	76.3
30	76.3	74.5	72.5	70.5	68.5	66.5	64.0	61.6	58.7	55.8	52.9
40	52.9	50.0	48.9	47.8	46.6	45.3	44.2	43.1	42.0	40.8	39.8
50	39.8	38.7	37.8	36.9	36.0	35.1	34.2	33.4	32.6	31.7	30.8
60	30.8	30.0	29.3	28.6	27.9	27.2	26.6	25.9	25.2	24.6	24.0
70	24.0	23.3	22.7	22.2	21.6	21.1	20.5	20.0	19.5	19.0	18.5
80	18.5	18.0	17.6	17.1	16.6	16.0	15.0	14.0	13.8	13.5	12.2
90	12.2	11.0	10.2	9.4	8.5	7.5	6.6	5.8	5.4	5.1	4.5
100	4.5	3.9	3.4	2.9	2.5	2.0	1.5	1.0	0.5	0	0
110	0	0	0	0	0	0	0	0	0	0	0

Table A7. Conversion from CPS to fractional cloudiness for 500 mb. Units of CPS form the abscissa and tens of CPS form the ordinate. Cloud percent values are located in the interior of the table.

	0	1	2	3	4	5	6	7	8	9	10
0	100.0	100.0	99.8	99.5	99.3	99.0	98.6	98.2	97.7	97.2	96.7
10	96.7	96.2	95.7	95.2	94.7	94.2	93.6	92.9	92.2	91.5	90.6
20	90.6	89.8	88.9	88.0	87.0	86.1	85.2	84.2	83.0	81.7	80.7
30	80.7	79.7	78.2	76.7	74.4	72.1	69.8	67.5	65.0	62.5	60.0
40	60.0	57.5	56.0	54.6	53.2	51.7	50.2	48.8	47.4	45.9	44.5
50	44.5	43.0	42.0	41.9	41.4	40.8	40.2	39.7	39.2	38.6	38.0
60	38.0	37.5	36.4	35.2	34.0	32.9	31.8	30.6	29.4	28.3	27.2
70	27.2	26.0	25.4	24.8	24.2	23.6	23.0	22.4	21.8	21.2	20.6
80	20.6	20.0	19.5	19.0	18.5	18.0	17.5	17.0	16.0	15.0	13.8
90	13.8	12.5	11.2	9.8	8.6	7.5	6.3	5.1	3.8	2.5	1.2
100	1.2	0	0	0	0	0	0	0	0	0	0
110	0	0	0	0	0	0	0	0	0	0	0

Table A8. Conversion from CPS to fractional cloudiness for 300 mb. Units of CPS form the abscissa and tens of CPS form the ordinate. Cloud percent values are located in the interior of the table.

	0	1	2	3	4	5	6	7	8	9	10
0	100.0	100.0	99.8	99.5	99.3	99.0	98.6	98.2	97.7	97.2	96.7
10	96.7	96.2	95.7	95.2	94.7	94.2	93.6	92.9	92.2	91.5	90.6
20	90.6	89.8	88.9	88.0	87.0	86.1	85.2	84.2	83.0	81.7	80.7
30	80.7	79.7	78.2	76.7	74.4	72.1	69.8	67.5	65.0	62.5	60.0
40	60.0	57.5	56.0	54.6	53.2	51.7	50.2	48.8	47.4	45.9	44.5
50	44.5	43.0	42.0	41.9	41.4	40.8	40.2	39.7	39.2	38.6	38.0
60	38.0	37.5	36.4	35.2	34.0	32.9	31.8	30.6	29.4	28.3	27.2
70	27.2	26.0	25.4	24.8	24.2	23.6	23.0	22.4	21.8	21.2	20.6
80	20.6	20.0	19.5	19.0	17.0	15.0	13.8	12.5	11.2	9.8	8.6
90	8.6	7.5	6.3	5.1	3.8	2.5	1.2	0	0	0	0
100	0	0	0	0	0	0	0	0	0	0	0
110	0	0	0	0	0	0	0	0	0	0	0

Appendix B: Relationship between CPS and dew point depression.

The relationship as presented in Crum (1987) between CPS (in mb) and dew point depression (in Kelvin) used in ADVCLD is given by the equation,

$$CPS = \{B_0(p) + T_{dd}B_1(p)\}T_{dd} \quad (B.1)$$

where T_{dd} is the dew point depression. $B_0(p)$ and $B_1(p)$ are given by

$$B_0(p) = B_{00} + pB_{01} \quad (B.2)$$

$$B_1(p) = B_{10} + pB_{11} \quad (B.3)$$

where p is pressure and B_{00} , B_{01} , B_{10} , and B_{11} are constants with values

$$B_{00} = 1.41985$$

$$B_{01} = 1.34466 \times 10^{-2}$$

$$B_{10} = -1.39131 \times 10^{-2}$$

$$B_{11} = -6.69419 \times 10^{-5}$$

Appendix C: MM5 forecast cycles and initialization models used.

The MM5 forecast cycles used in this study are tabulated below together with the model that was used to provide the initial and boundary conditions. Tables C1-C4 correspond to August-November, respectively.

Table C1. MM5 forecast cycles used together with model that was used to provide the initial and boundary conditions for August 1997.

Date	Time(UTC)	Initialization Model
23	00/12	NOGAPS/NOGAPS
24	00/12	NOGAPS/NOGAPS
25	12	NOGAPS
26	00/12	NOGAPS/NOGAPS
27	12	NOGAPS
28	00/06	NOGAPS/NOGAPS
29	12	NOGAPS
30	00/12	NOGAPS/NOGAPS
31	00/12	NOGAPS/NOGAPS
31	18	NOGAPS

Table C2. MM5 forecast cycles used together with model that was used to provide the initial and boundary conditions for September 1997.

Date	Time(UTC)	Initialization Model
01	12	NOGAPS
02	00	NOGAPS
03	00/12	NOGAPS/NOGAPS
04	00	NOGAPS
05	00/12	NOGAPS/NOGAPS
06	00/12	NOGAPS/NOGAPS
07	00/12	NOGAPS/NOGAPS
08	00/12	NOGAPS/NOGAPS
09	00/12	NOGAPS/NOGAPS
10	00/12	AVN/NOGAPS
11	00/12	NOGAPS/NOGAPS
12	00	NOGAPS
13	00/12	NOGAPS/NOGAPS
14	00/12	NOGAPS/NOGAPS
15	00/12	NOGAPS/NOGAPS
16	00	NOGAPS
17	12	NOGAPS
18	06	NOGAPS
19	00/12	NOGAPS/NOGAPS
20	00/12	NOGAPS/NOGAPS
21	00	NOGAPS
22	00/12	NOGAPS/AVN
23	00	NOGAPS

Table C3. MM5 forecast cycles used together with model that was used to provide the initial and boundary conditions for October 1997.

Date	Time(UTC)	Initialization Model
07	12	NOGAPS
08	00/12	NOGAPS/NOGAPS
09	00/12	NOGAPS/NOGAPS
10	00/12	NOGAPS/NOGAPS
11	00/09	NOGAPS/NOGAPS
12	00/12	NOGAPS/NOGAPS
13	00/12	NOGAPS/NOGAPS
14	00/12	NOGAPS/NOGAPS
15	00/12	NOGAPS/NOGAPS
16	00	NOGAPS
17	00/12	NOGAPS/NOGAPS
18	00/06	NOGAPS/AVN
19	00/12	NOGAPS/NOGAPS
20	00	NOGAPS
21	00	NOGAPS
22	00	NOGAPS
23	00	NOGAPS
24	00/12	NOGAPS/NOGAPS
26	00/12	NOGAPS/NOGAPS
27	00/12	AVN/AVN
28	12	NOGAPS
29	00/12	NOGAPS/NOGAPS

Table C4. MM5 forecast cycles used together with model that was used to provide the initial and boundary conditions for November 1997.

Date	Time(UTC)	Initialization Model
12	12	AVN
13	00/12	AVN/NOGAPS
15	00/12	AVN/NOGAPS
16	00/12	NOGAPS/AVN
17	00/12	AVN/NOGAPS
18	12	NOGAPS
19	00/12	AVN/AVN

Appendix D: Sigma (σ) Coordinate System Description.

A sigma coordinate system has the desirable attribute that the ground is always at the same level in the vertical. It is thus termed a “terrain-following” coordinate system.

In MM5 it is defined to be:

$$\sigma = \frac{p - p_t}{p_s - p_t} \quad (\text{D.1})$$

where p is the pressure at the height under consideration, p_t is a constant pressure which defines the top of the model (100 mb for MM5), and p_s is the surface pressure. Sigma values range from 1 (surface) to 0 (100 mb).

The MM5 uses a staggered grid structure in the vertical with vertical velocity being calculated on the 26 “full” sigma levels, while all other prognostic variables are calculated on the 25 “half” sigma levels. The 26 valid MM5 “full” sigma levels are:

01 - 1.00	10 - 0.80	19 - 0.35
02 - 0.99	11 - 0.75	20 - 0.30
03 - 0.98	12 - 0.70	21 - 0.25
04 - 0.96	13 - 0.65	22 - 0.20
05 - 0.94	14 - 0.60	23 - 0.15
06 - 0.92	15 - 0.55	24 - 0.10
07 - 0.90	16 - 0.50	25 - 0.05
08 - 0.87	17 - 0.45	26 - 0.00
09 - 0.84	18 - 0.40	

The 25 “half” sigma levels are located approximately half the distance between the 26 “full” sigma levels listed above, and hence the terms “full” and “half”.

Appendix E: Pressure levels used by MM5.

The pressure levels used by MM5 are:

01 - 1100 mb	12 - 550 mb
02 - 1050 mb	13 - 500 mb
03 - 1000 mb	14 - 450 mb
04 - 950 mb	15 - 400 mb
05 - 925 mb	16 - 350 mb
06 - 850 mb	17 - 300 mb
07 - 800 mb	18 - 250 mb
08 - 750 mb	19 - 200 mb
09 - 700 mb	20 - 150 mb
10 - 650 mb	21 - 100 mb
11 - 600 mb	

Appendix F: Total cloud condensate threshold values for the vertical column method.

The threshold values used to convert total cloud condensate to fractional cloudiness amounts for the vertical column method are found below in Table F1.

Table F1. Total cloud condensate thresholds used to convert to FC amounts for the vertical column method. FC amounts are expressed in percent while total cloud condensate is in units of kg of condensate per kg of air.

Total Cloud Condensate (TCC) Thresholds in kgkg^{-1}	Fractional Cloudiness Amounts in Percent
$\text{TCC} < 7.0 \times 10^{-11}$	0
$7.0 \times 10^{-11} \leq \text{TCC} < 1.0 \times 10^{-10}$	5
$1.0 \times 10^{-10} \leq \text{TCC} < 5.0 \times 10^{-10}$	10
$5.0 \times 10^{-10} \leq \text{TCC} < 7.0 \times 10^{-10}$	15
$7.0 \times 10^{-10} \leq \text{TCC} < 1.0 \times 10^{-9}$	20
$1.0 \times 10^{-9} \leq \text{TCC} < 6.0 \times 10^{-9}$	25
$6.0 \times 10^{-9} \leq \text{TCC} < 2.0 \times 10^{-8}$	30
$2.0 \times 10^{-8} \leq \text{TCC} < 7.0 \times 10^{-8}$	35
$7.0 \times 10^{-8} \leq \text{TCC} < 2.0 \times 10^{-7}$	40
$2.0 \times 10^{-7} \leq \text{TCC} < 7.0 \times 10^{-7}$	45
$7.0 \times 10^{-7} \leq \text{TCC} < 1.0 \times 10^{-6}$	50
$1.0 \times 10^{-6} \leq \text{TCC} < 4.0 \times 10^{-6}$	55
$4.0 \times 10^{-6} \leq \text{TCC} < 7.0 \times 10^{-6}$	60
$7.0 \times 10^{-6} \leq \text{TCC} < 1.0 \times 10^{-5}$	65
$1.0 \times 10^{-5} \leq \text{TCC} < 3.0 \times 10^{-5}$	70
$3.0 \times 10^{-5} \leq \text{TCC} < 5.0 \times 10^{-5}$	75
$5.0 \times 10^{-5} \leq \text{TCC} < 7.0 \times 10^{-5}$	80
$7.0 \times 10^{-5} \leq \text{TCC} < 9.0 \times 10^{-5}$	85
$9.0 \times 10^{-5} \leq \text{TCC} < 2.0 \times 10^{-4}$	90
$2.0 \times 10^{-4} \leq \text{TCC} < 4.5 \times 10^{-4}$	95
$\text{TCC} \geq 4.5 \times 10^{-4}$	100

Appendix G: Total cloud condensate threshold values for the layered method.

Three different sets of threshold values were used in the implementation of the layered method. The division into three sets was done to simulate the dependence of cloud water content on temperature. The sets corresponded to low-level clouds (950 mb - 750 mb), mid-level clouds (700 mb - 400 mb), and high-level clouds (350 mb - 200 mb), and the threshold values for these three sets are listed in Tables G1-G3, respectively.

Table G1. Total cloud condensate thresholds used to convert to FC amounts for MM5 model layers between 950 mb and 750 mb. FC amounts are expressed in percent while total cloud condensate is in units of kg of condensate per kg of air.

Total Cloud Condensate (TCC) Thresholds in kgkg^{-1}	Fractional Cloudiness Amounts in Percent
$\text{TCC} < 9.0 \times 10^{-13}$	0
$9.0 \times 10^{-13} \leq \text{TCC} < 1.0 \times 10^{-12}$	5
$1.0 \times 10^{-12} \leq \text{TCC} < 3.0 \times 10^{-12}$	10
$3.0 \times 10^{-12} \leq \text{TCC} < 5.0 \times 10^{-12}$	15
$5.0 \times 10^{-12} \leq \text{TCC} < 1.0 \times 10^{-11}$	20
$1.0 \times 10^{-11} \leq \text{TCC} < 5.0 \times 10^{-11}$	25
$5.0 \times 10^{-11} \leq \text{TCC} < 1.0 \times 10^{-10}$	30
$1.0 \times 10^{-10} \leq \text{TCC} < 5.0 \times 10^{-10}$	35
$5.0 \times 10^{-10} \leq \text{TCC} < 1.0 \times 10^{-9}$	40
$1.0 \times 10^{-9} \leq \text{TCC} < 6.0 \times 10^{-9}$	45
$6.0 \times 10^{-9} \leq \text{TCC} < 4.0 \times 10^{-8}$	50
$4.0 \times 10^{-8} \leq \text{TCC} < 1.0 \times 10^{-7}$	55
$1.0 \times 10^{-7} \leq \text{TCC} < 5.0 \times 10^{-7}$	60
$5.0 \times 10^{-7} \leq \text{TCC} < 2.0 \times 10^{-6}$	65
$2.0 \times 10^{-6} \leq \text{TCC} < 8.0 \times 10^{-6}$	70
$8.0 \times 10^{-6} \leq \text{TCC} < 1.0 \times 10^{-5}$	75
$1.0 \times 10^{-5} \leq \text{TCC} < 4.0 \times 10^{-5}$	80
$4.0 \times 10^{-5} \leq \text{TCC} < 7.0 \times 10^{-5}$	85
$7.0 \times 10^{-5} \leq \text{TCC} < 1.5 \times 10^{-4}$	90
$1.5 \times 10^{-4} \leq \text{TCC} < 3.5 \times 10^{-4}$	95
$\text{TCC} \geq 3.5 \times 10^{-4}$	100

Table G2. Total cloud condensate thresholds used to convert to FC amounts for MM5 model layers between 700 mb and 400 mb. FC amounts are expressed in percent while total cloud condensate is in units of kg of condensate per kg of air.

Total Cloud Condensate (TCC) Thresholds in kgkg^{-1}	Fractional Cloudiness Amounts in Percent
$\text{TCC} < 2.0 \times 10^{-13}$	0
$2.0 \times 10^{-13} \leq \text{TCC} < 3.0 \times 10^{-13}$	5
$3.0 \times 10^{-13} \leq \text{TCC} < 5.0 \times 10^{-13}$	10
$5.0 \times 10^{-13} \leq \text{TCC} < 7.0 \times 10^{-13}$	15
$7.0 \times 10^{-13} \leq \text{TCC} < 2.0 \times 10^{-12}$	20
$2.0 \times 10^{-12} \leq \text{TCC} < 8.0 \times 10^{-12}$	25
$8.0 \times 10^{-12} \leq \text{TCC} < 3.0 \times 10^{-11}$	30
$3.0 \times 10^{-11} \leq \text{TCC} < 9.0 \times 10^{-11}$	35
$9.0 \times 10^{-11} \leq \text{TCC} < 4.0 \times 10^{-10}$	40
$4.0 \times 10^{-10} \leq \text{TCC} < 9.0 \times 10^{-10}$	45
$9.0 \times 10^{-10} \leq \text{TCC} < 5.0 \times 10^{-09}$	50
$5.0 \times 10^{-09} \leq \text{TCC} < 4.0 \times 10^{-08}$	55
$4.0 \times 10^{-08} \leq \text{TCC} < 1.0 \times 10^{-07}$	60
$1.0 \times 10^{-07} \leq \text{TCC} < 6.0 \times 10^{-07}$	65
$6.0 \times 10^{-07} \leq \text{TCC} < 1.0 \times 10^{-06}$	70
$1.0 \times 10^{-06} \leq \text{TCC} < 7.0 \times 10^{-06}$	75
$7.0 \times 10^{-06} \leq \text{TCC} < 1.0 \times 10^{-05}$	80
$1.0 \times 10^{-05} \leq \text{TCC} < 5.0 \times 10^{-05}$	85
$5.0 \times 10^{-05} \leq \text{TCC} < 9.0 \times 10^{-05}$	90
$9.0 \times 10^{-05} \leq \text{TCC} < 2.5 \times 10^{-04}$	95
$\text{TCC} \geq 2.5 \times 10^{-04}$	100

Table G3. Total cloud condensate thresholds used to convert to FC amounts for MM5 model layers between 350 mb and 200 mb. FC amounts are expressed in percent while total cloud condensate is in units of kg of condensate per kg of air.

Total Cloud Condensate (TCC) Thresholds in kg kg^{-1}	Fractional Cloudiness Amounts in Percent
$\text{TCC} < 8.0 \times 10^{-14}$	0
$8.0 \times 10^{-14} \leq \text{TCC} < 1.0 \times 10^{-13}$	5
$1.0 \times 10^{-13} \leq \text{TCC} < 2.0 \times 10^{-13}$	10
$2.0 \times 10^{-13} \leq \text{TCC} < 6.0 \times 10^{-13}$	15
$6.0 \times 10^{-13} \leq \text{TCC} < 1.0 \times 10^{-12}$	20
$1.0 \times 10^{-12} \leq \text{TCC} < 5.0 \times 10^{-12}$	25
$5.0 \times 10^{-12} \leq \text{TCC} < 1.0 \times 10^{-11}$	30
$1.0 \times 10^{-11} \leq \text{TCC} < 6.0 \times 10^{-11}$	35
$6.0 \times 10^{-11} \leq \text{TCC} < 1.0 \times 10^{-10}$	40
$1.0 \times 10^{-10} \leq \text{TCC} < 6.0 \times 10^{-10}$	45
$6.0 \times 10^{-10} \leq \text{TCC} < 3.0 \times 10^{-09}$	50
$3.0 \times 10^{-09} \leq \text{TCC} < 1.0 \times 10^{-08}$	55
$1.0 \times 10^{-08} \leq \text{TCC} < 6.0 \times 10^{-08}$	60
$6.0 \times 10^{-08} \leq \text{TCC} < 2.0 \times 10^{-07}$	65
$2.0 \times 10^{-07} \leq \text{TCC} < 7.0 \times 10^{-07}$	70
$7.0 \times 10^{-07} \leq \text{TCC} < 3.0 \times 10^{-06}$	75
$3.0 \times 10^{-06} \leq \text{TCC} < 8.0 \times 10^{-06}$	80
$8.0 \times 10^{-06} \leq \text{TCC} < 3.0 \times 10^{-05}$	85
$3.0 \times 10^{-05} \leq \text{TCC} < 8.0 \times 10^{-05}$	90
$8.0 \times 10^{-05} \leq \text{TCC} < 1.5 \times 10^{-04}$	95
$\text{TCC} \geq 1.5 \times 10^{-04}$	100

Bibliography

- Cantrell, L., Captain, USAF, Programmer/Analyst, Cloud Models Team, AFWA, Offutt Air Force Base. Personal Correspondence.
- Cotton, W. R. and R. A. Anthes, 1989: *Storm and Cloud Dynamics*. Academic Press, 883 pp.
- Crum, T. D., 1987: *AFGWC Cloud Forecast Models*. AFGWC/TN-87/001. Air Force Global Weather Central, 66 pp.
- Fye, F. K., 1978: *The AFGWC Automated Cloud Analysis Model*. AFGWC/TN-78/002. Air Force Global Weather Central, 97 pp.
- Grell, G. A., J. Dudhia, and D. R. Stauffer, 1995: *A Description of the Fifth-Generation Penn State/NCAR Mesoscale Model (MM5)*. NCAR/TN-398+STR. National Center for Atmospheric Research, Boulder, CO, 122 pp.
- Hamill, T. M., R. P. D'Entremont, and J. T. Bunting, 1992: A description of the Air Force Real-Time Nephanalysis Model. *Wea. Forecasting*, **7**, 288-306.
- Kalbfleisch, J. G., 1979: *Probability and Statistical Inference II*. Springer-Verlag.
- Kiess, R. B. and W. M. Cox, 1988: *The AFGWC Automated Real-Time Cloud Analysis Model*. AFGWC/TN-88/001. Air Force Global Weather Central, 81 pp.
- Kopp, T., Team Chief, Cloud Models Team, AFWA, Offutt Air Force Base. Personal Correspondence.
- Kvamstø, N. G., 1991: An investigation of diagnostic relations between stratiform fractional cloud cover and other meteorological parameters in numerical weather prediction models. *J. Appl. Meteor.*, **30**, 200-216.
- Larson, H. J., 1982: *Introduction to Probability Theory and Statistical Inference*. John Wiley & Sons, 637 pp.
- Mocko, D., and W. Cotton, 1995: Evaluation of fractional cloudiness parameterizations for use in a mesoscale model. *J. Atmos. Sci.*, **52**, 2884-2901.
- Nehrkorn, T., M. Mickelson, M. Zivkovic, and L. W. Knowlton, 1994: *Evaluation of NWP and cloud forecasts from the Phillips Laboratory Global Spectral Model*. PL-TR-94-2296, Phillips Laboratory, Hanscom Air Force Base, 216 pp.

- Norquist, D. C., H. S. Muench, D. L. Aiken, and D. C. Hahn, 1994: *Diagnosing cloudiness from global numerical weather prediction model forecasts*. PL-TR-94-2211, Phillips Laboratory, Hanscom Air Force Base, 139 pp.
- Seaman, N. L., Z. Guo, and T. P. Ackerman, 1995: Evaluation of Cloud Prediction and Determination of Critical Relative Humidity for a Mesoscale Numerical Weather Prediction Model. *Proceedings of the Fifth ARM Science Team Meeting*, San Diego, CA, Atmospheric Radiation Measurement Session Papers, 273-275.
- Spero, T., Team Chief, MM5 Model Team, AFWA, Offutt Air Force Base. Personal Correspondence.
- Sundqvist, H., E. Berge, and J. E. Kristjánsson, 1989: Condensation and cloud parameterization studies with a mesoscale numerical weather prediction model. *Mon. Wea. Rev.*, **117**, 1641-1657.
- Trapnell, R. N., 1992: *Cloud curve algorithm test program*. PL-TR-92-2052, Phillips Laboratory, Hanscom Air Force Base, 170 pp.
- Wilks, D. S., 1995: *Statistical Methods in the Atmospheric Sciences*. Academic Press, 467 pp.
- Wonsick, M., Captain, USAF, Programmer/Analyst, Cloud Models Team, AFWA, Offutt Air Force Base. Personal Correspondence.
- Zamiska, A. and P. Giese, 1995: *RTNEPH, USAFETAC Climatic Database Users Handbook No. 1*. USAFETAC/UN-86/01 (Rev). USAF Environmental Technical Applications Center, 15 pp.

Vita

Brian D. Pukall was born 16 April 1969 in Antigo, Wisconsin. In May 1991, he was a summa cum laude graduate of Concordia College in Moorhead, Minnesota. He received a Bachelor of Arts degree in mathematics from Concordia. Brian earned his commission as an Air Force officer by completing ROTC courses at North Dakota State University in Fargo, North Dakota and was commissioned in June 1991. Brian was called to active duty in the Air Force in April 1992 and was assigned to Florida State University (FSU) to complete the Basic Meteorology Program (BMP). While at FSU he was inducted into Chi Epsilon Pi, the meteorology honor society. Upon completion of BMP, he was assigned to Aviano AB, Italy in May 1993. Brian served in the capacities of duty forecaster and Wing Weather Officer while at Aviano. At Aviano, he had the opportunity to directly support several real-world NATO operations including DELIBERATE FORCE. He also took advantage of his time in Italy to become proficient in Italian. After a little over three years in Italy, Brian was assigned to the Air Force Institute of Technology (AFIT) to earn a Master of Science degree in dynamic meteorology. While at AFIT he was inducted into Tau Beta Pi, the national engineering honor society.

Brian is married to the former Alessandra Arzenton of Pordenone, Italy. They were married on 30 September 1995 and have a daughter, Vittoria, who is one year old.

Permanent Address:

W14675 1st Ave.
Gleason, WI 54435

REPORT DOCUMENTATION PAGE			Form Approved OMB No. 0704-0188	
Public reporting burden for this collection of information is estimated to average 1 hour per response, including the time for reviewing instructions, searching existing data sources, gathering and maintaining the data needed, and completing and reviewing the collection of information. Send comments regarding this burden estimate or any other aspect of this collection of information, including suggestions for reducing this burden, to Washington Headquarters Services, Directorate for Information Operations and Reports, 1215 Jefferson Davis Highway, Suite 1204, Arlington, VA 22202-4302, and to the Office of Management and Budget, Paperwork Reduction Project (0704-0188), Washington, DC 20503.				
1. AGENCY USE ONLY (Leave blank)		2. REPORT DATE March 1998		3. REPORT TYPE AND DATES COVERED Master's Degree Thesis
4. TITLE AND SUBTITLE A Comparison of Advect Cloud Model and Fifth-Generation Mesoscale Model Total Fractional Cloud Forecasts				5. FUNDING NUMBERS
6. AUTHOR(S) Brian D. Pukall, Capt, USAF				
7. PERFORMING ORGANIZATION NAME(S) AND ADDRESS(ES) Michael K. Walters, LtCol, USAF AFIT/ENP 2950 P. Street Wright-Patterson AFB, OH 45433 DSN 785-3636 x4681, Comm (937) 255-3636 x4681, e-mail: mwalters@afit.af.mil				8. PERFORMING ORGANIZATION REPORT NUMBER AFIT/GM/ENP/98M-08
9. SPONSORING/MONITORING AGENCY NAME(S) AND ADDRESS(ES) Randy J. Lefevre, Maj, USAF Air Force Weather Agency 106 Peacekeeper Drive Suite 2N3 Offutt AFB, NE 68113-1408 DSN 271-4671 Comm (402) 294-4671 e-mail lefevrer@afwa.af.mil				10. SPONSORING/MONITORING AGENCY REPORT NUMBER
11. SUPPLEMENTARY NOTES				
12a. DISTRIBUTION AVAILABILITY STATEMENT Approved for public release; distribution unlimited				12b. DISTRIBUTION CODE
13. ABSTRACT (Maximum 200 words) <p>Total fractional cloudiness (FC) forecasts from the advect cloud (ADVCLD) model and total FC forecasts diagnosed from the relative humidity and total cloud condensate (snow, ice, rain water, and cloud water) fields from the fifth-generation mesoscale model (MM5) were statistically and subjectively compared to determine which model produced the better total FC forecasts from August through November 1997 for a forecast window centered on Bosnia. The real-time nephanalysis (RTNEPH) model was used to represent the true state of the atmosphere. ADVCLD and MM5 forecasts were also compared against a persistence forecast to provide a minimal skill baseline. The Air Force Weather Agency (AFWA) provided all model data.</p> <p>The Kvamsto and Sundqvist schemes were used to transform the relative humidity forecasted at individual grid points by MM5 into a total FC forecast. Two other methods, the vertical column and layered methods, based on threshold techniques and devised by the author were used to transform the total cloud condensate forecasted by MM5 into a total FC forecast.</p> <p>The results indicate that ADVCLD produced the better total FC forecasts for the first 33 hours of the 36-hr forecast period despite having a tendency to produce too much cloudiness. Overall, the MM5 displayed a significant negative bias in both the relative humidity and total cloud condensate fields. The MM5 was found to significantly underforecast cloud cover over the Adriatic Sea and slightly overforecast cloudiness over mountainous regions. ADVCLD demonstrated skill against</p>				
14. SUBJECT TERMS CLOUD FORECASTING, MESOSCALE MODEL, NUMERICAL WEATHER PREDICTION, FRACTIONAL CLOUDINESS				15. NUMBER OF PAGES 157
				16. PRICE CODE
17. SECURITY CLASSIFICATION OF REPORT Unclassified		18. SECURITY CLASSIFICATION OF THIS PAGE Unclassified		19. SECURITY CLASSIFICATION OF ABSTRACT Unclassified
				20. LIMITATION OF ABSTRACT UL